

JAERI-M

7 9 4 9

ANNUAL REPORT OF THE
OSAKA LABORATORY FOR RADIATION CHEMISTRY
JAPAN ATOMIC ENERGY RESEARCH INSTITUTE

(No. 11)

April 1, 1977-March 31, 1978

October 1978

Osaka Laboratory for Radiation Chemistry

日 本 原 子 力 研 究 所
Japan Atomic Energy Research Institute

この報告書は、日本原子力研究所が JAERI-M レポートとして、不定期に刊行している研究報告書です。入手、複製などのお問い合わせは、日本原子力研究所技術情報部（茨城県那珂郡東海村）あて、お申しこしください。

JAERI-M reports, issued irregularly, describe the results of research works carried out in JAERI. Inquiries about the availability of reports and their reproduction should be addressed to Division of Technical Information, Japan Atomic Energy Research Institute, Tokai-mura, Naka-gun, Ibaraki-ken, Japan.

Osaka Laboratory for Radiation Chemistry
Japan Atomic Energy Research Institute
25-1 Mii-minami machi, Neyagawa
Osaka, Japan

JAERI-M 7949

ANNUAL REPORT OF THE
OSAKA LABORATORY FOR RADIATION CHEMISTRY
JAPAN ATOMIC ENERGY RESEARCH INSTITUTE
(No. 11)

April 1, 1977 - March 31, 1978

(Received October 9 , 1978)

This report describes research activities of Osaka Laboratory for Radiation Chemistry, JAERI during one year period from April 1, 1977 through March 31, 1978. The latest report, for 1977, is JAERI-M 7355.

Detailed descriptions of the activities are presented in the following subjects: studies on reactions of carbon monoxide and hydrogen; polymerization under the irradiation of high dose rate electron beams; modification of polymers, degradation, cross-linking, and grafting.

Previous reports in this series are:

Annual Report, JARRP, Vol. 1	1958/1959*
Annual Report, JARRP, Vol. 2	1960
Annual Report, JARRP, Vol. 3	1961
Annual Report, JARRP, Vol. 4	1962
Annual Report, JARRP, Vol. 5	1963
Annual Report, JARRP, Vol. 6	1964
Annual Report, JARRP, Vol. 7	1965
Annual Report, JARRP, Vol. 8	1966
Annual Report, No. 1, JAERI 5018	1967
Annual Report, No. 2, JAERI 5022	1968
Annual Report, No. 3, JAERI 5026	1969
Annual Report, No. 4, JAERI 5027	1970
Annual Report, No. 5, JAERI 5028	1971
Annual Report, No. 6, JAERI 5029	1972
Annual Report, No. 7, JAERI 5030	1973
Annual Report, No. 8, JAERI-M 6260	1974
Annual Report, No. 9, JAERI-M 6702	1975
Annual Report, No. 10, JAERI-M 7355	1976

*Year of the activities

Keywords: Electron Beam Irradiation, γ -Irradiation, Carbon Monoxide-Hydrogen Reaction, Methane, Radiation-Induced Reaction, Polymerization, Grafting, Polymer Modification, Cross-Linking, Vinyl Monomer, Dienes, Polystyrene, Polyvinyl Chloride Fiber, Polyester Fiber, Wholly Aromatic Polyamide, Cellulose Triacetate Film Dosimeter, Radiation Chemistry

昭和52年度日本原子力研究所 大阪研究所年報

日本原子力研究所 大阪研究所

(1978年10月9日受理)

本報告は、大阪研究所において昭和52年度に行なわれた研究活動を述べたものである。主な研究題目は、一酸化炭素と水素の反応ならびにそれに関連した研究、高線量率電子線照射による重合反応の研究、ポリマーの改質および上記の研究と関連して重合反応、高分子分解、架橋ならびにクラフト重合に関する基礎的研究などである。

日本放射線高分子研究協会年報	Vol. 1		1958/1959
日本放射線高分子研究協会年報	Vol. 2		1960
日本放射線高分子研究協会年報	Vol. 3		1961
日本放射線高分子研究協会年報	Vol. 4		1962
日本放射線高分子研究協会年報	Vol. 5		1963
日本放射線高分子研究協会年報	Vol. 6		1964
日本放射線高分子研究協会年報	Vol. 7		1965
日本放射線高分子研究協会年報	Vol. 8		1966
日本原子力研究所大阪研における放射線化学の基礎研究 No.1	JAERI	5018	1967
日本原子力研究所大阪研における放射線化学の基礎研究 No.2	JAERI	5022	1968
日本原子力研究所大阪研における放射線化学の基礎研究 No.3	JAERI	5026	1969
日本原子力研究所大阪研における放射線化学の基礎研究 No.4	JAERI	5027	1970
日本原子力研究所大阪研における放射線化学の基礎研究 No.5	JAERI	5028	1971
日本原子力研究所大阪研における放射線化学の基礎研究 No.6	JAERI	5029	1972
日本原子力研究所大阪研における放射線化学の基礎研究 No.7	JAERI	5030	1973
Annual Report, Osaka Lab., JAERI, No.8	JAERI-M	6260	1974
Annual Report, Osaka Lab., JAERI, No.9	JAERI-M	6702	1975
Annual Report, Osaka Lab., JAERI, No.10	JAERI-M	7355	1976

CONTENTS

I. INTRODUCTION	1
II. RECENT RESEARCH ACTIVITIES	
[1] Radiation Effects on the Reaction of Mixture of Carbon Monoxide and Hydrogen	
1. Irradiation of Gaseous Mixtures under Forced Circulation	6
2. Irradiation at Elevated Pressures at Static Condition	11
3. Reaction of the Irradiated Gaseous Mixture on Fischer-Tropsch Catalyst	14
4. Reactions in the Presence of Fluidized Bed Catalyst	17
5. Radiation Effects on CO-H ₂ -N ₂ O Mixtures in the Presence of Magnesium Oxide	22
6. Radiation Chemical Reaction of Methane in a Flow System	27
7. Spin Trapping of Radicals Produced by Irradiation of Gas Mixtures of CO and H ₂	32
[2] Polymerization of Vinyl Monomers by High Dose Rate Electron Beams	
1. Polymerization of Styrene up to Higher Conversion by High Dose Rate Electron Beams ...	33
2. Radiation Polymerization of Styrene/Carbon- tetrachloride Mixture in a Wide Range of Dose Rate	38
3. Radiation Polymerization of Styrene/Ethylene Chloride Mixture in a Wide Range of Dose Rate .	52
[3] Radiation-Induced Polymerization of Dienes	

1. Polymerization of Isoprene	60
2. Polymerization of Chloroprene	64
[4] Modification of Polymers	
1. Surface Modification of Poly (Ethylene Terephthalate) Film by Radiation Induced Chlorination and Adhesion of Chlorinated Films	68
2. Preparation and Properties of Polyvinyl Chloride Fibers with Graft Branches of Poly (Aluminum Acrylate)	771
3. Radiation-Induced Graft Polymerization of Acrylic Acid onto Poly (Vinyl Chloride)	74
4. Wettability of Hydrated Cellulose and Poly (Vinyl Alcohol) Films	80
5. Formation of Electret in Polymers by High Energy Electron Irradiation	83
[5] Studies of Chain Rupture in Polyamides by Radiation and Mechanical Stretching	
1. Chain Rupture in Nylon 6 Fibers	89
2. Radical Formation in Wholly Aromatic Polyamides	92
[6] Studies on Radiation Dosimetry	
1. Survey of Wavelength Suitable for Optical Density Measurement Used for CTA Film Dosimeter	97
2. Coloration Mechanism of the CTA Dosimeter	102
III. LIST OF PUBLICATIONS	
[1] Published Papers	106
[2] Oral Presentations	108
IV. LIST OF SCIENTISTS	111

目 次

I	序文	1
II	研究活動	
(1)	CO-H ₂ 混合気体の放射線化学反応	
1.	循環気相反応装置による照射	6
2.	非循環・昇圧下の照射	11
3.	Fischer-Tropsch 触媒上における被照射混合気体の反応	14
4.	流動触媒存在下の反応	17
5.	MgO 存在下の CO-H ₂ -N ₂ O 混合気体の反応	22
6.	流通方式による CH ₄ の放射線化学反応	27
7.	CO-H ₂ 混合気体の照射によって生成するラジカルのスピン・トラッピング	32
(2)	高線量率電子線照射によるビニル・モノマーの重合	
1.	高重合率まで進めたスチレンの重合挙動	33
2.	広い線量率範囲におけるスチレン-四塩化炭素系の放射線重合	38
3.	広い線量率範囲におけるスチレン-塩化エチレン系の放射線重合	52
(3)	ジエン類の放射線重合	
1.	イソプレンの重合	60
2.	クロロプレンの重合	64
(4)	ポリマーの改質	
1.	放射線塩素化によるポリエチレンテレフタレート・フィルムの表面改質と接着性	68
2.	ポリアクリル酸アルミニウム・グラフト鎖をもつ ポリ塩化ビニル・繊維の合成と性質	71
3.	ポリ塩化ビニルへのアクリル酸の放射線グラフト重合	74
4.	水和セルロースとポリビニルアルコールの漏れ	80
5.	電子線照射による高分子エレクトレットの生成	83
(5)	ポリアミドの放射線および機械的切断の研究	
1.	ナイロン6の主鎖切断	89
2.	全芳香族ポリアミドにおけるラジカル生成	92
(6)	線量測定の研究	
1.	CTA フィルム線量計の光学密度測定波長の選定	97
2.	CTA フィルム線量計の着色機構	102
III	発表記録	
(1)	論文など	106
(2)	口頭発表	108
IV	研究者一覧表	111

I. INTRODUCTION

Osaka Laboratory was founded in 1958 as a laboratory of the Japanese Association for Radiation Research on Polymers (JARRP), which was organized and sponsored by some fifty companies interested in radiation chemistry of polymers. The JARRP was merged with Japan Atomic Energy Research Institute (JAERI) on June 1, 1967, and the laboratory changed its name from Osaka Laboratory, JARRP to Osaka Laboratory for Radiation Chemistry, JAERI. The research activities of Osaka Laboratory have been oriented towards the fundamental research on radiation chemistry.

The results of the research activities of the Laboratory were published from 1958 until 1966 in the Annual Reports of JARRP which consisted essentially of original papers. During the period between 1967 and 1973, the publication had been continued as JAERI Report which also consisted mainly of original papers. From 1974, the Annual Report has been published as JAERI-M Report which contains no original papers, but presents outlines of the current research activities in some detail. Readers who wish to have more information are advised to contact with individuals whose names appear under subjects.

The present annual report covers the research activities of the Laboratory between April 1, 1977 and March 31, 1978.

Most of the studies carried out in the Laboratory are continuation from the previous year, emphasis being laid on two fields; one is "Effect of radiation on the reaction of carbon monoxide and hydrogen" and the other, "Radiation-induced polymerization by high dose rate electron beams".

Our new high dose rate electron accelerator (HDRA) has been operated since May 31, 1975, and many results have been obtained using the HDRA.

More quantitative data have been accumulated using the irradiation apparatus for gases under forced circulation on the mixtures of carbon monoxide and hydrogen; G values of the

products were obtained for wide ranges of reaction conditions such as molar ratio of carbon monoxide to hydrogen in the reactant gas, presence or absence of cold traps to remove condensable products to prevent them from further irradiation, and pressure of the reactant around atmospheric pressure. The study on the effect of reactant pressure on G (product) is extended over 7000 Torr using a small reaction vessel of batch type and obtained preliminary results that the G values of the most products did not decrease with increasing pressure, which encourages us to design an irradiation apparatus for circulated gas under moderate pressures.

Since the presence of catalyst in the reactant mixture was found to affect the distribution of the products significantly, we studied the reaction of irradiated gaseous mixture over the Fischer-Tropsch catalyst at various temperatures to examine the contribution of radiation chemical reaction and catalytic reaction separately to overall reaction.

Quantitative comparison of the composition of the gas mixture before and after the passage of the catalyst shows that formaldehyde was reduced to methanol at lower temperatures between 80 - 200°C and oxygen containing products were reduced to hydrocarbons or decomposed at higher temperatures. No evidence that radiation chemically produced intermediates are involved in the reaction was obtained under the reaction conditions employed this year. However, we confirmed the presence of the radiation chemically produced intermediates by spin trapping ESR technique.

The data required for operation of the fluidized bed catalytic reactor were experimentally obtained for various combinations of solids and gases, so that we can carry out the radiation chemical reaction of gaseous mixture of carbon monoxide and hydrogen in the presence of fluidized bed catalyst in which the temperature during irradiation will be more uniform than that in the fixed bed catalyst. Preliminary results seem to confirm the previous experimental results using fixed bed catalytic reactor.

In view of the fact that methane will be an important

resource for obtaining future chemical raw materials and is closely correlated with hydrogen, carbon monoxide, water, or carbon dioxide in that these compounds are convertible from one another by the reaction involving these species, we initiated preliminary study on radiation chemical reaction of methane under broad ranges of reaction conditions including the presence of solid catalyst.

A brief survey was carried out on optical density change to absorbed dose for cellulose triacetate (CTA) film containing various amounts of triphenyl phosphate (TPP) at wavelength between 240 nm and 280 nm in order to find out the optimum condition for dosimetry.

Most favorable result was obtained by use of CTA film containing 5% TPP and by taking optical density reading at 243 nm. The mechanism of the coloration is also studied.

Studies on the radiation-induced polymerization of styrene in bulk have been extended to two directions. One is the polymerization of styrene up to higher conversion and the other is solution polymerization of styrene.

Studies of the initial stage of bulk polymerization of styrene have been useful to know the mechanism of the polymerization by irradiation at high dose rates. For the practical point of view, experiments were carried out with moderately dried styrene up to higher conversion such as 90%. Dose rate was so chosen that the main product was ionic polymers. Both the rate and degree of polymerization decreased with increasing conversion. The decrease of the rate of polymerization could be accounted for quantitatively by the drop of the monomer concentration in the course of the polymerization.

Radiation-induced solution polymerization of styrene was taken up using carbontetrachloride and ethylene dichloride as solvent. The most important effect of the presence of such halogenated hydrocarbons is that they produce much more initiating radicals than styrene. By the irradiation of a unit dose, carbontetrachloride produces radicals 50 times that of styrene, but on the contrary it seems that carbontetra-

chloride produces only the same number of initiating ions as styrene or less.

Studies on kinetics and structure of the products were initiated this year on the bulk polymerization of dienes. In the case of isoprene, oligomers of average degree of polymerization of ca. 13 were obtained by both cationic and radical polymerization at high dose rate. The ^{13}C NMR spectrum indicates that the oligomers consist of 80% trans, 10% cis, and 10% vinyl types and possibly have vinyl groups on both ends of molecules. Since polymerization rate by radical mechanism for chloroprene is 40 times higher than that observed for isoprene, the cationic polymerization was found to contribute above 10^4 rad/sec, but the rate of polymerization at higher dose rate was one of the highest among those of cationically polymerizing monomers ever studied. The products thus obtained are viscous liquid containing oligomers of $\text{DP}=20$ and mostly of trans type (6 - 8% vinyl and ca. 2% cis type).

Heat shrinkage of polyvinyl chloride (PVC) was improved by grafting to a low degree such as 12% when PVC fibers were grafted with acrylic acid and subsequently treated with aluminum salts. Direct grafting of aluminum acrylate was also effective for the improvement of heat shrinkage, dyeability, and hygroscopicity.

Graft copolymerization of acrylic acid has been carried out onto PVC having average molecular weight from 30000 to 60000 which was suspended in a mixture containing water, ethylene dichloride and acrylic acid in order to obtain polymer having hydrophobic part and hydrophilic part as well.

The adhesive strength of the grafted polymer obtained in solutions of different composition against copper or iron plate showed maximum value at 5 - 10% of graft; grafted polymer obtained in the monomer solution containing larger amount of water showed higher adhesive strength, e.g., high values as 16 kg/cm^2 were obtained for copper plate, which suggests a practical use as structural adhesives.

It was found that one cupric ion was adsorbed by every two carboxylic groups contained in the graft polymer when the

graft polymer was immersed in aqueous solution containing excess amounts of cupric ions. This ratio of adsorbed cupric ion to carboxylic groups was independent of the molecular weight of PVC. Ninety-nine percent of cupric ions was removed from aqueous solution containing 100 ppm cupric ion by immersing the grafted polymer (graft percent of 15 - 18%) in the solution.

Studies have continued in order to prepare electret polymer film by irradiation. In order to get insight into the mechanism for the electret formation, the surface charge density in polypropylene film and the electrostatic field generated by electric charge trapped in polymethyl methacrylate substrate were measured as a function of time after irradiation. The results indicate that the amount of charge accumulated on the polypropylene film depends significantly on the electric charge trapped on the substrate.

To obtain further information of the mechanism for degradation by the irradiation, studies have been made on radicals formed by mechanical loading of the fibers of nylon 6, poly-m-phenylene iso-phthalamide(PIA) and poly-p-phenylene terephthalamide(PTA) by ESR technique. ESR signals are observed for PIA on stretching either in N_2 or in air, at room temperature or at low temperature, and the signals observed at low temperature were assigned to radical formed by scission of C-C(O) bond which links phenyl ring and amide group.

August 31, 1978

Tomomichi Kasamatsu, Head
Osaka Laboratory for Radiation Chemistry
Japan Atomic Energy Research Institute

II. RECENT RESEARCH ACTIVITIES

[1] Radiation Effects on the Reaction of Mixtures of Carbon Monoxide and Hydrogen1. Irradiation of Gaseous Mixtures under Forced Circulation

Preliminary results using the apparatus designed for irradiation of recycled gas were described in the last annual report¹⁾. In this year, the data on the product yields are obtained for various reaction conditions such as reactant composition (8 ~ 77 CO% by volume), pressure (450 ~ 1500 Torr) and presence or absence of cold traps (-72°C) which remove condensable products from the reaction mixture. The irradiations are carried out using electron beams from the HDRA (0.4 MeV, 0.5 mA, 400 sec) and dose rate determined by N₂O is $5.22 \times 10^{-4} \text{ eV} \cdot \text{molec}^{-1} \cdot \text{sec}^{-1}$.

Table 1 Material balance

Run No.		C-17	C-15	C-18
Total pressure (torr)		454	706	998
Absorbed energy ($\times 10^{21}$ eV)		3.98	6.16	8.73
Reactant consumed (mgr)	H ₂	4.3	5.2	5.9
	CO	23.8	29.3	33.3
	Total	28.1	34.5	39.2
Products collected (mgr)		27.62	28.97	28.02
Material balance				
$\frac{\text{Products collected}}{\text{Reactants consumed}} \times 100$		98 %	84 %	71 %
$\frac{\text{CO consumed (mole)}}{\text{H}_2 \text{ consumed (mole)}}$		1/2.5	1/2.5	1/2.5

Since the apparatus combined with a direct sampling system to a gaschromatograph can determine the yields of all products containing non-condensable products such as methane, ethane, and propane, which were not determined in the study where a batch type irradiation vessel was used, we examined the material balance of the reaction, the results of which are summarized in Table 1. Excellent material balance is established for run C-17 at 454 Torr, but the balance becomes poorer as the pressure of the reactant increases, probably because of the formation of high molecular weight compounds which are difficult to be recovered. The ratio of consumed hydrogen to carbon monoxide is 2.5 and almost independent of the pressure.

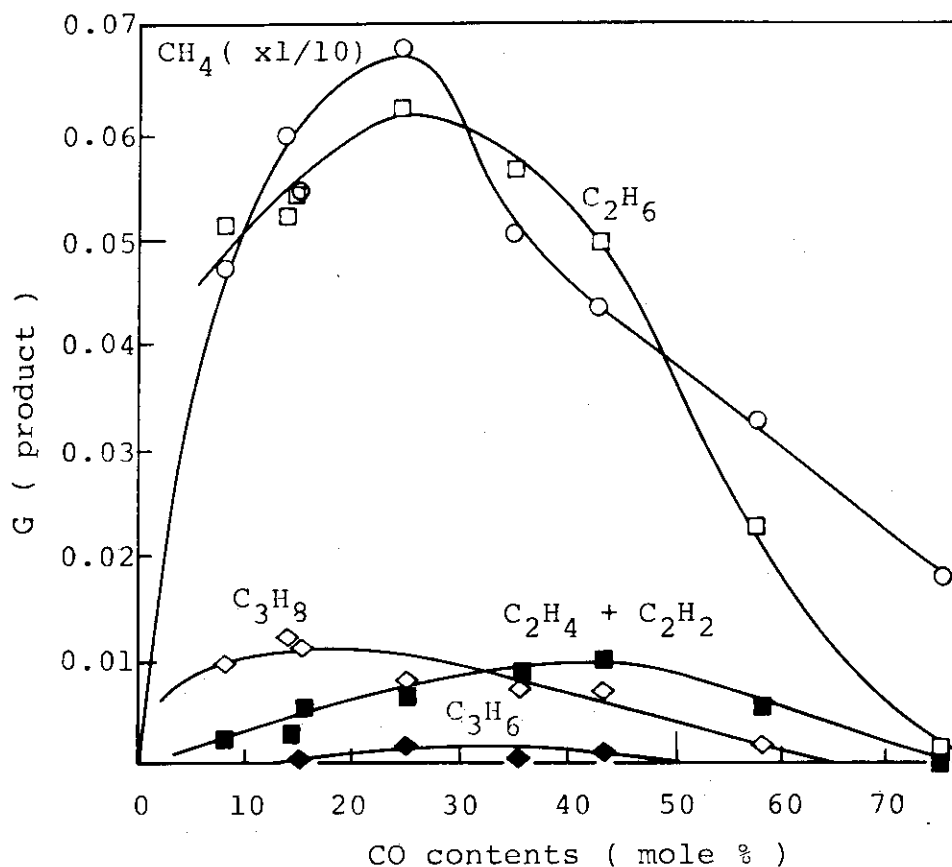


Fig. 1. G (product) vs. CO content in the reactant.
Irradiation conditions, 0.4 MeV, 0.5 mA, 0.12 ~ 0.18 Mrad/sec; Irradiation time, 400 sec; Flow rate of gas circulation, 45 l/min.

The relationships between G value of the products and CO content in the reactant at 1000 Torr reactant pressure are given in Fig. 1, 2 and 3 for hydrocarbons, aldehydes and cycloethers, and other oxygenates, respectively. Methane, ethane, and TEOX have maximum G values (G^{\max} values) at 25%, and G^{\max} values of HCHO, TOX, HCOOCH_3 appear at 15%, and G^{\max} value of C_2H_4 appears at 45% CO content. The G values of CO_2 , C_3O_2 and CH_3CHO increase with increasing CO content up to 77% and the G^{\max} (CH_3OH) comes below 5% CO content.

Most of the G (products) slightly decrease with increasing reactant pressure, but G (CH_3CHO), G (TOX), G ($\text{C}_2\text{H}_4 + \text{C}_2\text{H}_2$), and G (C_3H_8) remain constant. The G (TEOX) and G (-reactants) increase with increasing pressure. These facts may suggest

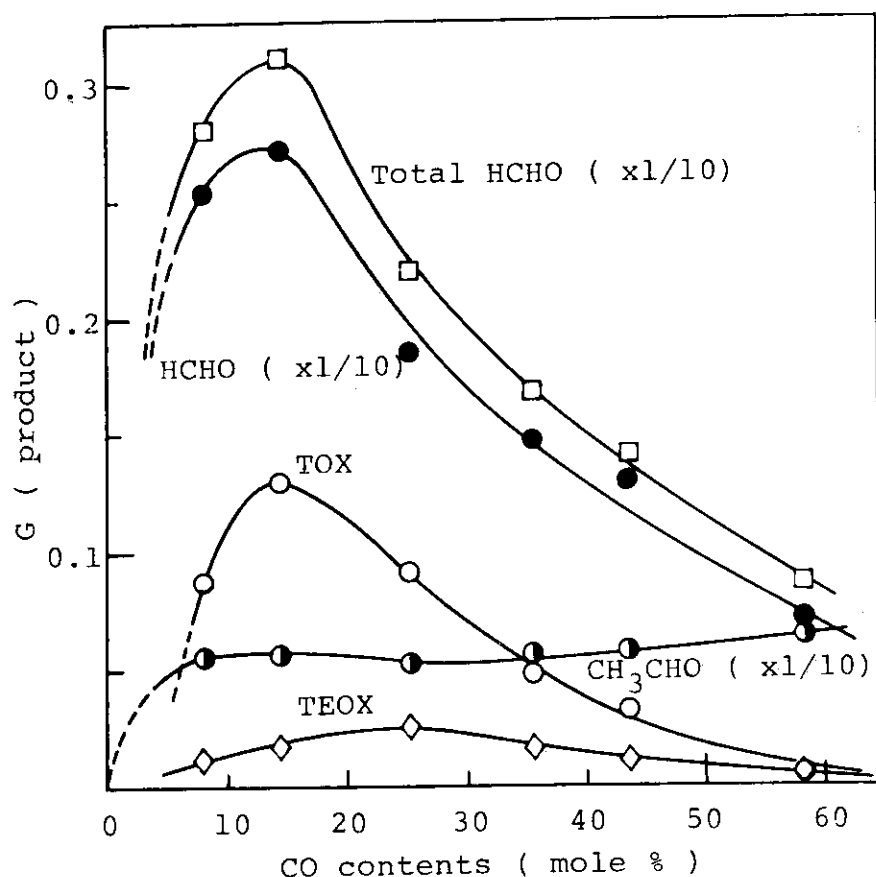


Fig. 2. G (product) vs. CO content in the reactant. Irradiation conditions and reaction conditions are described in the caption of Fig. 1.

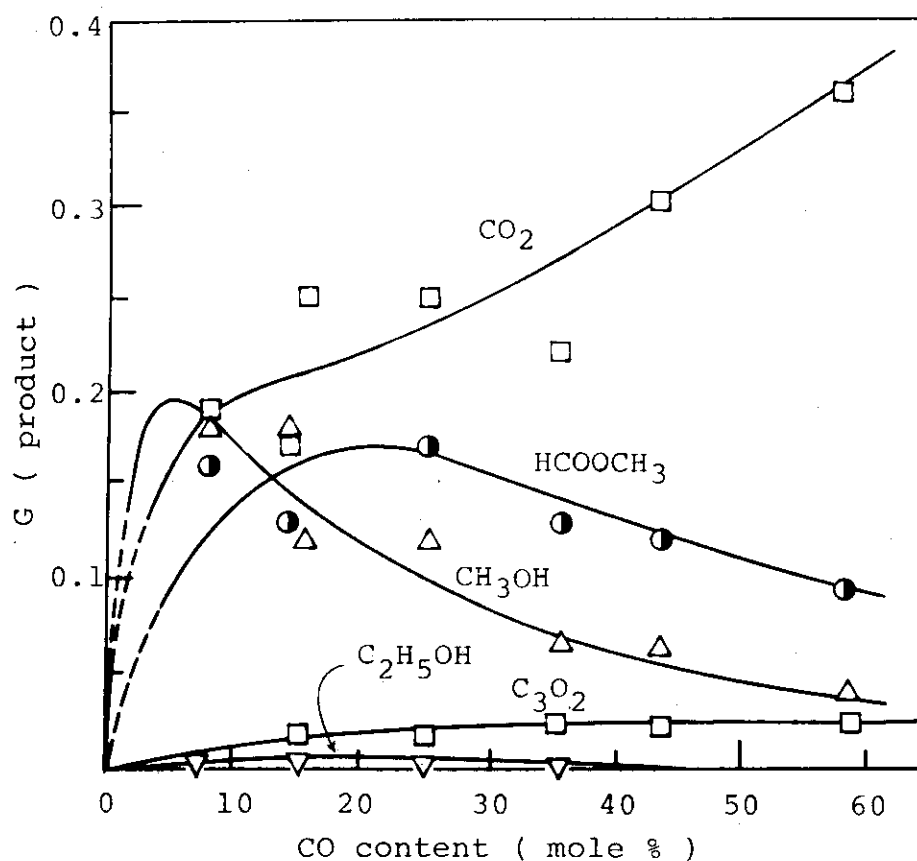


Fig. 3. G (product) vs. CO content in the reactant.
Irradiation conditions and reaction conditions
are described in the caption of Fig. 1.

that the conversion to unidentified products (possibly of high molecular weight) decreases the G values of the most products described above.

In Fig. 4, the yield of the products are given for the cases: (a) no gas circulation, (b) gas circulation without traps, and (c) gas circulation with two traps cooled at -72°C in series. The yield of formaldehyde decreases by the gas circulation, but significantly increases when the traps are used. The yields of methane and methyl formate also increase slightly while those of water, carbon dioxide and methanol decrease with the presence of the cold traps. Therefore, the use of cold traps in the circulating system to trap the condensable products to prevent them from recirculation

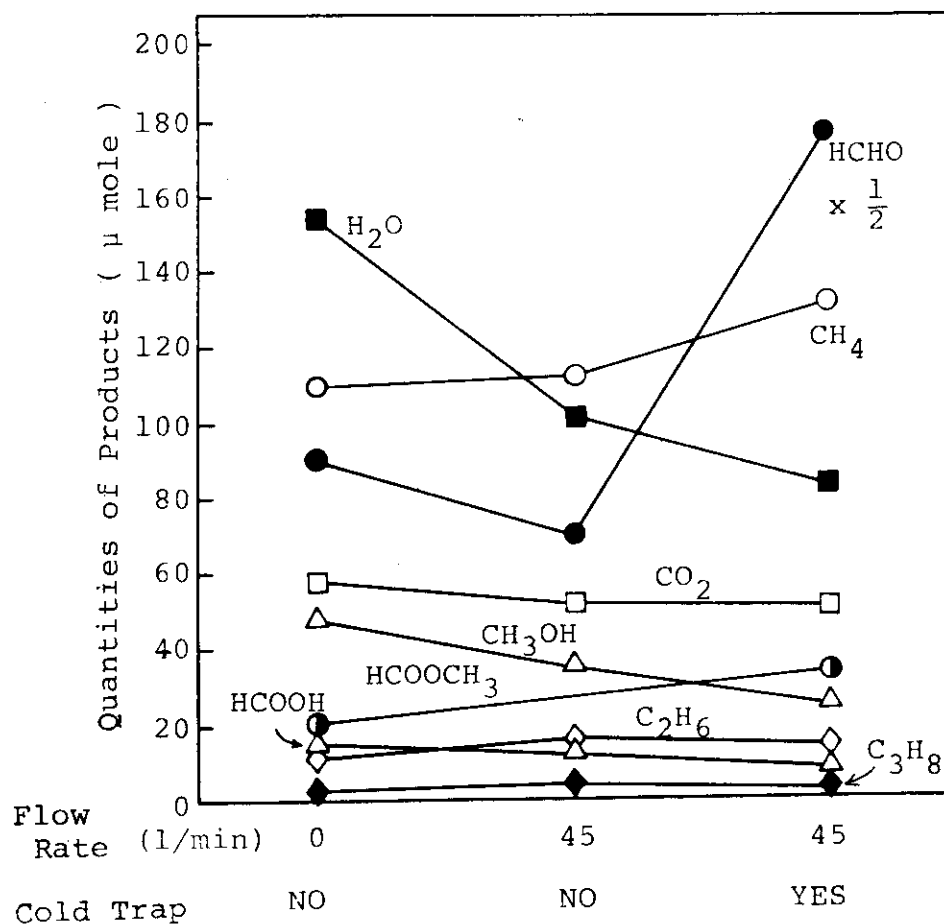


Fig. 4. Effect of cold traps on the yields of the products.
 Irradiation conditions, 0.4 MeV, 0.5 mA;
 Irradiation time, 400 sec; CO content, 25 vol%.

proves to be effective in obtaining high yields of condensable products and depressing the production of unwanted by-products like water or carbon dioxide. (S. Sugimoto, M. Nishii, T. Sugiura)

- 1) S. Sugimoto, M. Nishii, and T. Sugiura,
 JAERI-M 7355, 4 (1977).

2. Irradiation at Elevated Pressures at Static Condition

In the former annual report, it was described that the G values of the main products are independent of the reactant pressure up to 1000 Torr, indicating that the space time yields of most products can be increased linearly by increasing the reactant gas pressure. This finding has been further supported by the experimental results described in the foregoing section where an irradiation apparatus for circulating gas is used. Besides these results, G (TOX) was found to increase with increasing reactant pressure in the pressure range studied. Therefore, it is interesting to investigate the dependence of G (products) on the reactant pressure above 1000 Torr. For this purpose, we made an irradiation vessel of 2.66 l with a titanium window (5.0 cm diameter, 50 μ thick) on top and a Baratron sensor (type 130M-315BH-1000). The vessel can hold compressed gas up to 7000 Torr.

Irradiations are performed by electron beams from the HDRA (0.4 MeV, 0.1 mA) for 1000 seconds on the gaseous mixtures containing hydrogen and carbon monoxide of various compositions at -30°C. Dose rate absorbed by the N₂O gas in the vessel is estimated to be 7.50×10^{-5} eV.molecule⁻¹.sec⁻¹.

After irradiation, the reactants and products in the reaction vessel were pumped off through cold traps in which condensable products were collected. The products recovered from the cold traps were subjected to gaschromatography and mass spectrometry. The products which are not condensed in the traps were not analyzed.

In Fig. 1 and 2, the G values of the products from the reactant containing 15% CO are plotted against pressure of the reactant. It is clear from the figures that the G values of the products except TEOX do not change up to 6300 Torr. This means that the space time yields of the products increase linearly with increasing pressure. The scattering points of G (HCHO) make difficult to obtain definite conclusion, but it seems that G (HCHO) decreases at higher pressures above 5000 Torr. The G value of TOX formation, which shows positive

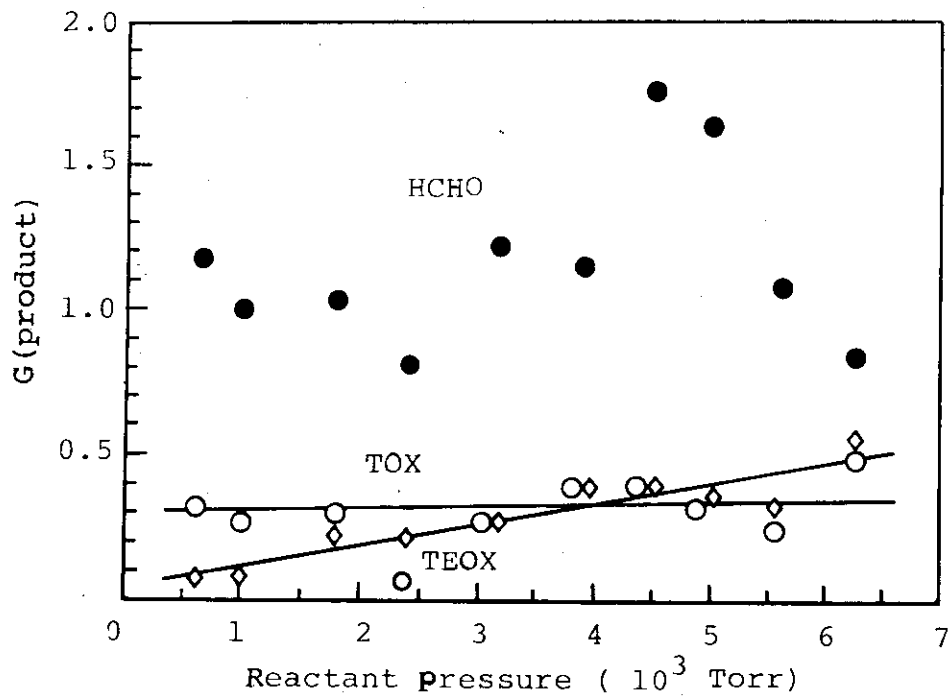


Fig. 1. G values of the products vs. reactant pressure.
CO content, 15%; Irradiation conditions, 0.4 MeV,
0.1 mA, 1.36×10^{-5} eV·molec⁻¹·sec⁻¹; Irradiation
time, 10^3 sec.

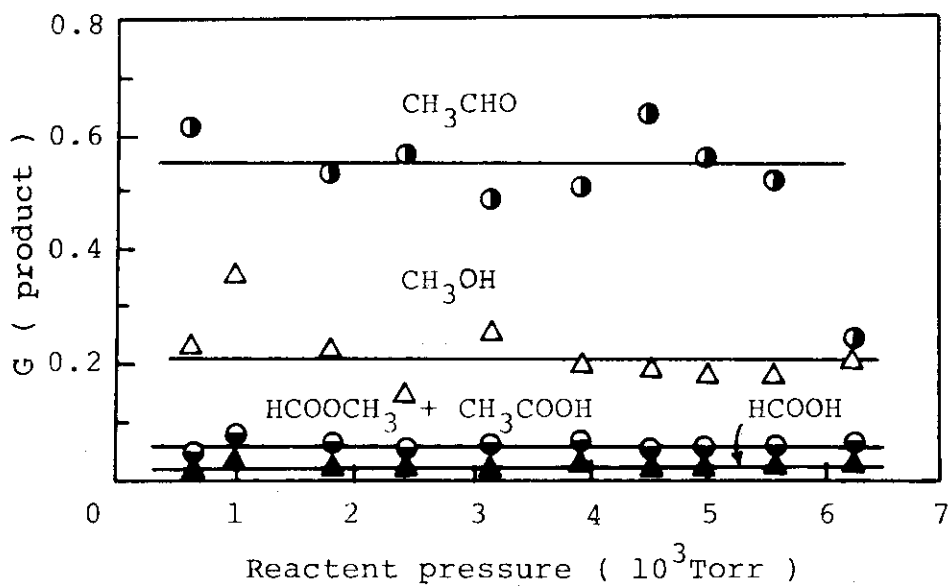


Fig. 2. G values of the products vs. reactant pressure.
Irradiation conditions are given in the caption
of Fig. 1.

pressure dependence in the previous report, is constant in the pressure range studied here; on the other hand the G value of TEOX formation increases with increasing reactant pressure, suggesting the presence of a precursor like $\text{CO}^+(\text{CO})_n (\text{H}_2)_m$ and m being shifted toward higher value at higher reactant pressures. The G values of the products averaged over whole pressure range studied are listed in Table 1.

Table 1 Averaged G (product) under the pressure range
600 - 6300 torr

Product	Averaged G (product)	Product yields (g/Nm ³ reactant · 10 ⁸ rad)
HCHO	1.2	0.88
TOX	0.33	0.73
TEOX	0.56*	1.6*
CH ₃ CHO	0.55	0.59
CH ₃ OH	0.21	0.16
HCOOCH ₃ + CH ₃ COOH	0.055	0.081
HCOOH	0.022	0.025
(CHO) ₂	0.022	0.031
CO ₂	0.067	0.072
H ₂ O	0.39	0.17

* maximum value

14.3 CO% at -28°C, volume 2.66 liters

At 5000 Torr and CO content of 15% the G values of HCHO, CH₃OH, CO₂ and CH₃CHO increase with increasing temperature, while those of TOX and TEOX decrease at higher temperature in the range from -64 to +77°C. The G value of HCOOCH₃ remains almost constant throughout the temperature range studied. It is noted that a product giving peak at m/e = 117 in the mass spectrum increases sharply with decreasing temperature, but the product is still unidentified. The temperature dependence

of G values found at 5000 Torr is somewhat different from those found in the experiments carried out at 600 Torr for some products; CH_3CHO , CH_3OH , but quite similar for other compounds; CO_2 , HCHO , TOX , HCOOCH_3 and $(\text{CHO})_2$.

G values of the products are found to depend on the composition of the reactant gas at 5000 Torr as were found in the experiment at an ordinary pressure (600 Torr). The G values of HCHO , CH_3CHO , CH_3OH , $\text{HCOOCH}_3 + \text{CH}_3\text{COOH}$, and $(\text{CHO})_2$ give maxima at 20, 30, 10, 10 and 12% CO contents, respectively. The G value of CO_2 becomes larger while that of $\text{TEOX} + \text{TOX}$ becomes lower as the CO content becomes higher. This behavior is similar to that reported at lower pressures, although the CO content giving the maximum G value for some products shifted. (S. Sugimoto, M. Nishii, T. Sugiura)

3. Reaction of the Irradiated Gaseous Mixture on Fischer-Tropsch Catalyst

It was reported previously¹⁾ that by passing an irradiated gaseous mixture of CO and H_2 over an Fe-Cu-KG catalyst kept at relatively low temperatures, the yields of methanol and ethanol are greatly increased as compared with those produced by simple irradiation of the CO- H_2 mixture. Such enhancement in the yields of alcohols was suggested to be due to catalytic hydrogenation of formaldehyde and acetaldehyde contained abundantly in the irradiated gas. The analysis system employed in that study, however, did not permit detection of formaldehyde so that we could not discuss the reaction quantitatively.

The principal purpose of the present study is to get data detailed enough to support the previous suggestion by studying the reaction again with adding an analysis system for formaldehyde. It was also of interest to see if evidence could be obtained for surface reaction of active species such as radicals and ions formed by irradiation of CO- H_2 .

A 1 : 6 mixture of CO and H_2 was irradiated in the irradiation vessel FIXCAT-II by electron beams of 600 KeV and 5 mA. The irradiated gas was led into a Pyrex reactor

Table 1 The Amounts of Products in gr/m³-Reactant

Type of method	1		2	
Delay time (sec)	—	60	—	0.8
Flow rates (ml/min)	120	150	150	300
H ₂	20	25	25	50
CO				
Temperatures (°C)	150	150	192	192
Irrad. zone	—	129	—	154
Catalyst				194 154
The amounts of products (gr/m ³ reactant)				
CO ₂	0.691	0.756	0.526	0.457
H ₂ O	1.556	1.798	1.470	1.616
CH ₄	0.082	0.080	0.067	0.069
C ₂ H ₄	<0.001	<0.001	0.001	0.001
C ₂ H ₆	0.016	0.016	0.012	0.012
C ₃ H ₆	<0.001	<0.001	<0.001	<0.001
C ₃ H ₈	0.014	0.014	0.009	0.010
HCHO	0.182	<0.001	0.203	<0.001
CH ₃ OH	0.018	0.237	0.024	0.235
CH ₃ CHO	0.039	<0.001	0.042	<0.001
HCOOCH ₃	0.014	0.011	0.011	0.010
C ₂ H ₅ OH + C ₄ H ₁₀	0.014	0.067	0.016	0.047
(C ₂ H ₅ OH)	(0.007)	(0.064)	—	—
				0.455
				1.278
				0.029
				<0.001
				0.004
				<0.001
				0.003
				0.172
				0.013
				0.176
				0.022
				0.004
				0.010
				—

Catalyst : Fe/Cu/KG (4/1/5, w/w)
Irradiation: 600 KeV, 5 mA

containing 2.8 g of Fe-Cu-KG (4 : 1 : 5 by wt.) catalyst attached 14 m downstream from FIXCAT-II through stainless steel tubing (Method 1). Delay time defined as time for the irradiated gas to reach the catalyst is estimated to be 60 sec for 140 ml/min of the flow rate of the feed gas. To see what happens at much shorter delay time as 0.4 sec, the second series of experiment was carried out with Method 2 where the reactor was attached 20 cm downstream from FIXCAT-II. In both Method 1 and 2, by adjusting a magnetic valve attached 5 cm upstream from the reactor, product yields were determined before and after the reaction of the irradiated gas. Analysis of formaldehyde was made by TCD of a gaschromatograph, Shimadzu GC-7A equipped with Porapak N columns.

Table 1 summarizes the typical data for the product yields together with the experimental conditions. Results obtained with Method 1 indicate that the catalyst kept at 129°C does not affect the yields of hydrocarbons, CO₂ and H₂O. The yields of methanol and ethanol, on the other hand, increase to about ten times of the corresponding yields produced by simple irradiation of CO-H₂, while formaldehyde and acetaldehyde were not detected in the gaschromatogram. The increments for the yields of both alcohols are nearly the same as the amounts of formaldehyde and acetaldehyde, respectively, lost by reaction with the catalyst. When the temperature of the catalyst was increased to 250°C, the catalytic reactions of CO-H₂ to produce hydrocarbons become predominant and no oxygenates are detectable.

Experiments with Method 2 gave results similar to those with Method 1, except that hydrogenation of acetaldehyde does not occur when the flow rate of the irradiated gas is as high as 350 ml/min. Accordingly, evidence was not obtained in the experimental conditions with Method 2 for surface reaction involving active species in the irradiated gas. The occurrence of catalytic hydrogenation found in the present study, however, seems a quite important information for analysis of radiation effects of CO-H₂ mixtures in the presence of Fe-Cu-KG catalyst where the surface reaction of the irradiated gas certainly

occurs more or less. (S. Nagai, H. Arai, K. Matsuda, M. Hatada)

- 1) S. Nagai, K. Matsuda and M. Hatada, JAERI-M 7355, 16 (1977).

4. Reaction in the Presence of Fluidized Bed Catalyst

In the studies on radiation chemical reactions in the presence of fixed bed catalyst, one of the most serious problems encountered was inhomogeneous temperature rise of the catalyst caused by electron beam irradiation. This is expected to be solved by use of a fluidized bed catalytic reactor, in which the distribution of temperature of the bed is more uniform.

In order to operate the fluidized bed catalytic reactor, gas velocity required for minimum fluidization, u_{mf} , and heat transfer coefficient between solid and wall, h_{ws} , should be known for various combinations of solid and gas expected in the experiments. Since many equations have been proposed to describe the relations between the properties of gas and solids and u_{mf} and h_{ws} ¹⁾, we tested these relationships with experiment carried out either on the fluidized bed reactor or on an equivalent substitute made of plastic (fluidized tester) to see which equation fits best to our apparatus.

The u_{mf} for small particles having small density, ρ_s , and small diameter, d_p , is calculated by the following equation:

$$u_{mf} = \frac{(\phi_s d_p)^2}{150} \cdot \frac{\rho_s - \rho_g}{\mu} \cdot g \cdot \frac{\epsilon_{mf}^3}{1 - \epsilon_{mf}} \quad (1)$$

where ϕ_s is a spheric factor for solid particle, ϵ_{mf} is a void fraction at minimum fluidization, and μ and ρ_g are viscosity and density of the gas, respectively.

Pressure drop across the bed and distributor is plotted against flow rate in Fig. 1 along with pressure drop across the distributor alone as an example; the experimental conditions are given in the caption to the figure. The difference

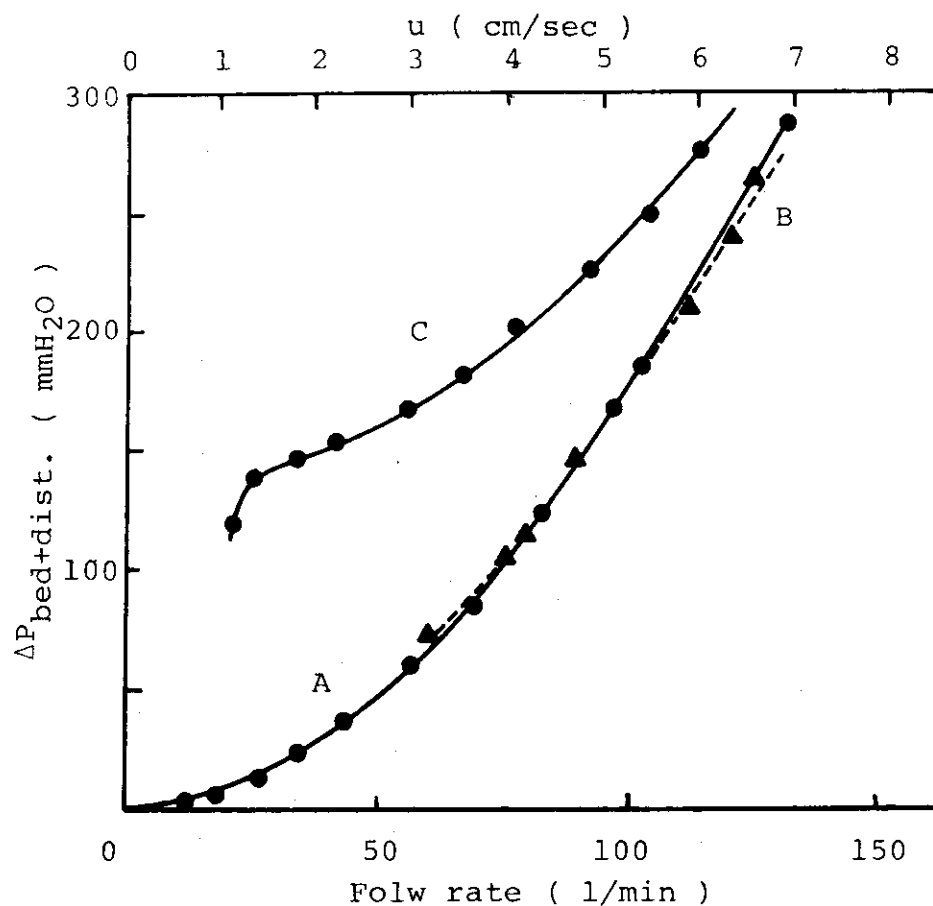


Fig. 1. Pressure drop vs. gas flow rate; curve A was obtained for air using a fluidization tester; curves B and C were obtained using the fluidizing catalytic bed reactor for air and nitrogen, respectively, with (B) or without (C) Al_2O_3 particles.

of the two curves gives net pressure drop across the bed, and the u_{mf} is calculated from the flow rate at which a knick point appears. The experimental results obtained under various conditions are compared with the calculated values in Table 1, in which qualitative agreements between the two are shown.

Absorbed electron energy in the fluidized bed is estimated from dose rate distribution in the reaction vessel measured by means of CTA film dosimeter. The dose rate distributions on

Table 1 Gas Velocity for Minimum Fluidization

Solid	d_p (μ)	Gas	u_{mf} calc (cm/sec)	u_{mf} obs (cm/sec)
Al ₂ O ₃	90	air	0.68	1.1
Al ₂ O ₃	90	N ₂	0.68	1.1
Al ₂ O ₃	90	H ₂ /CO(=3)	0.99	0.64
Fe/Cu/Al ₂ O ₃	90	H ₂ /CO(=3)	0.	2.1
Fe/Cu/Al ₂ O ₃	90	He	0.54	-
Fe/Cu/KG	297~420	N ₂	6.22	3.2
Fe/Cu/KG	150~250	N ₂	2.33	1.4
Fe/Cu/KG	150~250	H ₂ /CO(=3)	9.21	7.8
Fe/Cu/KG	<74	N ₂	0.14	0.15*

* by visual observation

Table 2 Temperature of Catalyst Bed

	h_{ws} (Kcal/m ² .hr.deg)	T_{bed} calc (°C)	T_{bed} obs (°C)	Q_i ($\frac{Kcal}{hr}$)
DOW-JACOB	439.3	78.9		
LEVENSPIEL-WALTON	152.1	171.4	200	1079.3
VAN HEERDEN	249.7	116.1		

Solid: Al₂O₃, d_p = 90 μ ; bed height, 23 cm; gas, H₂/CO = 3, 40 ℓ /min;
 electron accelerating voltage, 600 KeV; beam current, 5 mA; scanning width, 15 cm.

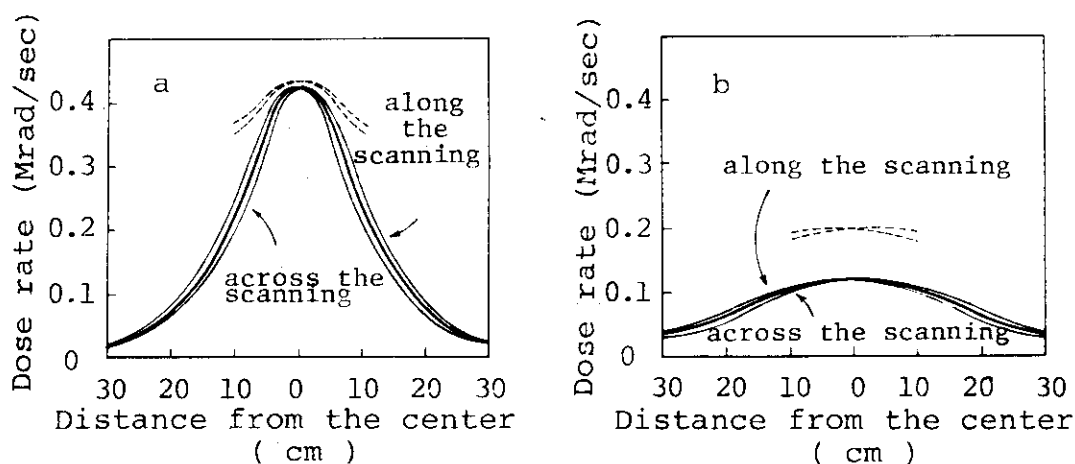


Fig. 2. Dose rate distribution under the irradiation window. Bed height, a) 23 cm and b) 3 cm; dotted lines, with wall; continuous lines, without wall; accelerating voltage, 600 KeV; beam current, 0.5 mA; scanning width, 15 cm.

the bed surface thus measured are shown in Fig. 2a and b for 23 cm and 3 cm bed heights, respectively. The heat input, Q_i estimated from the output energy from the accelerator (5 mA, 600 KeV), transmission efficiency along the beam path, directional scattering efficiency at the window and dose rate distribution is listed in Table 2.

The temperature of the catalyst bed, T_{bed} , can be calculated from the equations:

$$Q_{gs} = (T_{bed} - T_{gas}) \cdot u_0 \cdot \rho_g \cdot C_{pg} \quad (2)$$

$$Q_{ws} = (T_{bed} - T_{wall}) \cdot h_{ws} \cdot A \quad (3)$$

$$Q_i = Q_{gs} + Q_{ws} \quad (4)$$

where T_{gas} and T_{wall} are temperatures of gas and wall of the vessel, respectively, Q_{gs} and Q_{ws} are heat transferred between gas and solid, and that between wall and solid, respectively, h_{ws} is a heat transfer coefficient between wall and solid, A

is area of wall in contact with the solid, u_0 is a superficial velocity of the gas, ρ_g and C_{pg} are density and heat capacity of the gas, respectively. Approximate calculation demonstrates that the Q_{ws} is about eight times larger than Q_{gs} , and therefore, we neglect Q_{gs} in the calculation of T_{bed} . Several authors claim the equations to predict h_{ws} values from various parameters depending on properties of solid and gases

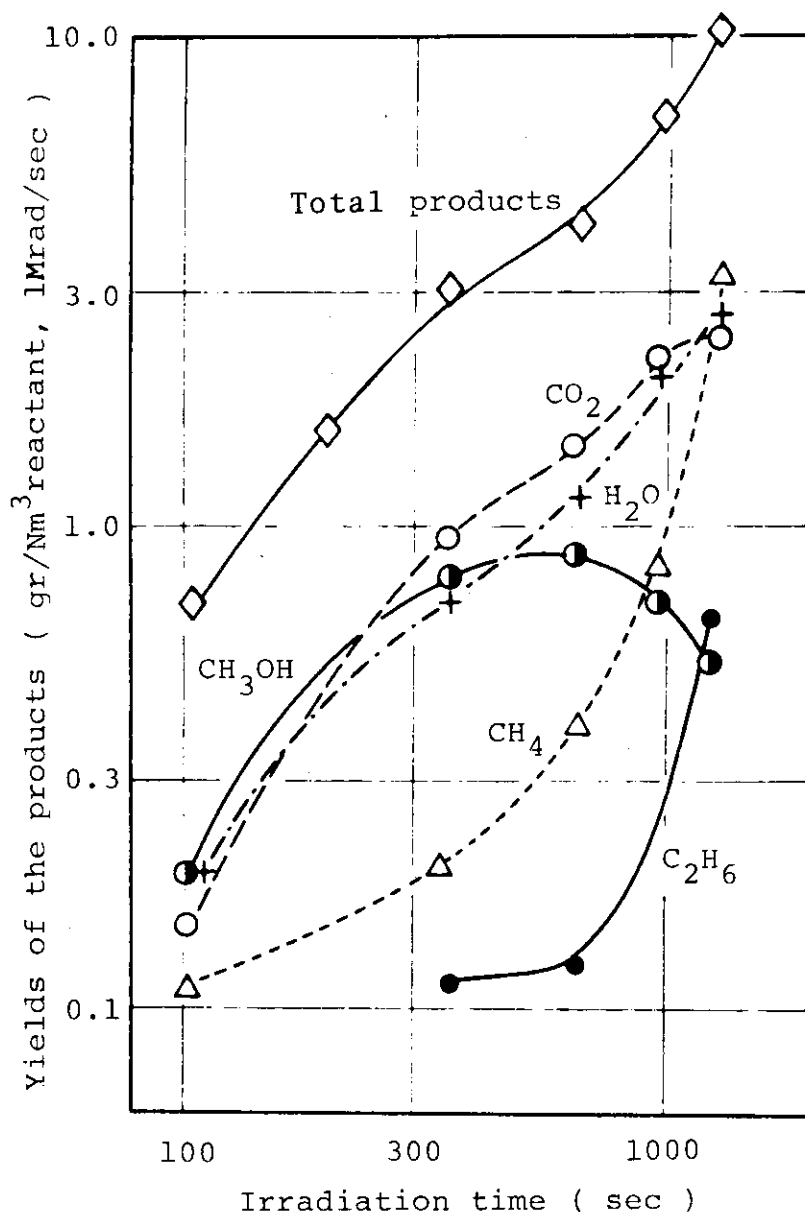


Fig. 3. Yields of the products vs. irradiation time.
Catalyst, Fe/Cu/KG = 4/1/5 by wt., 630 g;
Beam current, 7.5 mA.

involved. The comparison of experimental values with those calculated using h_{ws} (Table 2) indicates that Levenspiel-Walton's equation¹⁾ fits well to our data obtained with the fluidized bed catalytic reactor.

The analyses of the products are carried out using three gaschromatographs, gas samplers of which are connected in series to permit simultaneous analysis of broad spectrum of the products. A preliminary result obtained by 7.5 mA irradiation is given in Fig. 3 in which the amounts of the products produced in the system during irradiation are plotted against irradiation time. The other reaction conditions are given in the caption to the figure. Methanol was produced with sacrifice of formaldehyde as expected from the experimental results previously obtained using the fixed bed catalytic reactor, but considerable amount of water which was adsorbed on the catalyst makes the analysis of experimental results difficult. (K. Matsuda, S. Nagai, H. Arai, M. Hatada)

- 1) D. Kunii and O. Levenspiel, Fluidization Engineering, J. Wiley and Sons, 1969.

5. Radiation Effects on CO-H₂-N₂O Mixtures in the Presence of Magnesium Oxide

It has been reported recently¹⁾ that the dehydrogenation of some simple alkanes proceeds efficiently through the reaction with O⁻ ions adsorbed on magnesium oxide (MgO). Since alkanes are selectively produced by irradiation of CO-H₂ mixtures in the presence of an Fischer-Tropsch catalyst as reported previously²⁾, it was of interest to examine if the dehydrogenation of alkanes produced from CO-H₂ mixtures occurs to enhance the yields of olefins in the presence of MgO.

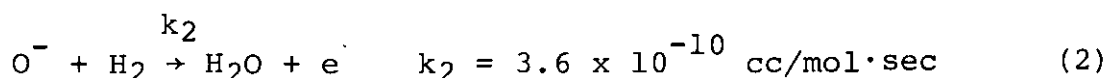
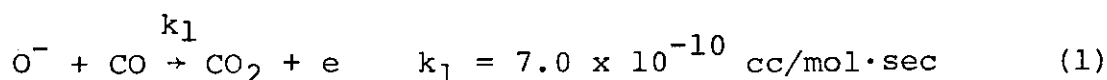
MgO was evacuated at 500°C for 8 hrs. A 1 : 6 mixture of CO in H₂ with or without 8.6% N₂O was irradiated with electron beams in the presence of 7 gr of the MgO. Product analysis

was made in the same manner as reported previously³⁾. For comparison purpose, effect of N₂O was studied on the radiolysis of the CO-H₂ mixture in the absence of MgO.

Table 1 compares the yields of the products in the presence of MgO with those in the absence of MgO. The products detected in the presence of MgO were low-molecular hydrocarbons, CO₂ and H₂O, but no oxygenates. The yield of H₂O in the presence of MgO was not determined.

As seen in Table 1, the addition of N₂O greatly enhances the yield of CO₂ while it depresses the yields of alkanes. In addition, the yields of ethylene and propylene are increased to appreciable amounts. It may also be seen that thermal reaction of the CO-H₂ mixture over MgO almost exclusively produces CO₂.

It is known that O⁻ ions react with CO and H₂ according to reactions (1) and (2),



where the rate constants are those reported in gas phase⁴⁾. If we assume that all the O⁻ ions formed from N₂O disappear through the reactions (1) and (2), the increment for the CO₂ yield by the N₂O addition is estimated to be 0.37 moles/m³-reactant in close agreement with 0.35 moles/m³-reactant observed. Aika et al¹⁾ have shown that C₂- and C₃-alkanes and alkenes adsorbed on MgO desorb completely at 150°C while adsorbed methanol and ethanol decompose to hydrocarbons and CO. Accordingly, our failure to detect oxygenates is ascribed to their adsorption and decomposition on MgO.

The yields of ethylene and propylene are increased as expected, but their increment is fairly low compared with the decrement in the corresponding alkanes. This is probably because of the preferential reaction of the O⁻ ions with CO and H₂ as described above and hydrogenation of olefins, if formed by irradiation as observed in the reactions over the

Table 1 The Amounts of Products in gr/m³-reactant¹⁾

N ₂ O	ml/min %	0	0	6.6 8.6	0
Irrad.	Kev mA	600 5	600 5	600 5	0
Catalyst		—	MgO	MgO	MgO
Temp.	(°C)	170	230	230	250
CH ₄		0.174	1.753	1.409	0.113
C ₂ H ₄		<0.001	0.002	0.005	0.020
C ₂ H ₆		0.038	0.787	0.587	0.020
C ₃ H ₆		<0.001	<0.001	0.001	0.016
C ₃ H ₈		0.031	0.101	0.064	0.005
HCHO		0.237			
CH ₃ OH		0.031			
CH ₃ CHO		0.039		<0.004	
HCOOCH ₃		0.029			
C ₂ H ₅ OH+C ₄ H ₁₀		0.023			
CO ₂		1.260	2.888	18.375	2.363
H ₂ O		2.715	—	—	—
Conv. of N ₂ O (%)		—	—	39.4	—

1) Reactor: Fixcat-II; Flow rate: H₂ 60 ml/min, CO 10 ml/min;

MgO: 7 gr.

Table 2 Effects of N₂O on the Amounts of Products (gr/m³-reactant)¹⁾

N ₂ O	ml/min %	0.00	0.66	3.7	7.2
		0.00	0.93	5.0	9.3
Temp. (°C)		170	170	170	170
CH ₄		0.174	0.153	0.093	0.060
C ₂ H ₄		<0.001	<0.001	<0.001	<0.001
C ₂ H ₆		0.038	0.021	0.008	0.002
C ₃ H ₆		<0.001	0.001	0.002	0.002
C ₃ H ₈		0.031	0.012	0.003	0.002
HCHO		0.237	0.004	0.017	0.006
CH ₃ OH		0.031	0.044	0.025	0.013
CH ₃ CHO		0.039	0.041	0.023	0.010
HCOOCH ₃		0.029	0.013	0.003	0.001
C ₂ H ₅ OH+C ₄ H ₁₀		0.023	0.017	0.006	0.002
CO ₂		1.260	1.706	3.281	4.725
H ₂ O		2.715	4.542	8.660	11.381
Conv. of N ₂ O (%)	—	—	11.2	10.4	8.2

1) Reactor: Fixcat-II; Flow rates: H₂ 60 ml/min, CO 10 ml/min;

Irradiation: 600 Kev, 5 mA.

Fe-Cu-KG catalyst²⁾. Therefore, it seems not possible to selectively get olefins in the method employed in the present study.

Table 2 summarizes the effects of N₂O on the radiolysis of the CO-H₂ mixture in the absence of solid catalyst. The most prominent effect observed is the increase in the yields of CO₂ and H₂O. With increasing N₂O content, the yields of alkanes decrease while those of ethylene and propylene increase. The oxygenates decrease in their yields as increasing N₂O content. Included in Table 2 is the conversion of N₂O obtained by GC analysis. The conversion due to direct radiolysis of N₂O estimated by the stopping power ratios of CO, H₂ and N₂O, adsorbed dose rate, and G (-N₂O) is at most 3.8% for 9.3% mixture of N₂O in the CO-H₂, so that the decomposition of N₂O in the radiolysis of CO-H₂-N₂O mixtures may occur predominantly through dissociative attachment of electrons produced from the CO-H₂ to produce O⁻ ions.

The increase of the yields of CO₂ and H₂O is similarly explainable as that over MgO. The yields of alkanes decrease in the order of CH₄<C₂H₆<C₃H₈ with the N₂O addition. This trend agrees well with the relative reactivity of alkanes toward O⁻⁵⁾. The increment of ethylene and propylene is, however, too low to explain the decrease in the yields of alkanes, and the decrease in the yields of alkanes would result not from the reaction with O⁻ but from some inhibition effect of N₂O on the formation of alkanes.

The decrement in the yield of methanol is low as compared to that of formaldehyde, which may suggest that methanol is not necessarily produced from formaldehyde. (S. Nagai, H. Arai, K. Matsuda, M. Hatada)

- 1) K. Aika and J.H. Lunsford, J. Phys. Chem., 81, (1977).
- 2) M. Hatada and K. Matsuda, JAERI-M 6702, 11 (1976).
- 3) K. Matsuda, S. Nagai, H. Arai and M. Hatada, JAERI-M 7355, 11 (1977).
- 4) T.O. Tiernan, "Interaction between Ions and Molecules," Ed. by P. Ausloos, P353, Plenum Press, New York and London (1975).

- 5) D.K. Bohme and F.C. Fehsenfeld, Can. J. Chem., 47, 2717 (1969).

6. Radiation Chemical Reaction of Methane in a Flow System

Among the various products from gaseous mixtures of carbon monoxide and hydrogen, we focused our attention to hydrocarbons, especially to lower olefins, because these compounds which are obtained in large quantity from petroleum resource are difficult to be synthesized from simple gases considered as a resource of raw materials for future chemical industry. Hydrocarbons can be synthesized from carbon monoxide and hydrogen by catalytic reactions, but methane is more preferable than this to produce because the reaction of methane is far simpler than that of carbon monoxide and hydrogen.

As an extension of the program of radiation chemical reaction of carbon monoxide and hydrogen, we initiated the present study to accumulate fundamental data on the radiation chemical reactions of methane under various reaction conditions, so that the experimental data will help us to know whether the radiation chemical reaction of methane is promising for the purpose.

Takachiho "Research" grade CH_4 (99.95 mole % minimum) was used without further purification. Irradiation of CH_4 was carried out using electron beams from the HDRA (0.6 MeV, 0.01~10 mA) with the flow reactor, FXCAT-II¹⁾ which has been used for irradiation of CO/H_2 mixtures. The irradiated gas from the reactor was analyzed by two gaschromatograph (Yanagimoto G 80 equipped with 3 m Porapak Q columns and Shimadzu GC 7A with 5 m VZ-7 columns). Absorbed electron energy in the reactant gas flow was determined as described previously¹⁾.

Fig. 1 shows the dependences of yields of the products on the residence time at the beam current of 0.5 mA. The yields of H_2 and saturated hydrocarbons increase linearly with increasing residence time. Similar results were obtained at 10 mA. On the other hand, the yields of unsaturated hydrocarbon level off for prolonged irradiation.

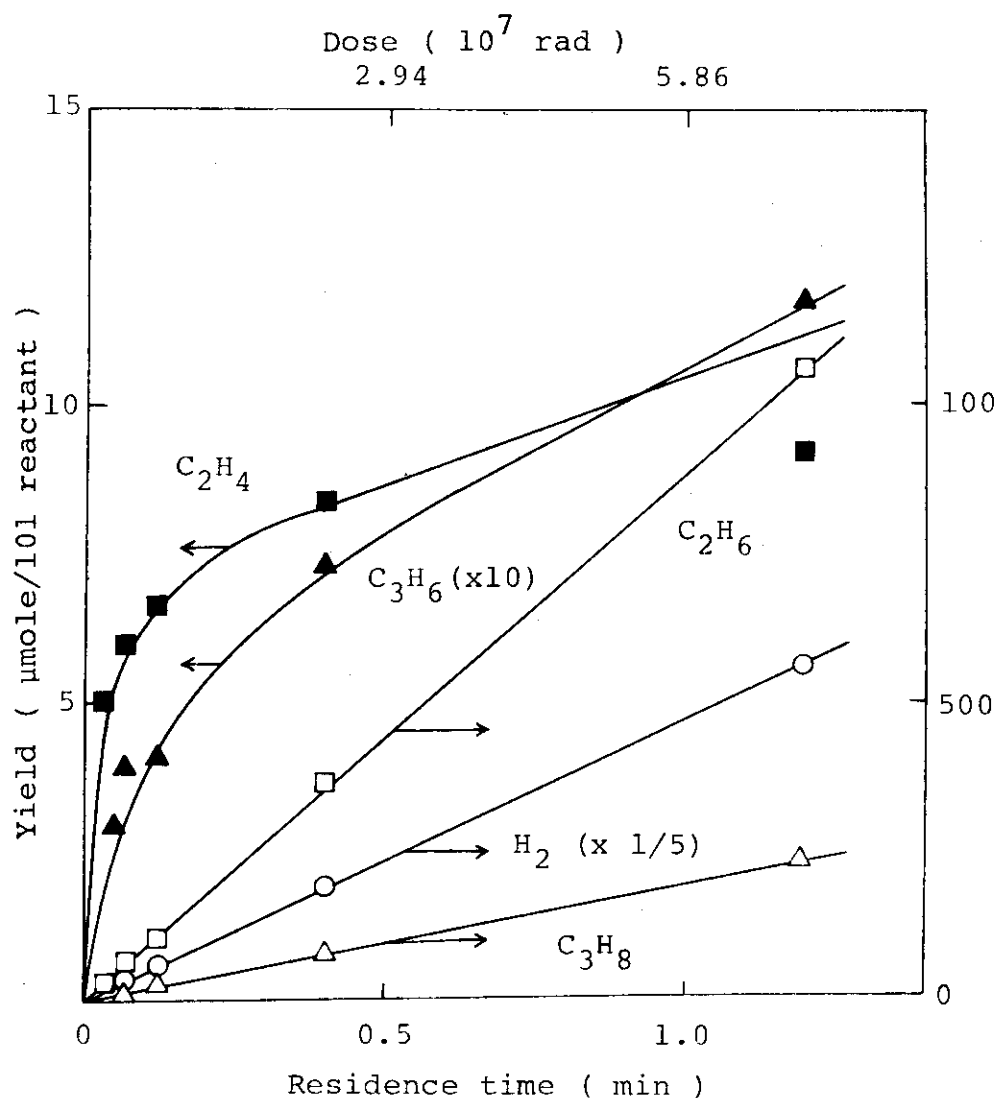


Fig. 1 Yields of the products vs. residence time.
Beam current, 0.5 mA; Dose rate, 0.77×10^5 rad/sec.

Fig. 2 shows the beam current effect on G values of the products at the flow rate of 100 ml/min. The G values of H_2 , C_2H_6 , and C_5H_{12} are little affected, while those of C_3H_8 , n- C_4H_{10} , and unsaturated hydrocarbons decrease with increasing beam current beyond 1 mA. The G value of iso- C_4H_{10} increases with increasing beam current. The temperature of the reactor was about 57°C at the beam current of 1 mA, 210°C at 5 mA, and 350°C at 10 mA, respectively; it was almost room temperature

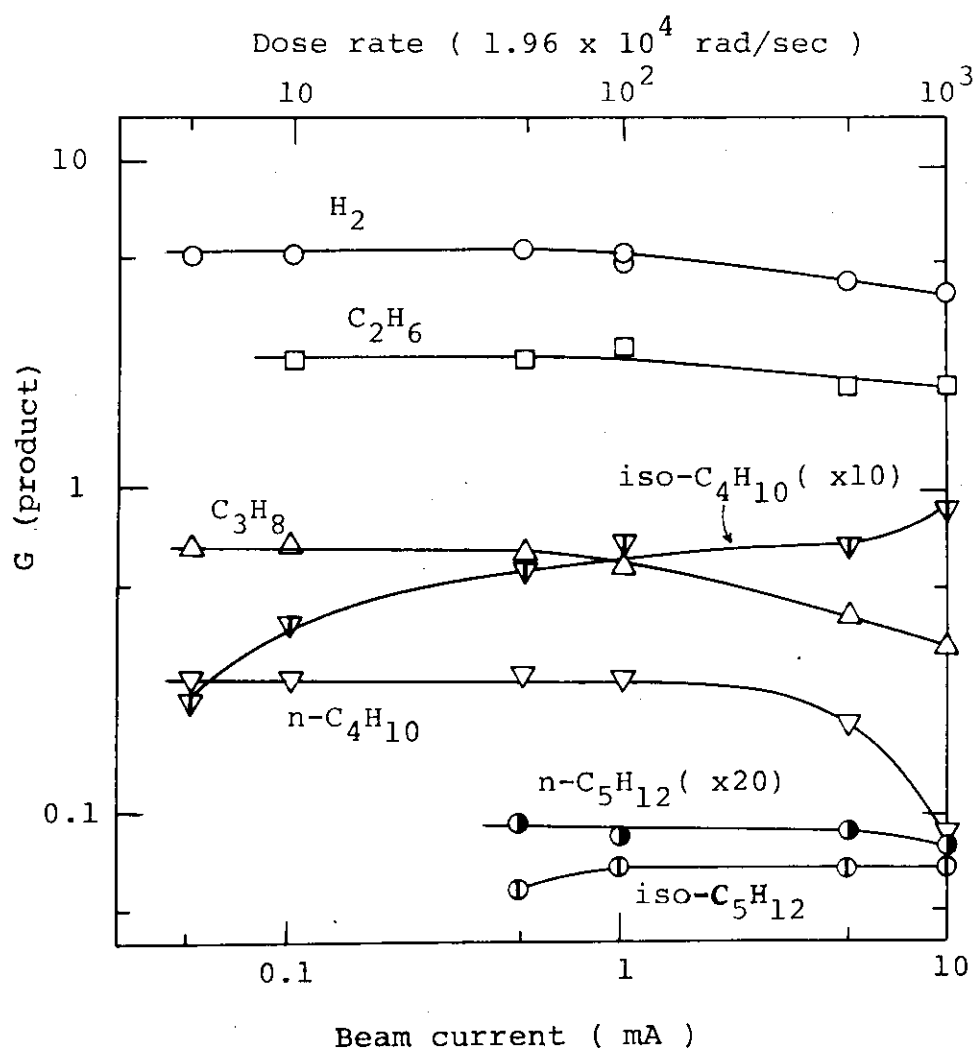


Fig. 2 G values of the products vs. beam current.
Flow rate, 100 ml/min.

below 0.5 mA. Therefore, the effect of the beam current on the G values found in the experiment may be understood as somewhat combined effect of the beam current and temperature.

To examine the effect of the reactor wall temperature, irradiation was carried out using the reactor kept at different temperatures by electric heater at the beam current of 0.5 mA. The results are shown in Figs. 3 and 4. The G values of H_2 , C_2 and C_3 saturated hydrocarbons scarcely vary with the temperature while those of higher paraffins except for $iso-C_4H_{10}$ decrease at higher temperature. The G value of $iso-C_4H_{10}$

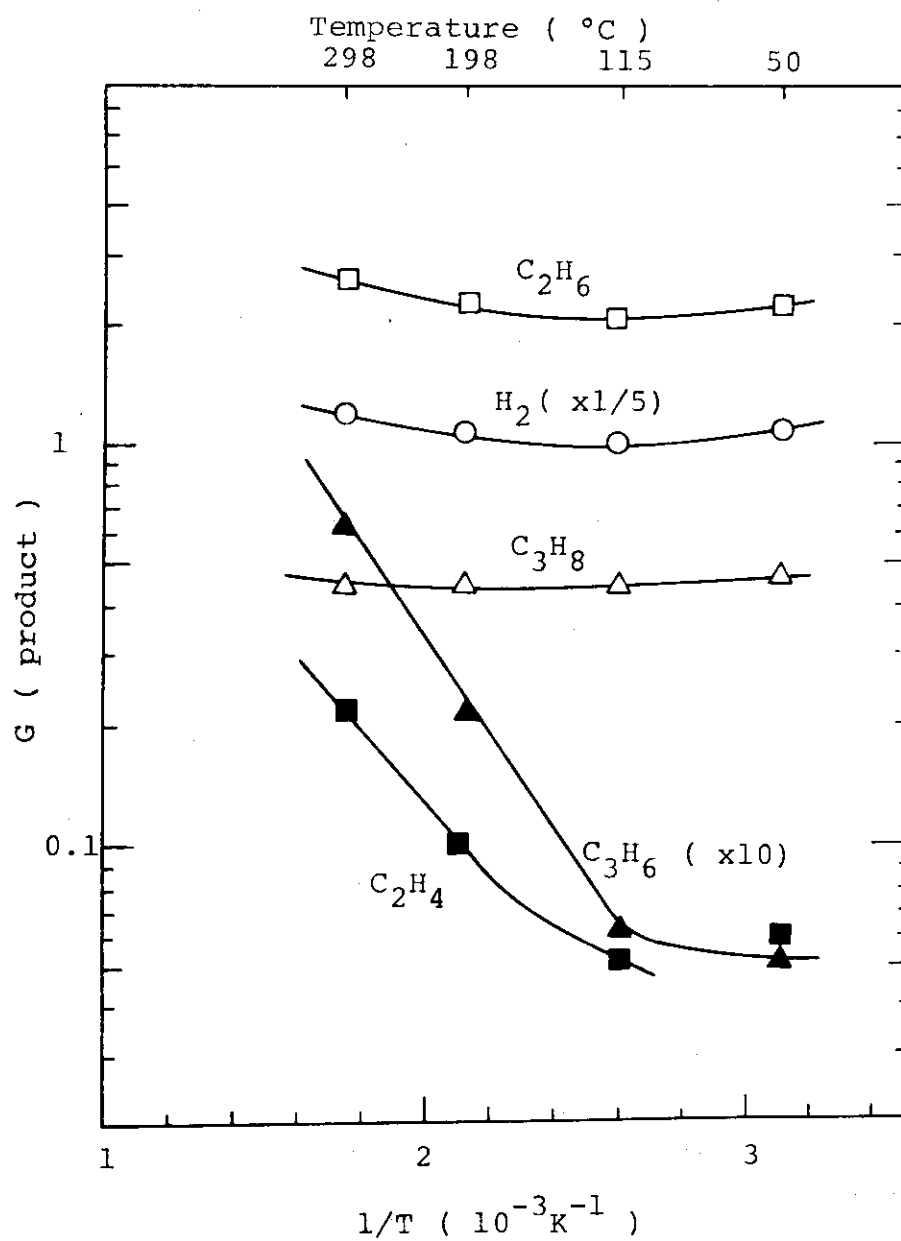


Fig. 3 G values of the products vs. $1/T$.
Beam current, 0.5 mA; Flow rate, 30 ml/min.

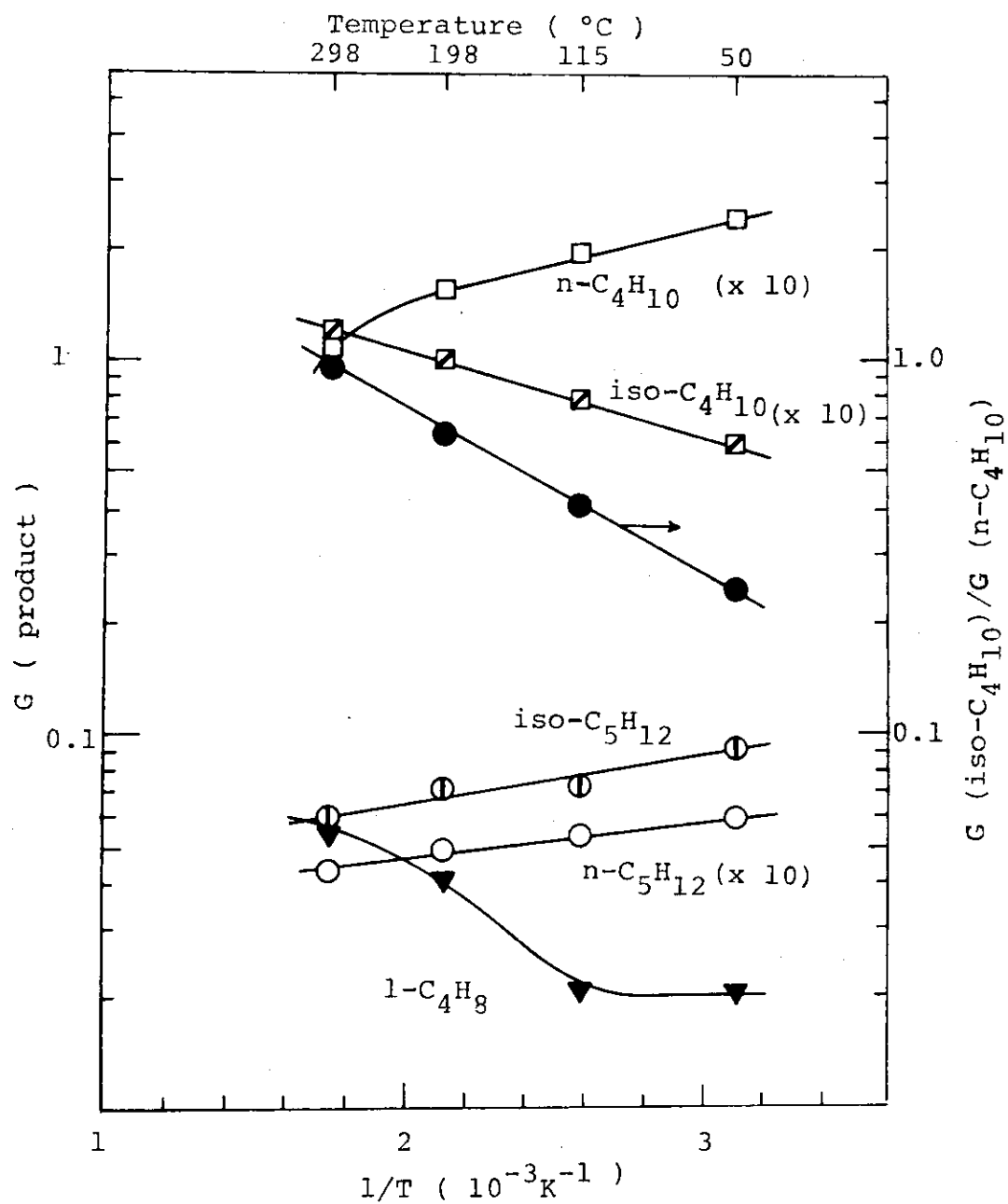


Fig. 4 G values of the products vs. $1/T$.

Beam current, 0.5 mA; Flow rate, 30 ml/min.

increases largely with increasing temperature. This fact may indicate that some of iso-C₄H₁₀ observed at 10 mA in Fig. 2 are from thermochemical reactions. On the other hand, the G values of olefins increase with increasing temperature. The details of this result are examined at present. (H. Arai, S. Nagai, K. Matsuda, M. Hatada)

- 1) K. Matsuda, S. Nagai, H. Arai, and M. Hatada, JAERI-M 7355, 11 (1977).

7. Spin Trapping of Radicals Produced by Irradiation of Gaseous Mixtures of CO and H₂

In the last annual report¹⁾, it was reported that H atoms and methyl radicals (CH₃) produced by irradiation of a CO-H₂ mixture were successfully detected by the spin trapping technique. A similar experiment was carried out with a mixture of CO and D₂, in which D atoms and CD₃ radicals were detected, thus confirming the previous finding. These results were already described in detail elsewhere²⁾. (S. Nagai, K. Matsuda, M. Hatada)

- 1) S. Nagai, K. Matsuda and M. Hatada, JAERI-M 7355, 21 (1977).
- 2) S. Nagai, K. Matsuda and M. Hatada, J. Phys. Chem., 82, 322 (1978).

[2] Polymerization of Vinyl Monomers by High Dose Rate
Electron Beams

1. Polymerization of Styrene up to Higher Conversion by High
Dose Rate Electron Beams

Polymerization of moderately dried styrene (water content 3.2×10^{-3} mole/l) is carried out up to higher conversion such as 90%. The dose rate of the electron beams is between 6×10^5 and 6×10^6 rad/sec, so that more than 90% of the product is consisted, at least at the initial stage of the polymerization, of ionic polymers.¹⁾ Not only the determination of the rate of polymerization but also that of molecular weight distribution by GPC is carried out.

Table 1 shows three typical results of the experiments.

Table 1 Polymerization of Moderately Dried Styrene
up to Higher Conversion

Dose rate, 6.0×10^5 rad/sec				
Time, sec	20	100	200	
Conv., %	12.5	64.6	90.7	
$R_p \times 10^2$ mole/l/sec	5.45	5.64	3.96	
$M \times 10^{-4}$	4.7	3.0	3.0	
Dose rate, 1.2×10^6 rad/sec				
Time, sec	20	60		
Conv., %	43.1	90.2		
$R_p \times 10$, mole/l/sec	1.87	1.31		
$M \times 10^{-4}$	3.9	2.9		
Dose rate, 6.0×10^6 rad/sec				
Time, sec	5	12	20	
Conv., %	27.4	38.8	51.3	
$R_p \times 10$, mole/l/sec	4.77	2.81	2.23	
$M \times 10^{-4}$	2.9	2.4	2.3	

It is clearly seen from the table that both the rate of polymerization and molecular weight decrease with increasing conversion.

The time-conversion curves are shown in Fig. 1. They may

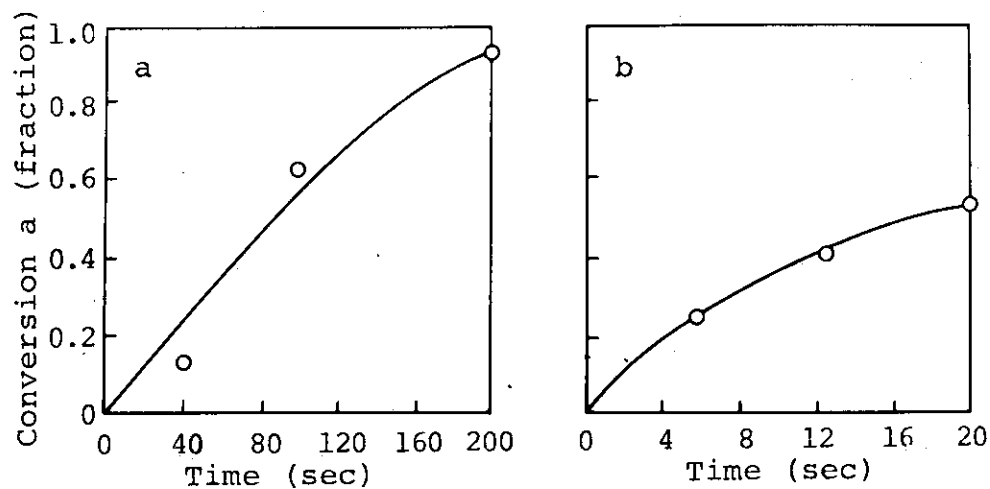


Fig. 1 Time conversion curves for the polymerization of styrene.
Dose rate: a, 6.0×10^5 rad/sec; b, 6.0×10^6 rad/sec.

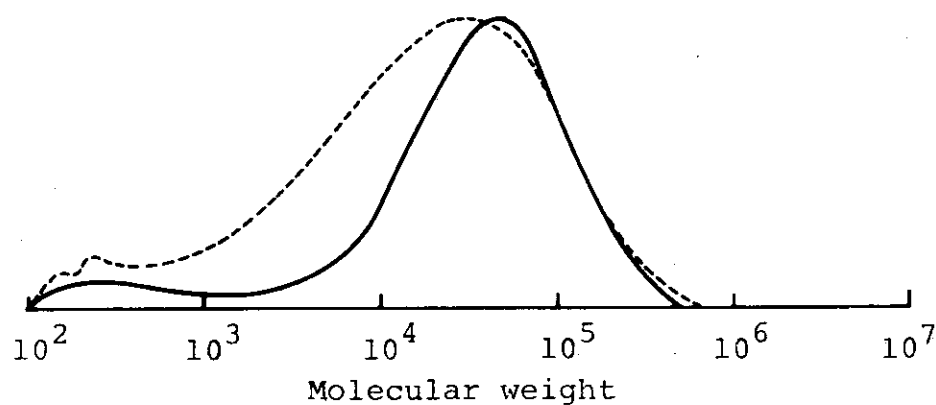


Fig. 2 Molecular weight distribution curves of polystyrene obtained by polymerization of styrene at a dose rate of 6.0×10^5 rad/sec.

	Irradiation time	Conversion
—	20 sec	12.5%
----	200 sec	90.7%

be regarded to be smooth though the number of the experimental points are rather too small. Molecular weight distribution curves by GPC are shown in Fig. 2 and Fig. 3. The curves of each series have similar shapes. They have one prominent peak of cationic polymers and small peaks of oligomers. Detailed observation of the curves indicates that the curves become broader in the direction of the lower molecular weight with increasing conversion, whereas the shapes at the higher molecular side remain almost unchanged.

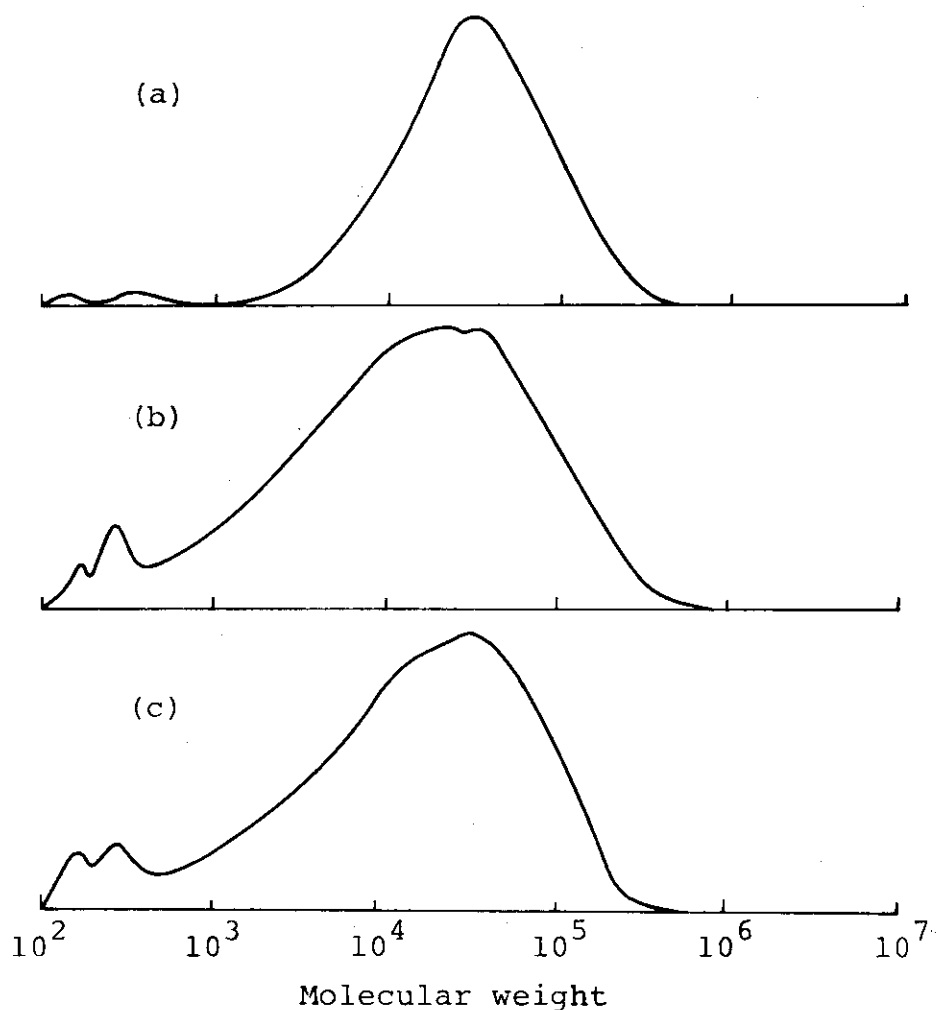


Fig. 3 GPC curves of polystyrene from moderately dried styrene at a dose rate of 6×10^6 rad/sec.

	Dose (Mrad)	Conversion (%)
a	30	27.4
b	72	38.8
c	120	51.3

The experimental results will be discussed briefly. The following two equations were theoretically deduced for the rate of cationic polymerization R_i of styrene and average degree of polymerization of cationic polymers \overline{DP}_i ,

$$R_i = \frac{k_{pi}}{k_{tx}} \frac{10G_i d \phi}{N} \frac{[M]}{[H_2O]} I \quad (1)$$

$$\frac{1}{\overline{DP}_i} = \frac{k_{tm}}{k_{pi}} + \frac{k_{tx}}{k_{pi}} \frac{[H_2O]}{[M]} \quad (2)$$

where, k_{pi} , k_{tm} and k_{tx} are rate constants of propagation, monomer transfer and termination with water molecule respectively. G_i , d , ϕ and N are G value for the initiating ion formation, density of styrene, numerical factor for normalizing radiation energy, and Avogadro's number. Further, $[M]$ and $[H_2O]$ are concentrations of monomer and water respectively and I is dose rate.

Applicability of the equations was shown for the initial stage of bulk polymerization of styrene in a wide range of dose rate and water content. For the purpose of employing these equations to the polymerization up to higher conversion it is assumed that all constants in the equation remain almost constant independent of the conversion. Then it is necessary to take into account the change of I , $[M]$ and $[H_2O]$. The values of I and $[M]$ are known. The question is the change of $[H_2O]$.

There is no question that the growing cationic chains terminate by interaction with water molecules; the mechanism of the termination reaction, however, has not yet been elucidated. The simplest assumption is that water molecule is consumed by the reaction. There is also possibility that the terminating activity is not lost by the termination reaction.

Equations (1) and (2) predict that R_i and \overline{DP}_i decrease with increasing conversion because $[M]$ decreases. The experimental results are in good agreement with the prediction. On the other hand, if water is consumed by the termination reaction, equation (2) predicts that smaller water content results in higher \overline{DP}_i . According to a trial calculation,

number of polymer molecules which are formed at 100% conversion by the termination reaction with water is, in the order of magnitude, the same as the water contained in the system; if it is assumed, therefore, that one water molecule is lost by one termination reaction, some indication of the effect to increase molecular weight with conversion is expected.

To detect the effect, $\log(1-a)$ vs. time curves are drawn, where a is the fraction of the polymer. The curves shown in Fig. 4 are straight lines, which means that the polymerization proceeds according to the monomolecular equation. This is in agreement with equation (1), when $[H_2O]$ does not change with conversion.

A simple explanation is that water is reproduced after the termination reaction. Another possibility is that OH

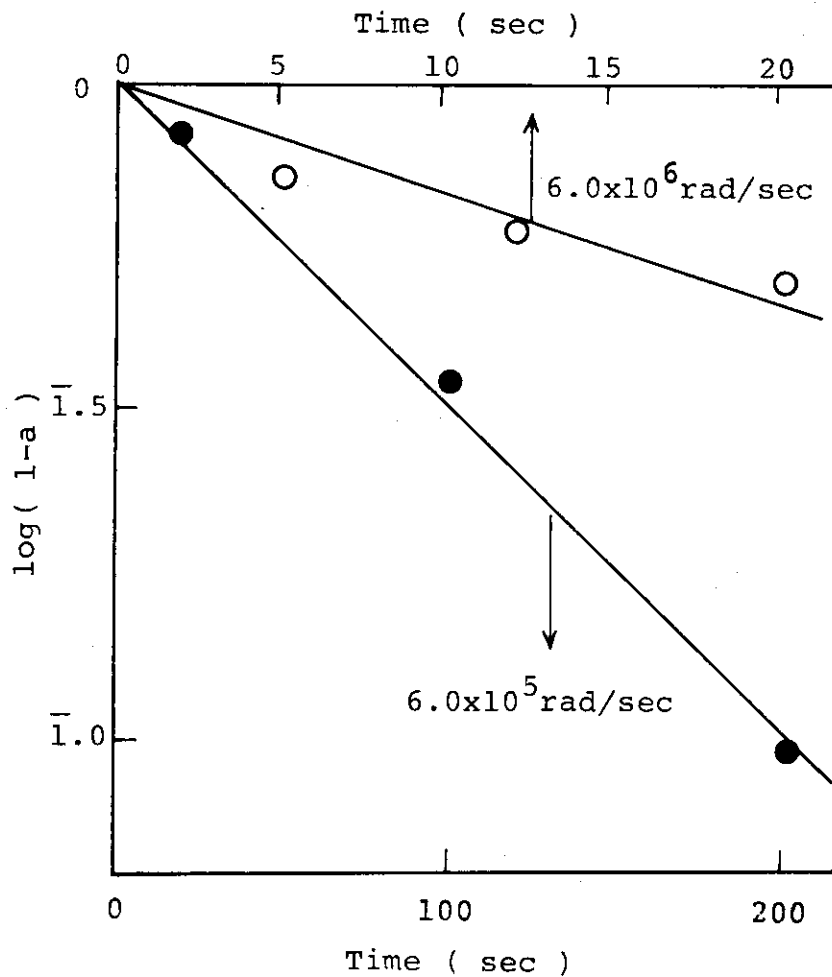


Fig. 4 Change of $\log(1-a)$ with time

group of H_2O is bound by the termination to the growing cationic chain end to form alcohol. That low molecular alcohol exhibits almost the same chain terminating effect as water is shown in Table 2.

Table 2 Comparison of Water and Methanol
as Terminating Agents

Additive*	conc. mole/l	conv. %	polmztn rate $R \times 10^3$ mole/l/sec
None	—	—	13
Water**	3.5×10^{-2}	5.15	1.5
Methanol	3.7×10^2	3.25	0.95

* Additive to m.d. styrene $[H_2O] = 3.2 \times 10^{-3}$ mole/l

** Water saturated styrene

Experiments are being continued to elucidate the mechanism to account for the reaction that water is not apparently consumed by the termination. (I. Sakurada, J. Takezaki, T. Okada)

- 1) I. Sakurada, T. Okada, Ka. Hayashi, J. Takezaki, JAERI-M 7355, 28 (1977); J. Takezaki, T. Okada, I. Sakurada, J. Appl. Polym. Sci., 21, 2683 (1977).

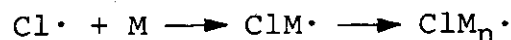
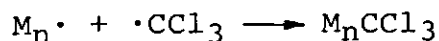
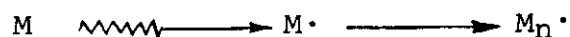
2. Radiation Polymerization of Styrene/Carbontetrachloride Mixture in a Wide Range of Dose Rate

The main subject of the experiment on the radiation polymerization of styrene/carbontetrachloride mixture is to see the effect of carbontetrachloride on the radical and cationic polymerization of styrene.

In the case of the radiation induced reaction of a binary mixture, there is some experimental difficulty to carry out a series of experiments of different styrene-carbontetrachloride

ratio at the same dose of the absorption energy of radiation. Therefore, for convenience sake, irradiation of a series of mixtures is carried out by a constant incident dose, and the absorbed dose for pure styrene in rad is used without correction also for the mixtures. This is more straight forward to the purpose, because general feature of the solution polymerization in halogenated hydrocarbons is a matter of interest in the present preliminary report.

In the case of radical polymerization, which is dominant in the region of low dose rate polymerization, it is expected that telomerization takes place. In the case of styrene/ CCl_4 , the typical reactions may be shown as follows:



G value for the radical formation of carbontetrachloride is reported to be one or two orders of magnitude greater than that for styrene; therefore, it is possible that the most part of radical polymers originates from solvent molecules in solvent rich systems. It is further probable that more or less similar reactions take place in the cationic polymerization also, and fragment of the solvent molecules are incorporated in the polymer.

Experiments in the present preliminary report were carried out with styrene/carbontetrachloride mixtures, whose styrene content was varied from 100 to 20 vol%; the range of dose rate was between 2.5 and 6.0×10^6 rad/sec. The irradiation was performed at room temperature, and the other details of the experiments are essentially the same as to the radiation

induced polymerization of bulk styrene in the previous reports¹⁾. Both styrene and carbontetrachloride were dried with calcium hydride, distilled and used for the experiments. Styrene dried in this manner contains about 2×10^{-2} mole/l H_2O .

The weight of polymers was determined not by the precipitation but by evaporation as previously. The conversion was calculated in weight percent of the polymer to the total initial weight of the reaction mixture as shown below.

$$\text{Conversion \%} = \frac{\text{wt. of polymer obtained}}{\text{wt. of initial reaction mixture}} \times 100 \quad (1)$$

It is unusual that carbontetrachloride, which does not polymerize in an usual sense, is treated as if it were monomer; this method of calculation is, however, natural and simple. If we calculate conversion based on the weight of styrene, we often find values, much larger than 100 as conversion percent. It seems, therefore, that more carbontetrachloride is incorporated in the polymer than expected under an assumption that carbontetrachloride plays only a role as a telogen in the polymerization of the present system. Due to the same reason, the rate of conversion or polymerization was expressed not in mole/l/sec but in g/l/sec.

Figure 1 shows time conversion curves for styrene/carbon-tetrachloride mixture of 20 vol% styrene content at three different dose rates. Curves appear to tend to level off at certain percents of conversion. The highest experimental conversion calculated by equation (1) are 17.9, 21.4 and 22.5% for the dose rates of 1.2×10^5 , 4.8×10^5 and 6.0×10^5 rad/sec, respectively. If only styrene is polymerized in the 20 vol% styrene solution, 100% styrene conversion is expected to give 12.5% conversion by equation (1). All experimental values of conversion are much higher than 12.5%, hence there is no doubt that an appreciable amount of carbontetrachloride is incorporated in the polymer.

The dose rate dependence of conversion rates of pure styrene and styrene/carbon-tetrachloride mixtures of 80 and 20

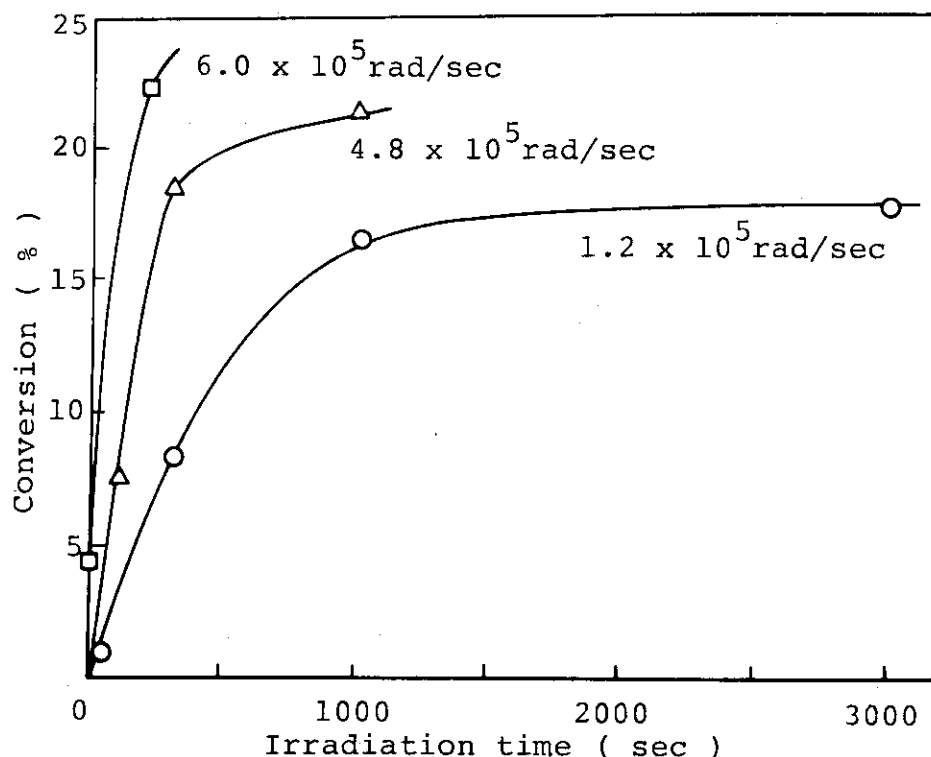


Fig. 1. Time conversion curve of styrene/carbontetrachloride of 20 vol% styrene content at various dose rates.

vol% styrene content are shown in Fig. 2. At a glance it is clear that the three curves for the widely different styrene concentrations have similar shapes and are located not so far from one another. Though the curves are drawn by a logarithmic scale and are insensible to small difference it is noteworthy that the curve for 80 vol% styrene is located in the low dose rate region about an order of magnitude higher than the pure styrene. It is further noteworthy that the difference of conversion rates between pure styrene and solution of 20 vol% styrene is very small.

Figure 3 shows mixture composition dependence of conversion rates at a dose rate of 6.0×10^5 (a) and 2.2×10^2 rad/sec (b). In this case also the rate of conversion is expressed in a logarithmic scale. It may be seen that both the curves are rather flat with nonprominent maxima. In curve b it is

noteworthy that the conversion rate becomes several times greater, when the styrene content of the mixture drops from 100 to 80 vol%. This corresponds to the observation of Fig. 2 that the 80 vol% styrene shows much higher conversion rate than pure styrene in the low dose rate region, and may be due to the much larger G-value of radical formation of carbon-tetrachloride than that of styrene. And further, it is well known, in the case of bulk polymerization of styrene, that the amount of radical polymers is dominant in the low dose rate region.

To obtain more details of the polymerization mechanism,

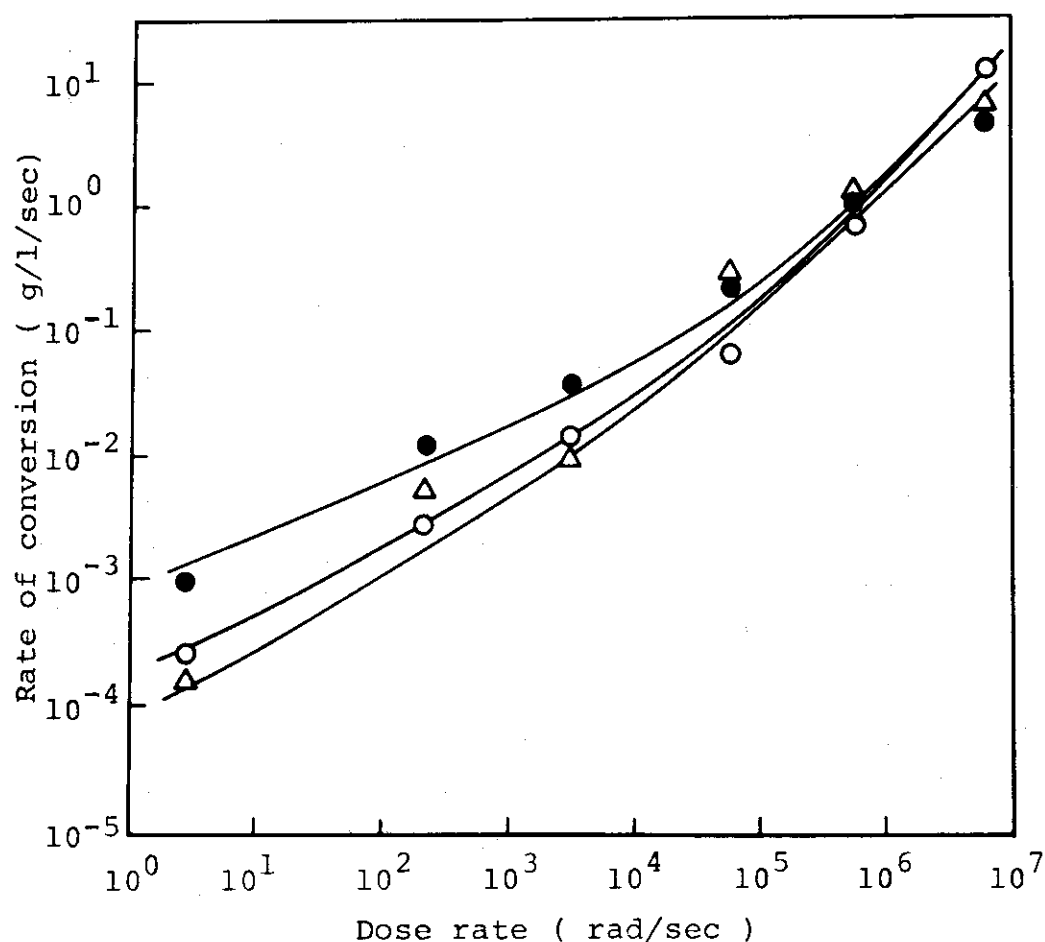


Fig. 2. Dose rate dependences of rate of total conversion in the polymerization of pure styrene (o) and styrene-carbon tetrachloride mixtures (•, 80 and Δ, 20 vol% styrene).

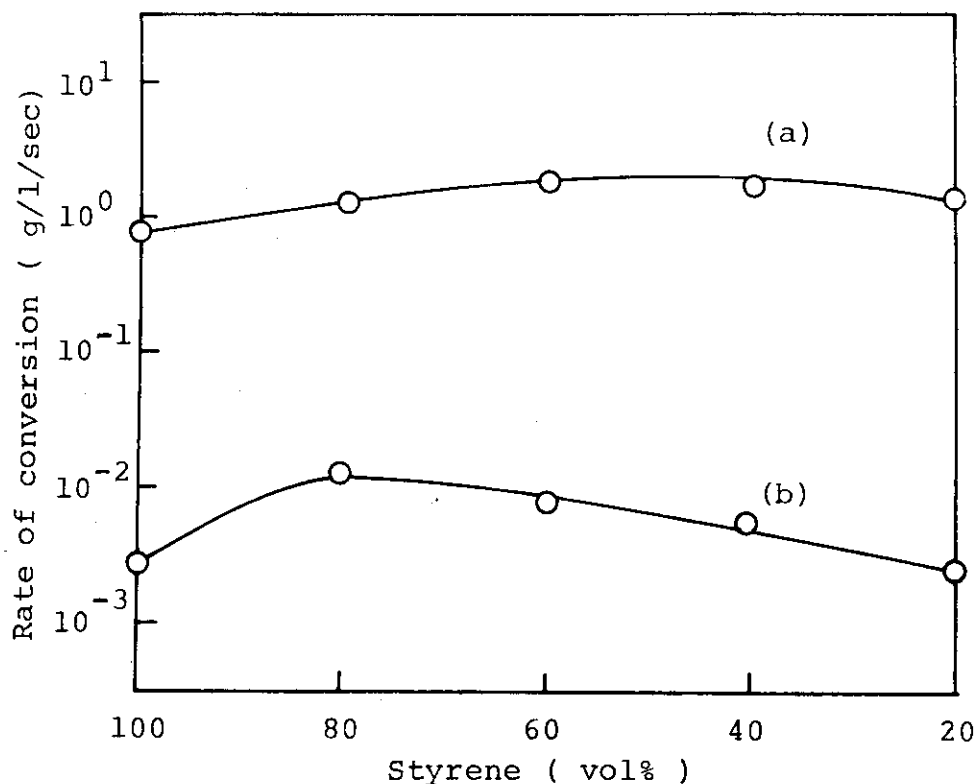


Fig. 3. Rate of total conversion of various styrene-carbontetrachloride mixtures at two different dose rates (a, 6.0×10^5 ; b, 2.2×10^2 rad/sec).

GPC analysis of the polymerization products was also carried out, and the typical curves are shown in Fig. 4 and 5 for the cases of radiation dose of 2.2×10^2 and 6.0×10^5 rad/sec. It may be not reasonable to use for such a product the same relation between molecular weight and elution volume as for pure polystyrene, but the same relation was employed for the calculation of the molecular weight of the products tentatively without correction.

As has already been shown in the previous report a GPC curve of polymerization product from the moderately dried styrene consists of three parts designated as fraction I, II and III. These fractions are oligomer, radical polymer and cationic polymer, respectively. As may be seen in Fig. 4 and 5 the GPC curves of the polymerization products of the mixtures may also be divided into the three fractions. Weight percent of the fractions at various styrene contents are shown in

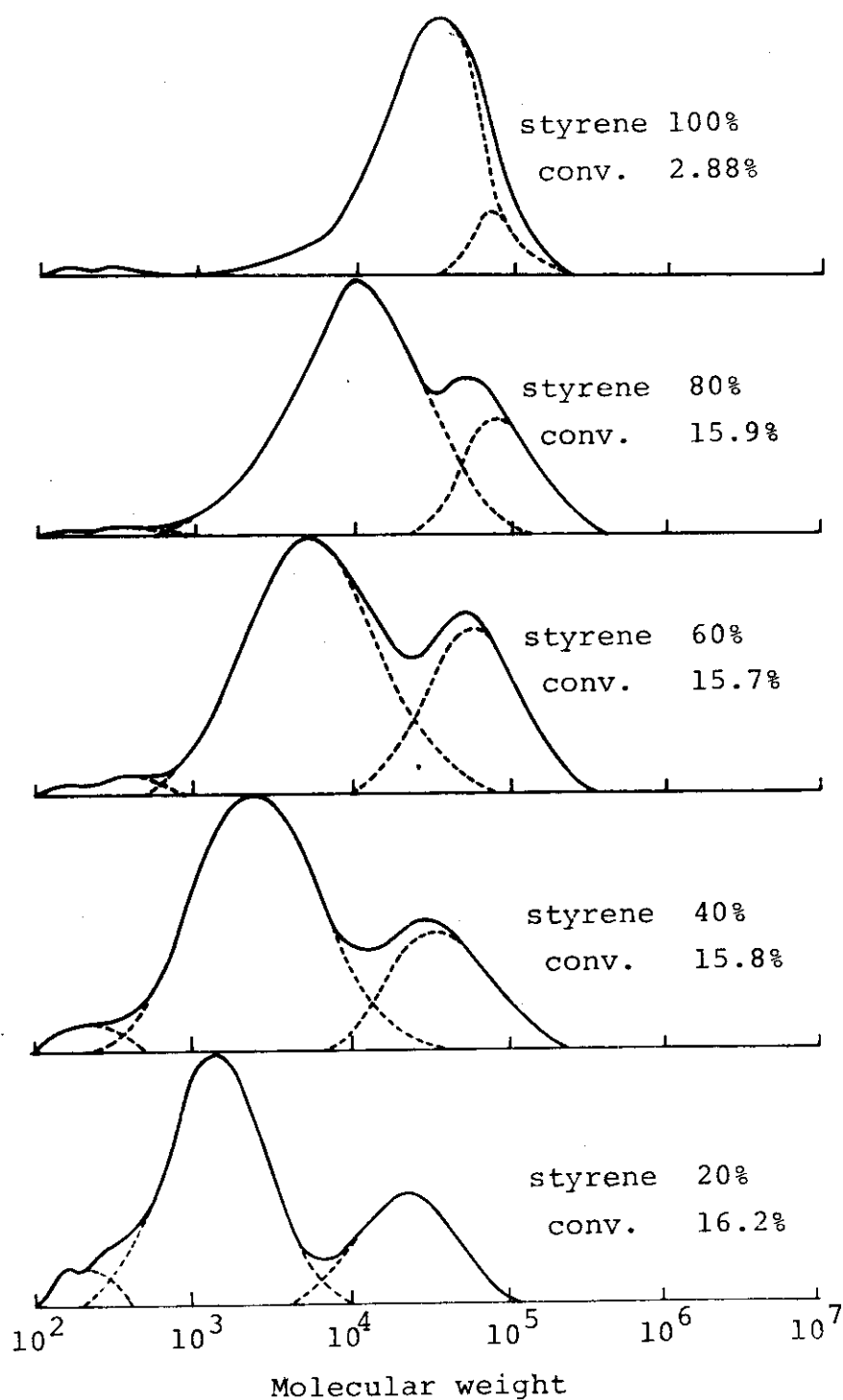


Fig. 4. Molecular weight distribution curves of polymerization product by GPC for styrene/carbon tetrachloride mixtures of various styrene contents at a dose rate 2.2×10^2 rad/sec.

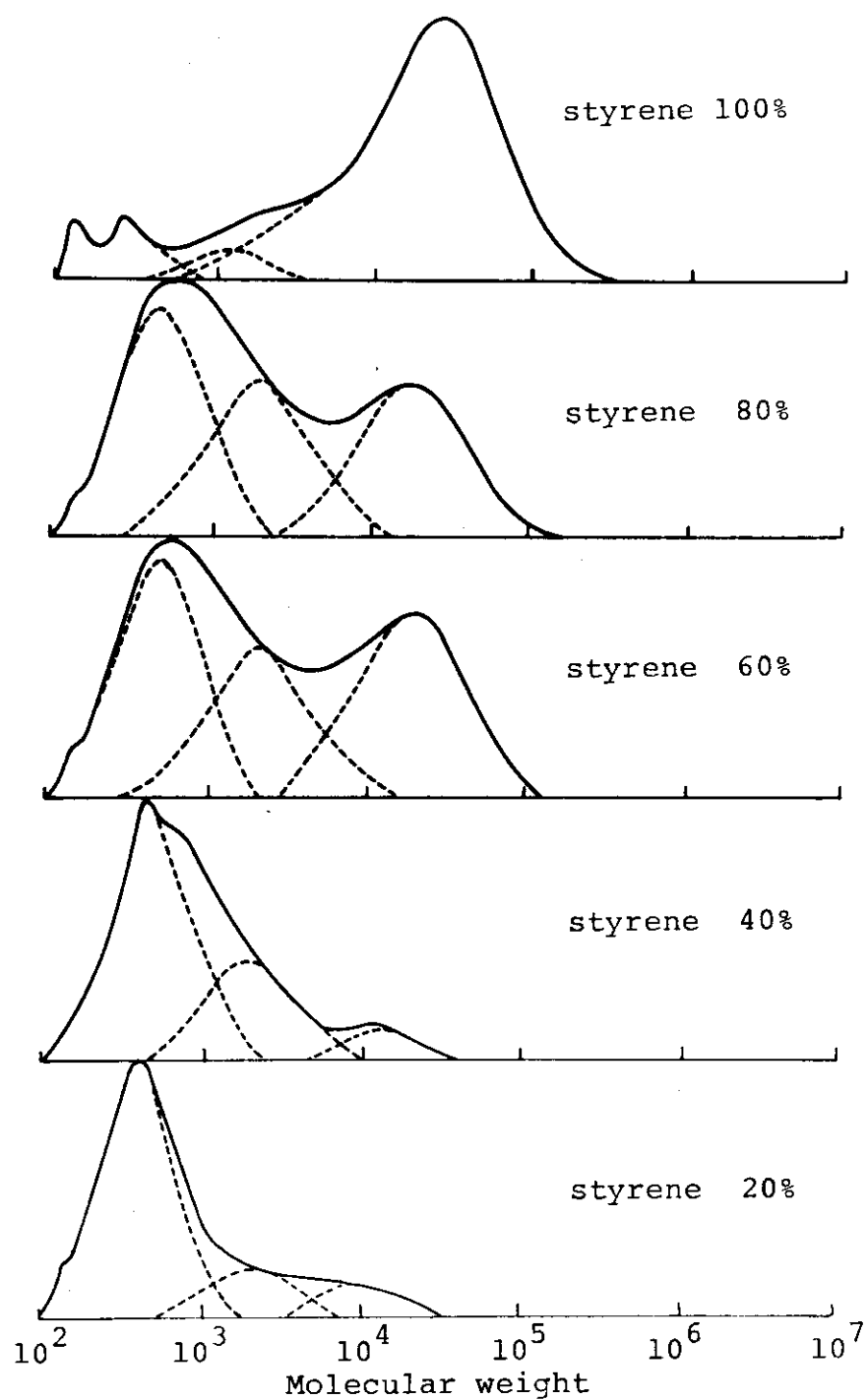


Fig. 5. Molecular weight distribution curves of polymerization product by GPC for styrene/carbon tetrachloride mixtures of various styrene contents at a dose rate 6.0×10^5 rad/sec.

Table 1.

Table 1 Weight percent of fractions I, II and III of polymerization product from styrene/carbontetrachloride mixtures of different styrene content.

Dose rate, 2.2×10^2 rad/sec						
Styrene cont. vol%		100	80	60	40	20
Fraction	I	1.0	2.3	2.6	3.6	5.1
"	II	82.9	75.6	65.4	69.8	66.9
"	III	16.1	22.1	32.0	26.6	28.0
Dose rate, 6.0×10^5 rad/sec						
Fraction	I	9.2	37.2	36.0	57.9	73.8
"	II	11.3	30.8	27.4	26.2	16.2
"	III	79.5	32.0	36.6	15.9	10.0

Though in the case of bulk polymerization there is no doubt that fractions II and III are radical and ionic polymers, because the results of GPC analysis agree with theoretical calculation, in the case of the polymerization of styrene/carbontetrachloride, however, it is more complicated especially when the styrene content is low or dose rate is high. Rates of conversion for the fractions I, II and III at two different dose rates of the mixtures of different styrene contents are shown in Fig. 6. All curves seem to be essentially flat, because in this case also a logarithmic scale was used; it may be seen, however, that the conversion rate increases enormously, except the case of fraction III at higher dose rate, with the drop of the styrene content from 100 to 80 vol%. The increase may be ascribed to the larger number of G-value of initiating radical formation of carbontetrachloride than styrene.

It is important from practical point of view that, with the same exception as above mentioned, the conversion rate of styrene/carbontetrachloride is greater than that of styrene

in bulk.

The dose rate dependence of the formation of various fractions is of interest. Figure 7 illustrates the relation for the 80 : 20 (vol) mixture. Only one common straight line is drawn for fractions I and III, because it may be regarded that points are scattered accidentally around a straight line. The exponent of the dose rate dependence is calculated to be 0.85. In the case of bulk polymerization of styrene, the exponent of the dependence was 1 both for fractions I and III. The exponent for fraction II is 0.55, which is in good agreement with 0.50 of fraction II in bulk polymerization. It is,

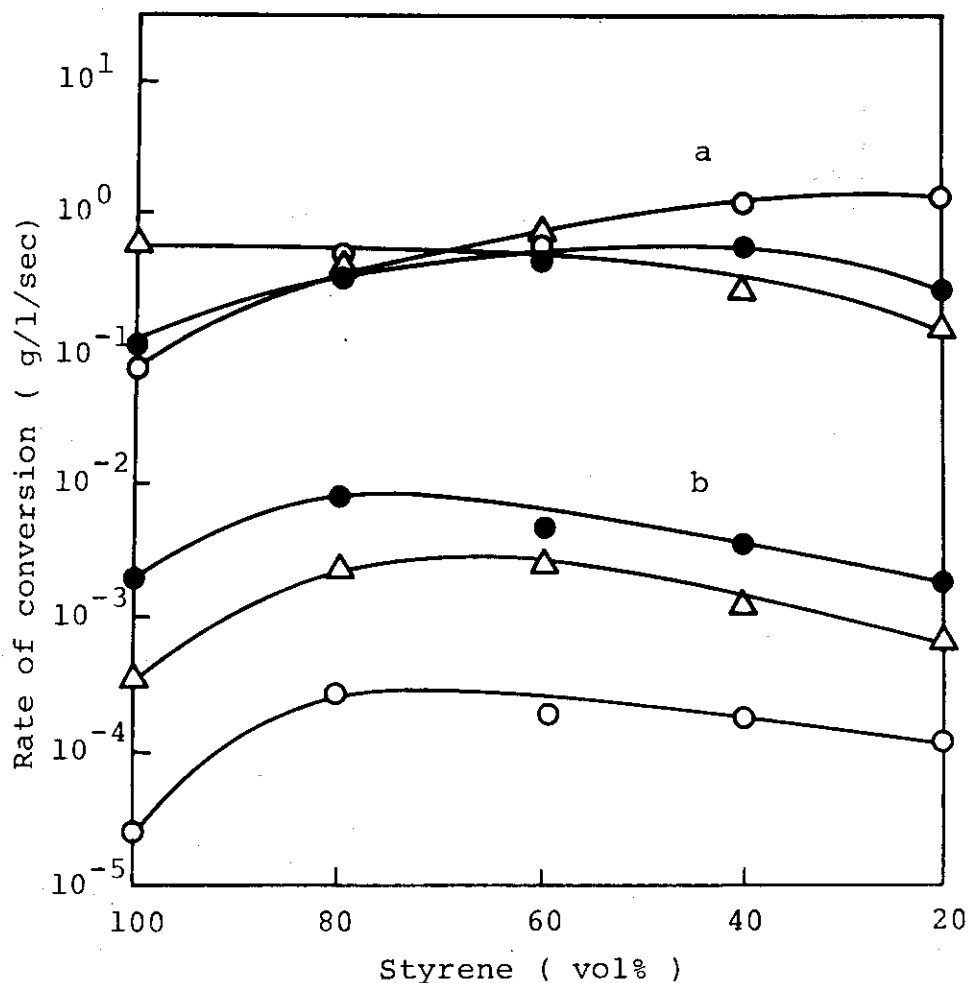


Fig. 6. Rate of conversions for fractions I (o), II (●) and III (Δ) in mixtures of styrene-carbontetrachloride at two different dose rates (a, 6.0×10^5 ; b, 2.2×10^2 rad/sec).

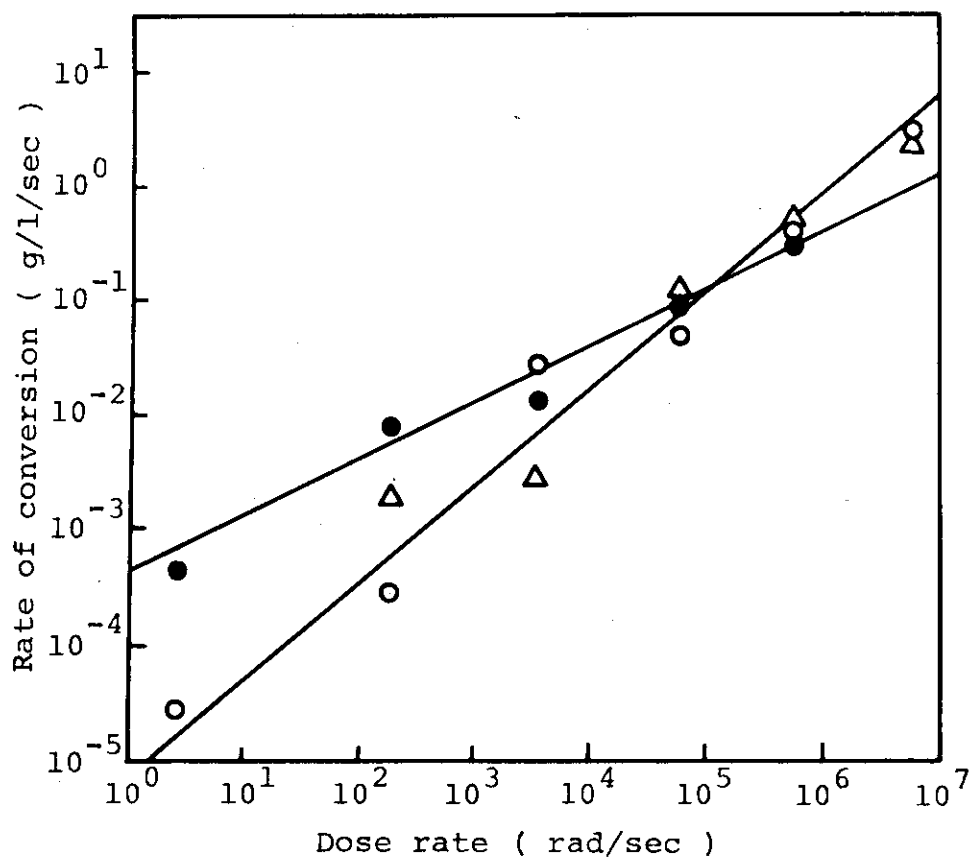


Fig. 7. Dose rate dependences of conversion rate for fractions I (o), II (●) and III (Δ) in 80 : 20 (vol.) mixture of styrene and carbontetrachloride.

therefore, likely that the essential feature of polymerization is retained at least in styrene/carbontetrachloride of 80 vol% styrene.

Dose rate dependence of the formation of various fractions in the case of much lower styrene content (20 vol%) is shown in Fig. 8. Three straight lines are drawn for fractions I, II and III, and the exponents calculated from the slopes are 0.92, 0.55 and 0.84, respectively. It may be concluded that the essential feature of the polymerization is kept unchanged even when the styrene content is lowered to 20 vol%.

Determination of the composition of the fractions has not yet been carried out; the molecular weight was estimated from the peaks of each fraction and given in Table 2 and 3 which

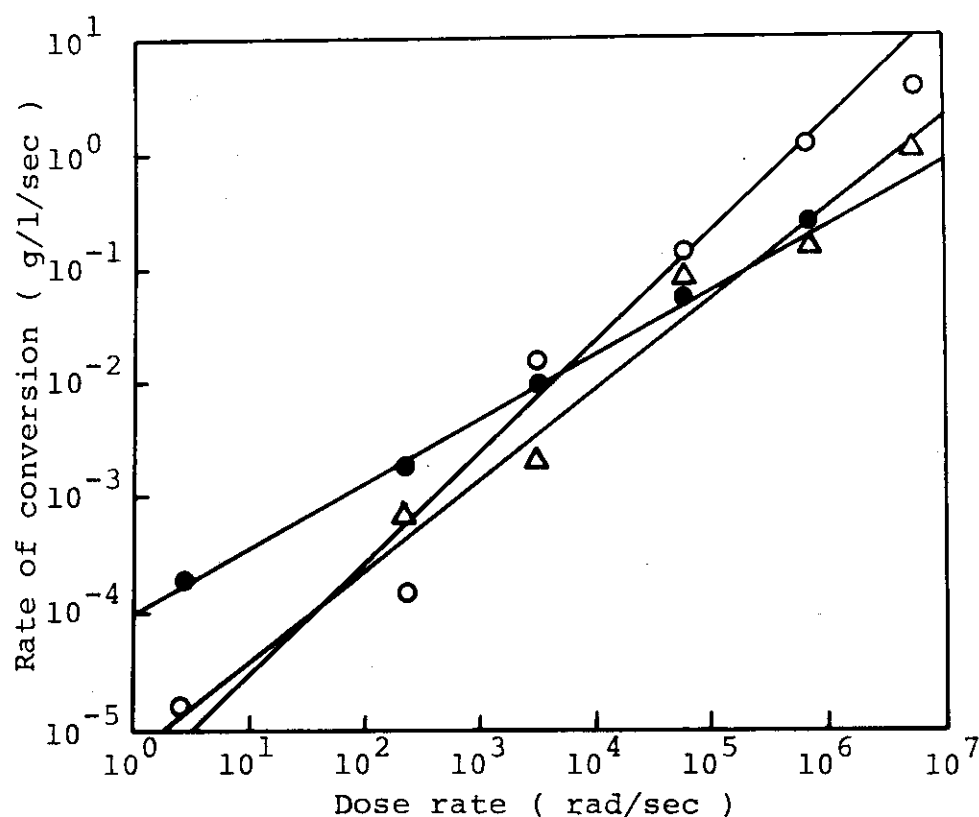


Fig. 8. Dose rate dependences of conversion rate for fractions I (o), II (●) and III (Δ) in 20 : 80 (vol.) mixture of styrene and carbontetrachloride.

contain also numerical values of the rates of conversion for the three fractions.

By use of the molecular weight and the conversion rate, the rate of polymer molecule formation in mole/l/sec and number of polymer molecules in mole/l/rad can be calculated.

Molecular weight of fraction I is almost independent of the styrene content and dose rate, and it seems to be apparently simple to discuss the results; however, that is not the case, because the mechanism of the formation of this fraction is not clear even in the case of bulk polymerization.

That the fraction II is formed by a radical mechanism has been shown in the bulk polymerization of styrene; in the case of the mixtures also it is probable that the radical mechanism accounts for the formation of fraction II, because the exponent

of the dose rate dependence of the rate of formation of this fraction is $1/2$ (see Fig. 7 and 8), which is typical for the mutual termination of growing radicals in the polymerization.

Table 2 Molecular Weight and Conversion Rate for Fractions I, II and III of Polymerization Products from Styrene/Carbontetrachloride Mixtures (Dose Rate: 2.2×10^2 rad/sec)

Styrene cont. vol%	100	80	60	40	20
Molecular weight, M					
I $M \times 10^{-2}$	2.7	2.7	2.7	2.7	2.7
II $M \times 10^{-3}$	32	8.6	5.2	2.2	1.3
III $M \times 10^{-4}$	6.4	6.6	5.9	3.6	2.1
Conversion rate, (g/l/sec)					
I (g/l/sec) $\times 10^{-4}$	0.244	2.55	2.00	1.93	1.40
II (g/l/sec) $\times 10^{-3}$	2.02	8.39	5.02	3.74	1.84
III (g/l/sec) $\times 10^{-3}$	0.393	2.45	2.46	1.43	0.77

Table 3 Molecular Weight and Conversion Rate for Fractions I, II and III of Polymerization Products from Styrene/Carbontetrachloride Mixtures (Dose Rate: 6.0×10^5 rad/sec)

Styrene cont. vol%	100	80	60	40	20
Molecular weight, M					
I $M \times 10^{-2}$	—	4.3	4.7	4.0	4.0
II $M \times 10^{-3}$	1.2	2.1	2.6	1.9	2.1
III $M \times 10^{-4}$	2.8	1.9	1.7	1.2	0.85
Conversion rate, (g/l/sec) $\times 10$					
I	0.82	4.72	6.77	10.8	12.1
II	1.01	3.91	5.51	4.90	2.66
III	7.12	4.06	6.88	2.97	1.64

If we concentrate our attention to the change of the feature of the polymerization owing to the drop of styrene content from 100 to 80 vol%, we can see in Table 2 that the molecular weight drops to about 1/4, whereas the conversion rate and the number of polymer molecules (the latter is not shown in the table) become about 4 and 15 times greater, respectively. The most important effect of carbontetrachloride is that it participates in the initiating radical formation. The rate of formation of the initiating radicals may be written as follows:²⁾

The rate of initiating radical formation in mole/l/sec

$$= (\phi_m [M] + \phi_s [S]) I \quad (2)$$

where ϕ_m and ϕ_s are factors of initiating radical formation for styrene and carbontetrachloride, respectively, and $[M]$ and $[S]$ are concentrations (mole/l) of styrene and carbontetrachloride, respectively. Under assumption of the termination by mutual reaction of the growing radicals and steady state for the concentration of radicals, ϕ_s/ϕ_m was calculated by use of the rates of conversion at 100 and 80 vol% styrene, and a value of about 50 was found for the ratio. The ratio of 50 can also explain quantitatively the drop of the molecular weight. At first chain transfer to carbontetrachloride was taken into account, but the calculation showed that the rate of chain transfer is so small compared to that of the termination, that it can be neglected.

In the case of the bulk polymerization of styrene it was reported that the G-value of the initiating radical formation of styrene is 0.66 independent of the dose rate and water content of styrene. G-value for the initiating radical formation of carbontetrachloride is therefore ca. 33, a value which is in fair agreement with values reported by other researchers.

In the case of fraction III, which is attributed to polymers by ionic mechanism in bulk polymerization and plays a dominant role at higher dose rate, the change of the molecular weight and conversion rate by an addition of carbontetra-

chloride is very small as Table 3 shows. The number of polymers per unit dose in mole/l/rad at 6.0×10^5 rad/sec is as follows;

Styrene vol%	100	80	60	40	20
(mole/l/rad) $\times 10^{11}$	4.2	3.6	6.8	4.1	3.2

The number of polymer molecules does not show remarkable change between 100 and 20 vol% styrene. The simplest explanation is that carbontetrachloride has similar G-value of initiating ion formation as styrene, though other explanation may also be possible.

Preliminary experiments on the effect of DPPH and n-butylamine on the polymerization of styrene/carbontetrachloride were also carried out. (I. Sakurada, J. Takezaki, T. Okada)

- 1) I. Sakurada, T. Okada, K. Hayashi and J. Takezaki, JAERI-M 7355, 28 (1977); J. Takezaki, T. Okada and I. Sakurada, J. Appl. Polymer Sci., 21, 2683 (1977).
- 2) A. Chapiro, Radiation Chemistry of Polymeric Systems, Interscience, New York, 1962, p 251-255.

3. Radiation Polymerization of Styrene/Ethylene Chloride Mixture in a Wide Range of Dose Rate

Instead of carbontetrachloride in the foregoing report¹⁾ ethylene chloride was used as a solvent for styrene and radiation polymerization was carried out in a wide range of dose rate, that is between 2.5 and 6.0×10^6 rad/sec. All experimental procedures and evaluations of the results are the same as the foregoing report, unless otherwise noted.

Figure 1 shows the rate of conversion of styrene/ethylene chloride mixtures at different dose rates. The dependence of the conversion rate on the styrene content is apparently more complicated than in the case of carbontetrachloride.

Fractionation by GPC was also carried out for the polymerization products, and it was found that they were mostly

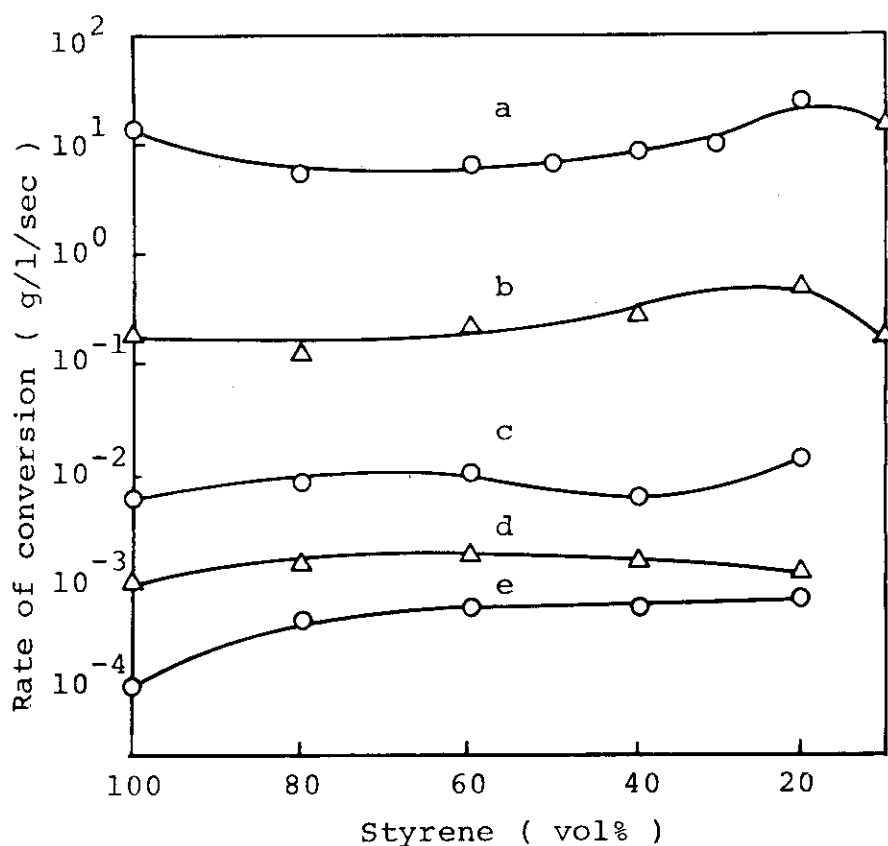


Fig. 1. Rate of total conversion of various styrene/ethylene chloride mixtures at different dose rates:
 (a) 6.0×10^6 , (b) 1.2×10^5 , (c) 1.1×10^3 ,
 (d) 4.3×10^2 , (e) 2.5 rad/sec.

consisted of three fractions i.e. fraction I, II and III; sometimes fraction IV with the molecular weight about 10^6 was found by the polymerization at very high dose rates.

Figure 2 shows a typical change of GPC curves with the styrene content of the system.

Percentage of the fractions of the products obtained at various dose rates from the mixtures of varying styrene contents is shown in Table 1. It is seen from the table that fraction II and III are dominants at the lower and higher dose rates, respectively. It is noteworthy that the highest content of fraction I is in the present case about 20%, whereas it often exceeded 70% in the case of styrene/carbontetrachloride.

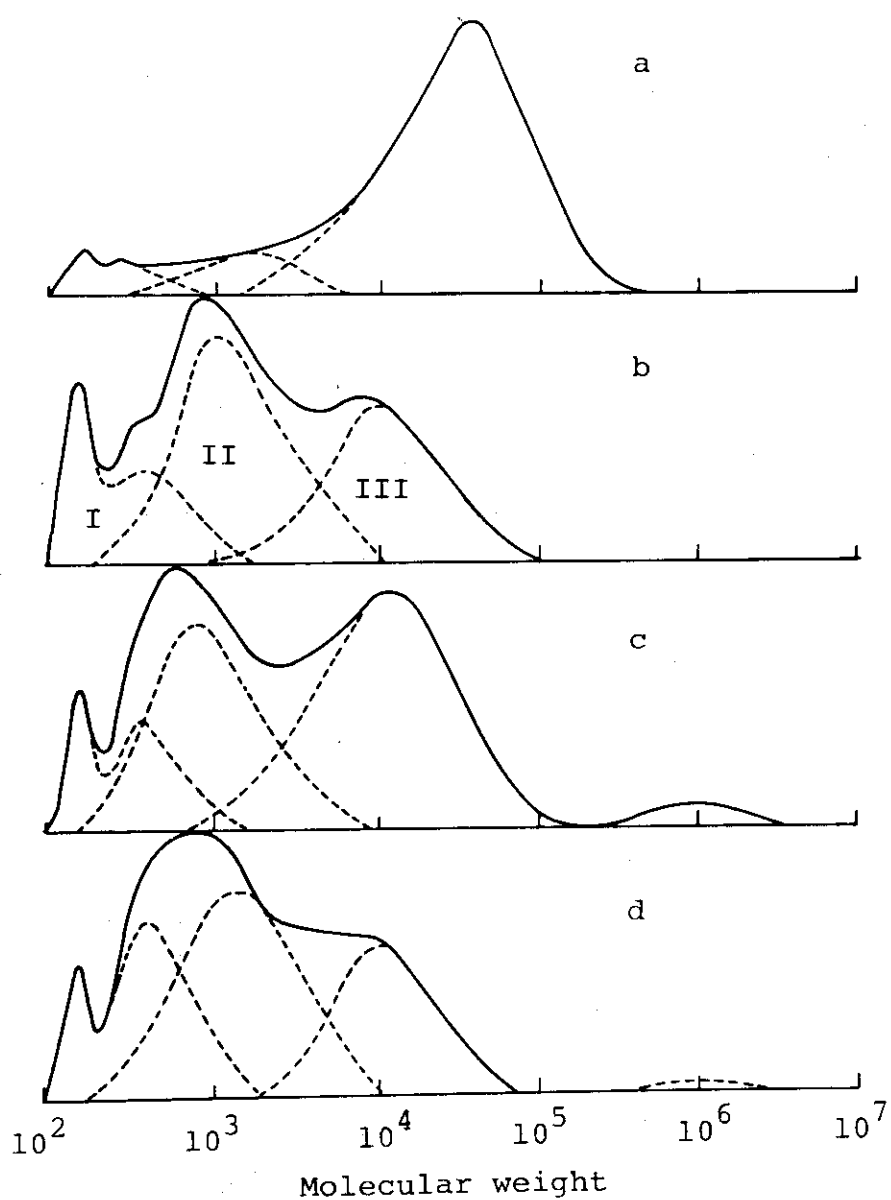


Fig. 2. Molecular weight distribution curves of polymerization product for styrene/ethylene chloride mixtures of various styrene contents at a dose rate of 1.2×10^5 rad/sec. Styrene content in vol%: (a) 100, (b) 80, (c) 60, (d) 50.

Table 1 Percentage of Fractions I, II, III and IV in the
Polymerization Products of Styrene/Ethylene
Chloride of Various Styrene Contents at Different
Dose Rates

Styrene cont. vol%	100	80	20
Dose rate 2.5 rad/sec			
Fr. I	13.0	6.9	8.8
Fr. II	87.0	93.1	91.2
Dose rate 4.3×10 rad/sec			
Fr. I	4.5	2.9	5.0
Fr. II	95.5	85.6	40.3
Fr. III	0	11.5	54.7
Dose rate 1.1×10^3 rad/sec			
Fr. I	16.4	18.5	6.3
Fr. II	58.5	73.0	74.8
Fr. III	25.1	8.4	18.9
Dose rate 1.2×10^5 rad/sec			
Fr. I	5.8	22.2	5.4
Fr. II	8.2	44.9	8.1
Fr. III	86.0	32.9	86.5
Dose rate 6.0×10^6 rad/sec			
Fr. I	13.1	16.2	9.5
Fr. II		6.9	17.5
Fr. III	89.3	71.1	73.0
Fr. IV	0	5.8	0

Figure 3 shows the dose rate dependence of the rate of conversion for fraction II at three different styrene contents (100, 80 and 20 vol%). The plots are straight lines and the exponents of the dose rate dependence are practically 0.50; one plot is for 100 and the other is for 80 vol% styrene. No curve was drawn for 20 vol% styrene, because the points are located near the drawn lines with somewhat larger scattering. It is important that the line for 80 vol% styrene is located above that for 100 vol% styrene. We will come back to this points later.

The dose rate dependence of the conversion rate for fraction III is shown in Fig. 4 for the three mixtures as in Fig. 3. The exponent of the dependence is practically one in this case, and it means clearly that the chemical mechanisms of the formation of fraction II and III are quite different each other.

As in the case of carbontetrachloride, the contribution of the solvent for the initiating radical formation will be

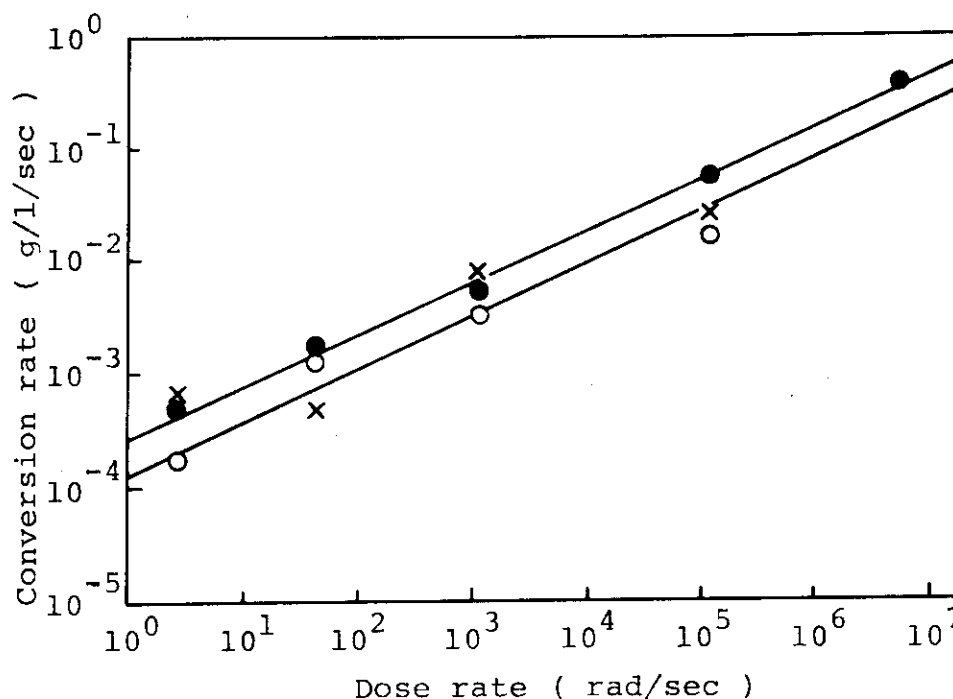


Fig. 3. Dose rate dependence of conversion rates for fraction II. Styrene content in vol%:
(o) 100, (●) 80, (x) 20.

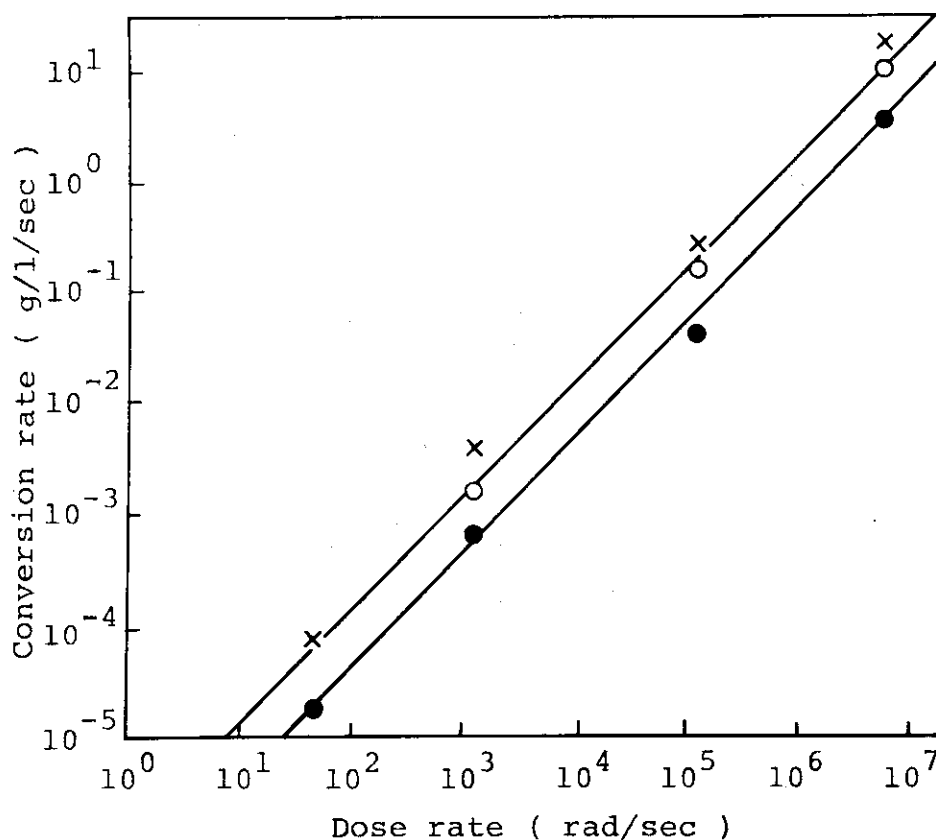


Fig. 4. Dose rate dependence of conversion rates for fraction III. Styrene content in vol%: (o) 100, (●) 80, (x) 20.

discussed with the following equation:²⁾

The rate of the initiating radical formation

$$= \phi_m[M] + \phi_s[S] \quad (1)$$

In this equation ϕ_m and ϕ_s are rate constants of initiating radical formation of the monomer M and the solvent S respectively.

If the rates of conversion of pure styrene and mixture are represented with R_0 and R , and the monomer concentrations with $[M]_0$ and $[M]$, respectively, the ratio of ϕ_s/ϕ_m is calculated from experimental value of R/R_0 with the following equation.

$$\left(\frac{R}{R_0}\right)^2 \cdot \left(\frac{[M]_0}{[M]}\right)^3 = \left(1 + \frac{\phi_s}{\phi_m} \cdot \frac{[S]}{[M]}\right) \quad (2)$$

The calculation was carried out for 80 vol% styrene solution. As R/R_0 an average value of 1.4 for the polymerization at lower dose rates was employed to find ϕ value of 8 as ϕ_s/ϕ_m . In the foregoing report a value of 50 was found for carbontetrachloride; it may be concluded that ethylene chloride produces far smaller number of initiating radicals. The G-value is calculated to be 5.3. Large differences in the polymerization products from the two binary mixtures, as for example, production of a large amount of fraction I in styrene/carbontetrachloride is probably closely connected to the large G-value of radical formation in carbontetrachloride.

In the case of molecular weight, it is necessary that chain transfer is considered; by the polymerization of styrene, however, it is well known that monomer transfer is negligible. It was shown in the system of styrene/carbontetrachloride that solvent transfer can also be neglected. In the present case also, it will be assumed that it is negligible and tried to see whether the change of the molecular weight can be explained solely by the mutual termination of the growing chains. Then we can use the following equation for the calculation of the ratio of the degree of polymerization of the product from pure styrene P_0 to that from mixture P.

$$\frac{P_0}{P} = \left(\frac{[M]_0}{[M]}\right)^{1/2} \left(1 + \frac{\phi_s[S]}{\phi_m[M]}\right)^{1/2} \quad (3)$$

As may be seen from the equation P_0/P is independent of the dose rate. Putting 8 for ϕ_s/ϕ_m in the equation, we find $P_0/P = 1.90$. Experimental values for the dose rates of 2.5, 4.3×10 and 1.1×10^3 rad/sec, were 2.56, 1.59 and 1.62 respectively. The agreement between the calculated and experimental values is fair, and there is no positive indication that chain transfer has to be taken into account.

As has already been mentioned fraction III is produced by ionic mechanism in pure styrene, and the exponent of the

dependence of the conversion rate on the dose rate is one. Styrene/ethylene chloride mixtures show the same dose rate dependence. It is seen from Fig. 4 that the straight line for 80 vol% styrene is located under that for pure styrene; the rate of conversion of pure styrene is about 4 times that of 80 vol% styrene. Probably this is due to termination of ionic chains by ethylene chloride. Further discussion will be given elsewhere. (I. Sakurada, J. Takezaki, T. Okada)

- 1) The present Annual Report. JAERI-M, 1978
- 2) A. Chapiro, Radiation Chemistry of Polymeric Systems, Interscience, New York, 1962, p 253-265.

[3] Radiation-Induced Polymerization of Dienes

1. Polymerization of Isoprene

For these years we have studied bulk polymerization of several vinyl compounds at high dose rate. It is found that in many monomers radical and cationic polymerizations take place at the same time. However, in methyl methacrylate and some alkyl acrylates only radical polymerization is found. In general the molecular weight (MW) of the polymer formed with radical mechanism is low at high dose rate while that of the polymer with cationic mechanism is independent of the dose rate. Therefore, to obtain polymer of medium chain length, it is advantageous to promote the cationic polymerization.

Among commercial oligomers, those from diene compounds are important in their use in adhesives, paints and liquid rubbers. Especially their large possibilities of modification seem to allow us much more extensive use in the future.

As a first step of diene studies, polymerization of isoprene is carried out. Details of the experimental procedure were described elsewhere¹⁾. Isoprene is used without further purification or drying.

Results of the polymerization at 25°C in a wide dose rate range are shown in Fig. 1. With γ -ray polymerization at a low dose rate, 7.0 - 234 rad/sec, R_p increases proportionately to the square root of the dose rate but \overline{DP}_n of the product decreases from 56 at 7.0 rad/sec to 22 at 234 rad/sec. These results indicate radical mechanism. R_p in a high dose rate region, 9×10^3 - 2×10^5 rad/sec by electron beams from a Van de Graaff accelerator is substantially higher than the extrapolation of R_p at low dose rate. An addition of 1.8 mole/l triethylamine (TEA) reduces the rate down to the expected level of the radical polymerization as shown in the figure. \overline{DP}_n of the product at high dose rate is approximately 13 independent of the dose rate.

A typical MW distribution of the product at high dose

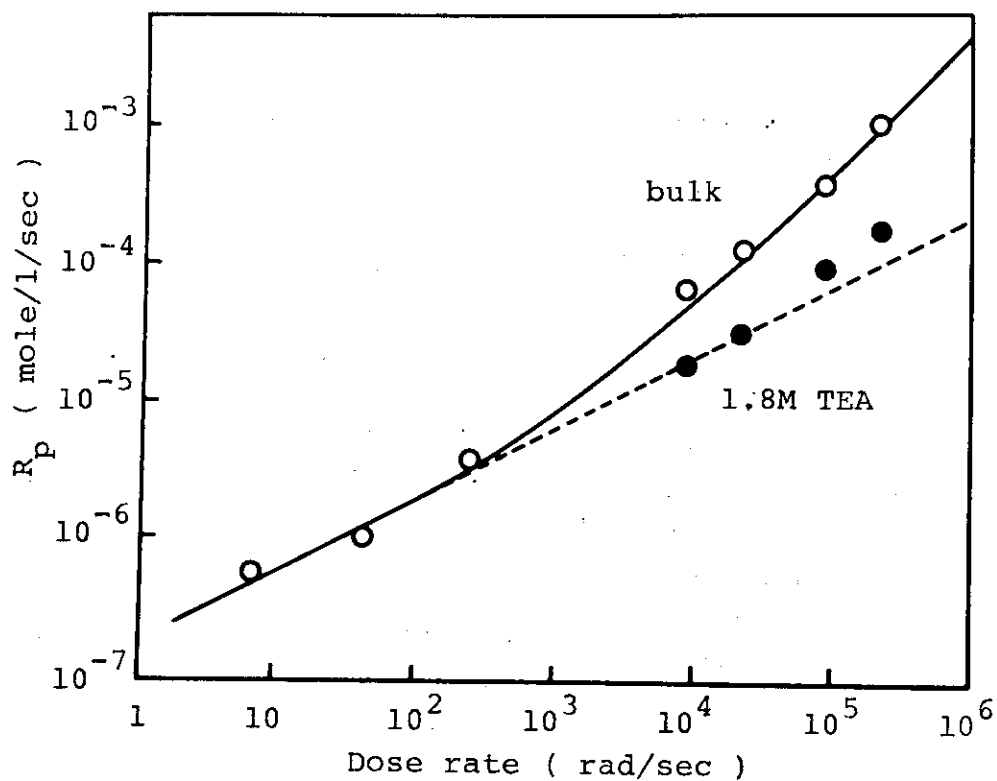


Fig. 1. Dose rate dependence of R_p of isoprene at 25°C.

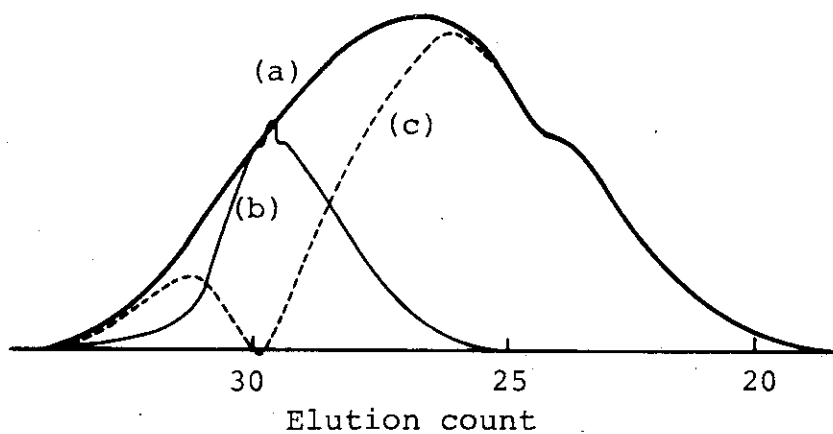


Fig. 2. MW distributions of the product irradiated at the dose rate of 2.2×10^4 rad/sec for 2,000 sec.
(a) bulk, (b) in the presence of 1.8 mole/l triethylamine, (c) result of subtraction.

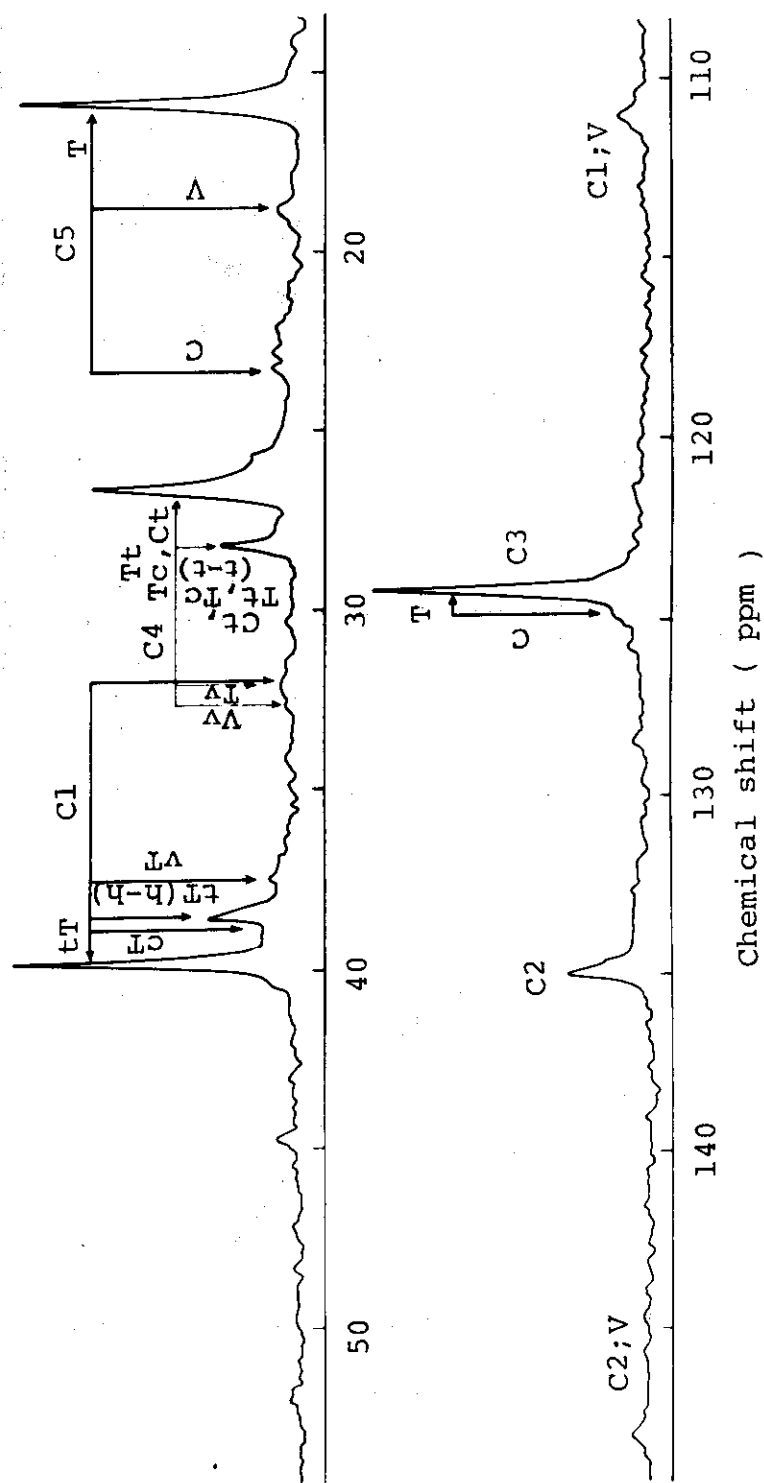


Fig. 3. ^{13}C -NMR spectra of the product at the dose rate of 2.2×10^5 rad/sec.
Upper spectrum, paraffinic part; lower spectrum, olefinic part.

rate is shown with curve (a) in Fig. 2. The distribution is always very broad. Curve (b) is a distribution of the product in the presence of TEA, presumably a distribution of radical product. A graphical subtraction of curve (b) from curve (a) gives a two-peaked distribution as shown with curve (c). The main fraction of high MW is obviously a product of cationic polymerization. The small peak of low MW is considered to be due to a product which is capable of cationic propagation as was supposed for the similar product in isobutyl vinyl ether.

Structure of the products is studied by ^{13}C -NMR as shown in Fig. 3. It is composed mainly of trans-1,4 unit (T) including head-to-head and tail-to-tail abnormalities with small fractions of cis-1,4 (C) and vinyl (V) units. Assignment for each peak is also described in the figure. Small letters, t, c and v mean trans, cis and vinyl units adjacent to the observing unit in a diad structure, respectively. The nomenclature of carbon atoms is, $\overset{1}{\text{CH}_2}=\overset{2}{\text{C}}(\overset{5}{\text{CH}_3})-\overset{3}{\text{CH}}=\overset{4}{\text{CH}_2}$. Relatively small peaks at 22.2 - 22.7, 25.8, 45.6 and 51.7 ppm are unassigned and probably intrinsic to these oligomeric polyisoprenes. Fractions of trans, cis and vinyl units evaluated from their relative intensities of absorptions of C5 atoms are given in Table 1. The fraction of vinyl unit is also estimated from

Table 1 Microstructure of Polyisoprenes

Sample		A67	A70	A60+A71
Dose rate (rad/sec)		2.2×10^5	230	7.0
$\overline{\text{DP}}_n$		13	22	56
Trans (%)	[C5; 16.0]	80	76	75
Cis (%)	[C5; 23.4]	9	14	18
Vinyl (%)	[C5; $\overset{17.7}{\sim}$ $\overset{18.8}{\sim}$]	11	10	7
	[C1; $\overset{109}{\sim}$ $\overset{112}{\sim}$]	10	11	9

its absorption at 111.1 ppm and the value agrees well with that evaluated from the absorption of C5 atoms. From the table, structural difference between the high and the low dose rate products or products with cationic and radical mechanism is only a little; a slightly greater cis content at low dose rate but a little change in vinyl fraction in spite of substantial change in \overline{DP}_n . (K. Hayashi, T. Okada, S. Okamura)

1) JAERI-M 6702, 42 and 87 (1976).

2. Polymerization of Chloroprene

It is well known that chloroprene polymerizes readily with radical initiators in contrast to its poor reactivity with cationic catalysts. Bulk polymerization of chloroprene at high dose rate was carried out to study the kinetic behavior of the polymerization and characteristic of the product.

The rate of polymerization as a function of dose rate is

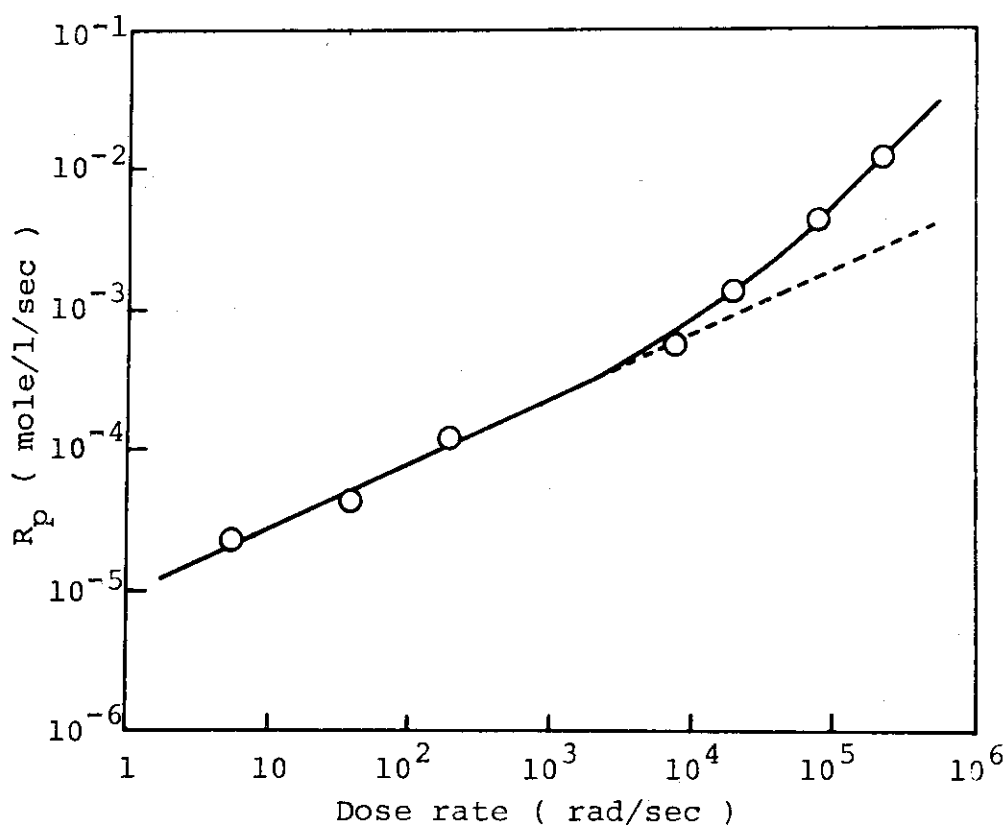


Fig. 1. Dose rate dependence of R_p of chloroprene at 25°C.

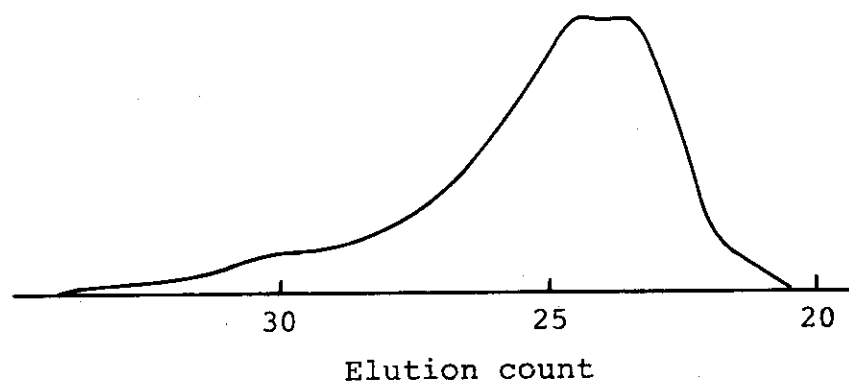


Fig. 2. MW distribution of the product at 8.3×10^4 rad/sec.

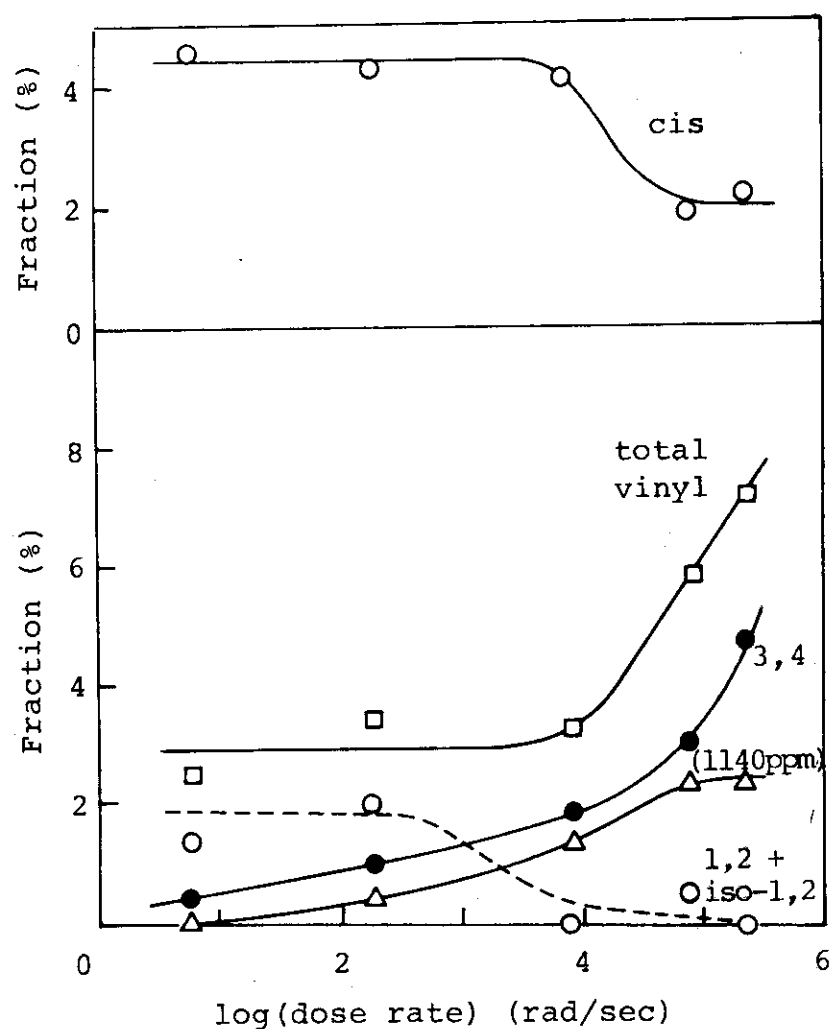


Fig. 3. Fraction of cis-1,4 and vinyl unit in polychloroprene.

shown in Fig. 1. In γ -ray polymerization between 5.9 - 192 rad/sec, R_p increases proportionately to the square root of the dose rate and the molecular weight (MW) of the product decreases with increasing dose rate as expected in ordinary radical polymerization. R_p at high dose rate deviates from the extrapolation of the radical polymerization probably because of the contribution of the cationic polymerization. R_p at 2×10^5 rad/sec is as high as twelve times that of isoprene and almost the same as that of styrene, for which the highest R_p has been attained so far except methyl and ethyl acrylates.

MW distribution of the high dose rate product is shown in Fig. 2. As a common trend of the product at high dose rate, the MW distribution is broad but it is notable that the

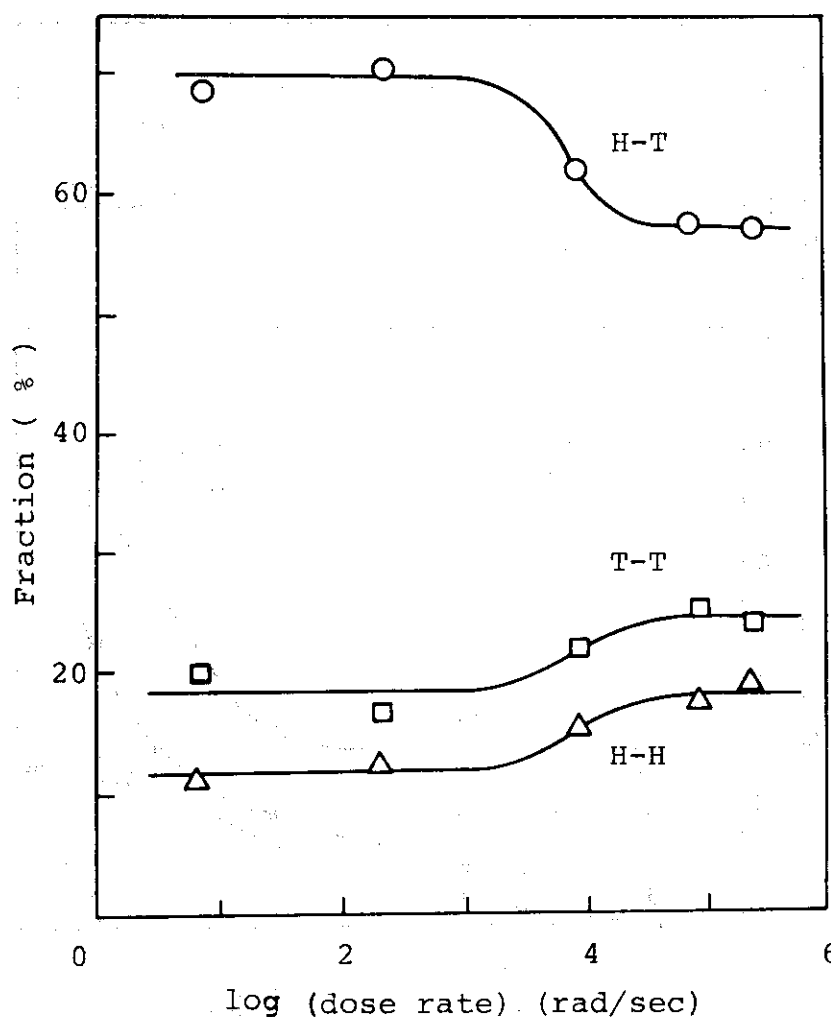


Fig. 4. Fraction of structural abnormalities in trans sequence of polychloroprene.

abundance of oligomers whose MW is less than 1,000 (elution count higher than 28.5) is relatively small in this product. \bar{M}_n value for this product by vapor pressure osmometry is 2,400. Polymerizations at 10 and -10°C give products of a little higher MW but almost no change in R_p .

Microstructure of polychloroprene is studied by ^{13}C -NMR. As the case of polyisoprene, the product is composed mainly of trans-1,4 unit with small fractions of cis-1,4 and vinyl units. Using Coleman's assignment¹⁾, changes of cis and vinyl fractions with dose rate are shown in Fig. 3. At high dose rate, cis unit decreases slightly while sum of vinyl units increases. Abnormalities of the central unit in all trans triad are also shown as a function of the dose rate in Fig. 4. Fractions of head-to-head and tail-to-tail linkage increase at high dose rate. From Fig. 3 and 4, it is found that the microstructure of low dose rate product is different from that at the dose rate of ca. 10^4 rad/sec or higher. This seems to be related to the appearance of the cationic polymerization. (K. Hayashi, T. Okada, S. Okamura)

1) M. M. Coleman, D. L. Taub, and F. G. Brame, Rubber Chem. and Tech., 50, 49 (1977).

[4] Modification of Polymers1. Surface Modification of Poly (Ethylene Terephthalate) Film by Radiation-Induced Chlorination and Adhesion of Chlorinated Film

The surface modification of poly (ethylene terephthalate) (PET) film by radiation-induced chlorination was carried out to enhance adhesive performance of the film.

Commercially available PET film ("Lumilar", 0.096 mm thick) was employed and irradiated in chlorine gas with γ -rays at room temperature. The Cl-content of the film was calculated from the weight increase of the film. By γ -ray irradiation of

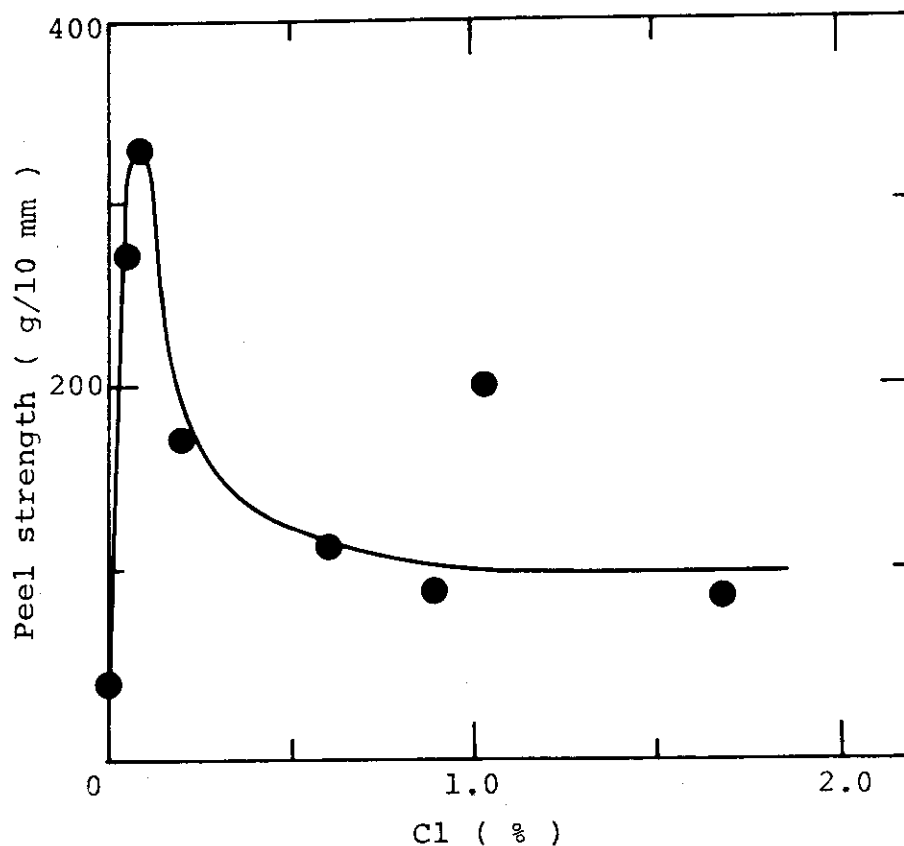


Fig. 1. Peel strength of a PET film-epoxy type adhesive bond as a function of the Cl-content of the film. Adhesive: "Smikadyne A 019-HE".

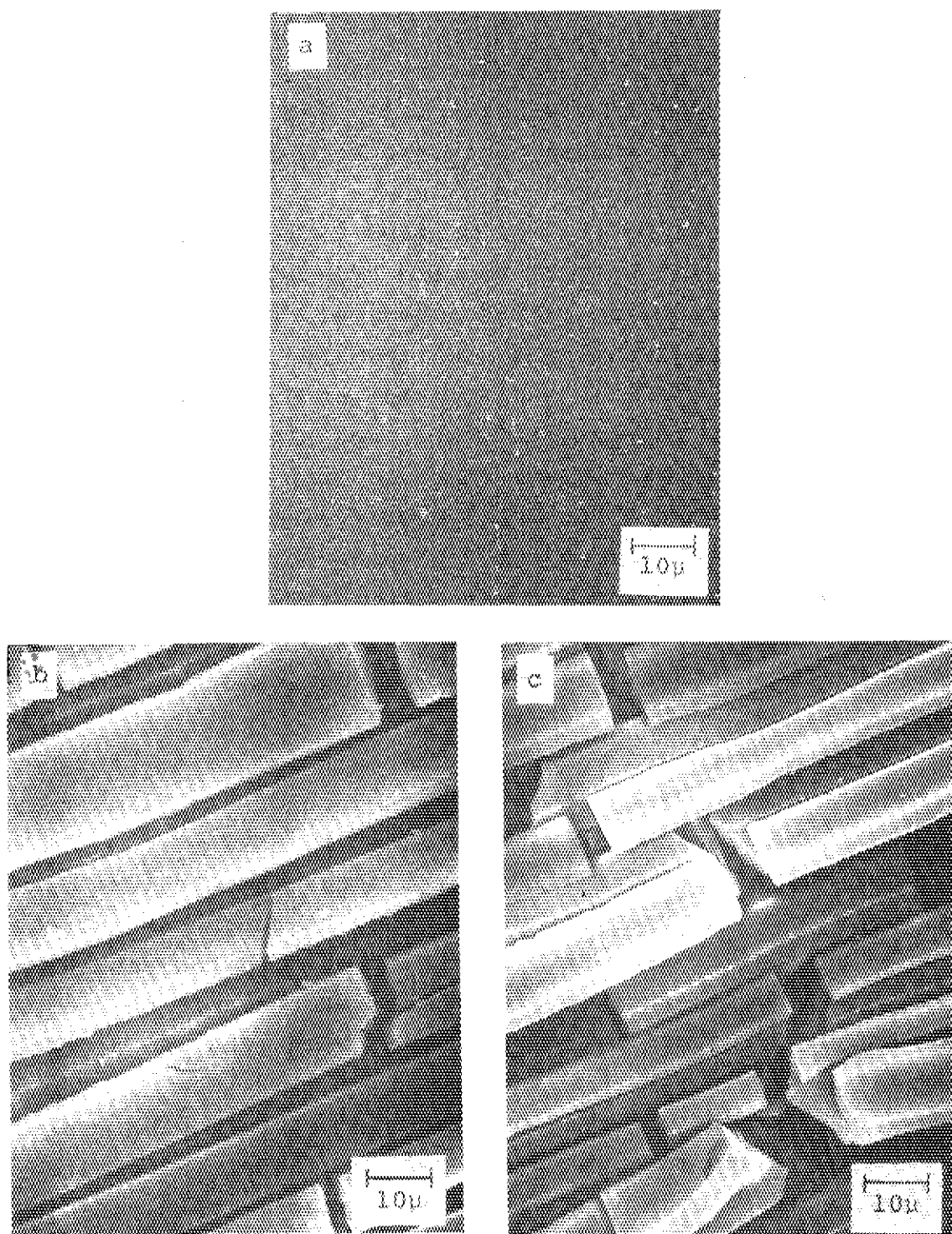


Fig. 2. Electron scanning micrographs of ethylene diamine treated (at 80°C for 1 hr.) PET films.
Cl-content (%): a, 0; b, 0.29; c, 1.3.

0.5 Mrad at a dose rate of 3.0×10^4 rad/hr Cl-content attained to a value of 1% (based on the weight of the original film), but further irradiation gave almost no effect to enhance the Cl-content.

The effect of the Cl-content on the contact-angle of a water droplet on the film was studied. The curve of contact-angle vs. Cl-content showed a maximum at a Cl-content of about 0.3%.

Adhesion tests of the chlorinated film were carried out using epoxy type and polychloroprene type adhesives and an acrylic type pressure-sensitive adhesive. In the peel test for the epoxy type adhesive the chlorinated film showed a sharp maximum strength at a Cl-content of 0.1%, which was ten times larger than the original film (see Fig. 1). Only a small increase in peel strength was observed when the tests were carried out with the other two types of adhesive.

To examine the reason for the enhancement of the peel strength at a low Cl-content the structure of the film surface was observed by scanning electron microscopy (SEM). No appreciable difference was observed between the chlorinated and original films.

Since most common epoxy type adhesive contains hardener having amino groups, the surface structure of the films treated with ethylene diamine was also examined by SEM.

The chlorinated PET film showed after the ethylene diamine treatment rough surface structure, and the roughness increases with increasing Cl-content. On the other hand the unchlorinated film showed smooth surface without any appreciable change of the surface structure by the treatment with ethylene diamine (see Fig. 2).

The above SEM observations lead to the following explanation to the sharp maximum of the peel strength; chlorinated surface becomes rough, when it is in contact with a hardener having amino groups, and enhances the peel strength by so-called anchor effect at a low Cl-content. By further increase of the Cl-content, however, the peel strength decreases due to the destruction of the film. (T. Okada, K. Kaji)

2. Preparation and Properties of Polyvinyl Chloride Fibers with Graft Branches of Poly (Aluminum Acrylate)

We have reported previously^{1),2)} on the preparation and properties of polyvinyl chloride (PVC) fibers with graft branches of calcium salt of polyacrylic acid (Ca-PAA). In the present experiments aluminum salt of polyacrylic acid (Al-PAA) is taken up instead of Ca-PAA. The main object is, in this case also, to obtain PVC fibers with higher temperature of heat shrinkage.

There are two methods to prepare PVC-g-poly (aluminum acrylate) (Al-AA). One is two step method, where free acrylic acid is grafted to PVC, and then PVC-g-PAA is converted to

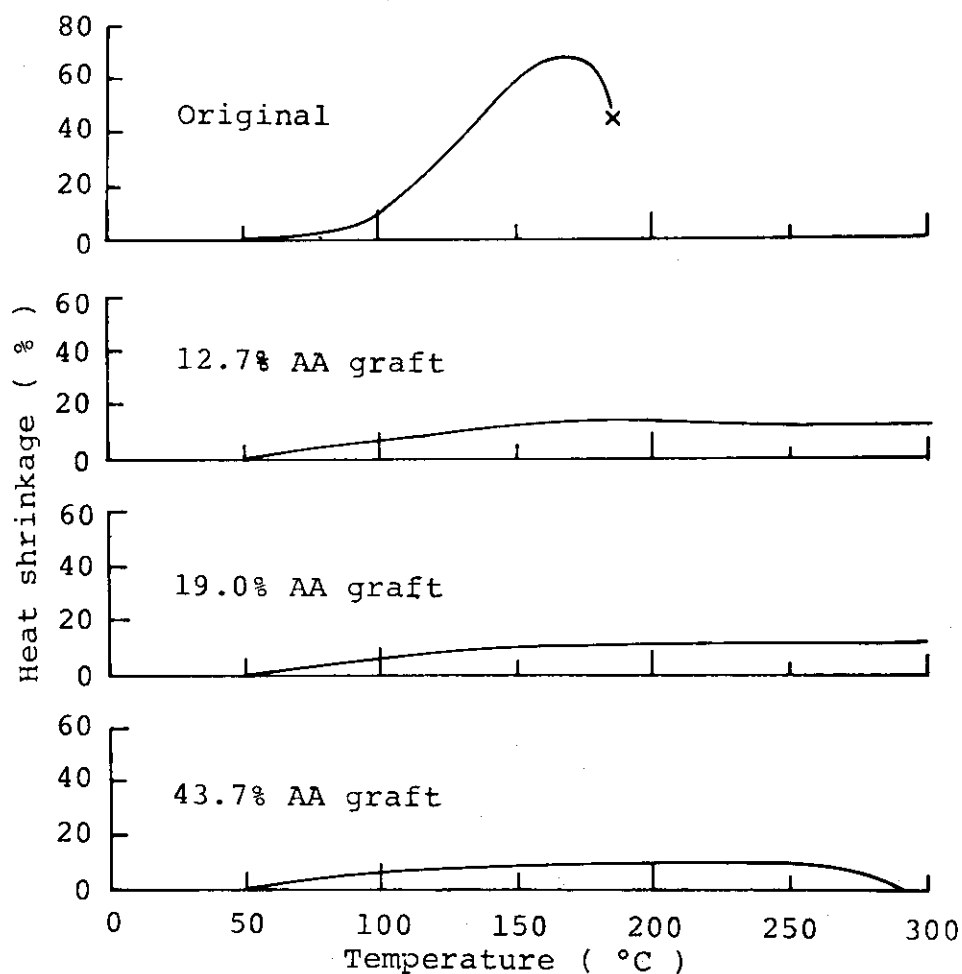


Fig. 1. Heat shrinkage of PVC-g-poly (aluminum acrylate) fibers prepared by two step method.

PVC-g-poly (Al-AA) by treatment with aqueous solution of a suitable aluminum salt such as aluminum acetate. The second method is the direct method and aluminum acrylate is directly grafted onto PVC to obtain PVC-g-poly (Al-AA).

Fig. 1 shows heat shrinkage of PVC graft fiber with poly (Al-AA) prepared by the two step method. It is seen from the figure that the degree of grafting as low as 12% is effective to enhance the heat shrinkage temperature to a remarkable extent. It seems that the effect of aluminum is somewhat greater than calcium for the enhancement of the temperature of heat shrinkage.

The direct grafting with aluminum acrylate was carried out as follows; PVC fiber swelled with a mixture of ethylene dichloride and methanol was dipped in aqueous solution of aluminum acrylate containing a small amount of CuSO_4 to prevent homopolymerization outside of the fiber and then the mixture was irradiated with γ -rays of Co 60.

Fig. 2 shows the plots of percent graft against irradiation

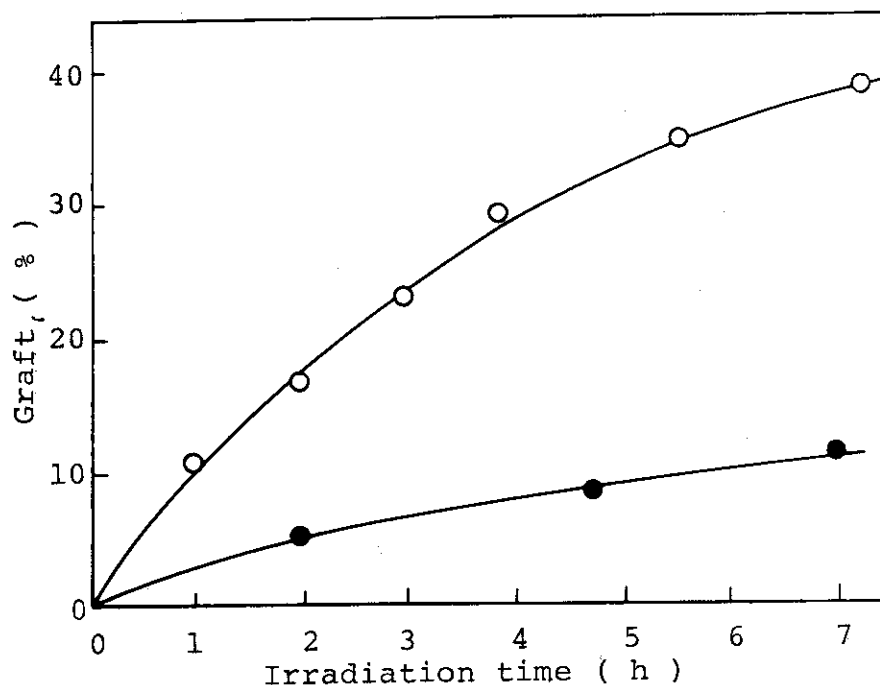


Fig. 2. Grafting of aluminum acrylate onto polyvinyl chloride fiber at 22°C. Dose rate: (○) 1.7×10^5 rad/h, (●) 1.9×10^4 rad/h.

time at 1.7×10^5 and 1.9×10^4 rad/h. At the dose rate of 1.7×10^5 rad/h, one hour irradiation is needed to attain 10% graft. It means that the rate of grafting is nearly the same as that of calcium acrylate.

Aluminum acrylate graft polyvinyl chloride fibers have high heat shrinkage temperature, especially when the graft fiber has been heat-treated. Fig. 3 shows the heat-shrinkage of aluminum acrylate graft fibers against temperature. The fiber of 37% graft retains its fiber form even above 300°C , and gives a maximum shrinkage of 40% which is much lower than that of the original fiber. When this graft fiber is heat-treated at 180°C for 5 min, the maximum heat shrinkage decreases to 20%.

When properties of PVC fibers with graft branches of aluminum salt of polyacrylic acid prepared by two step and

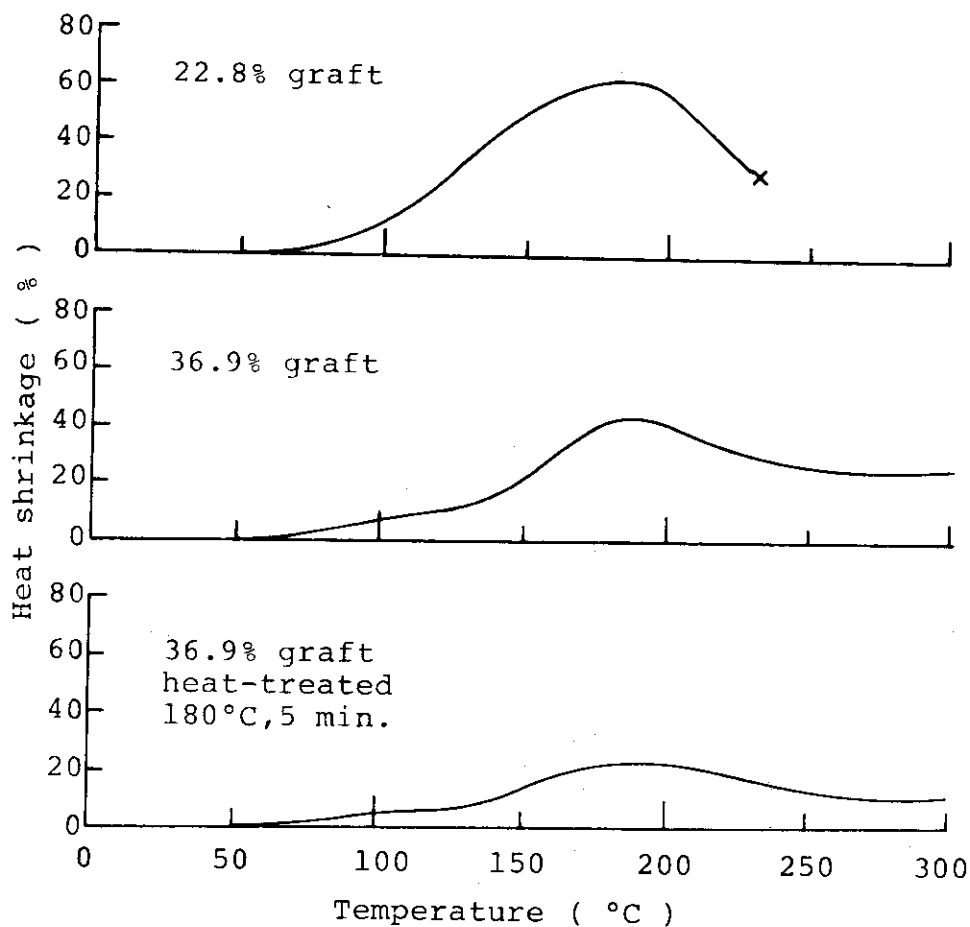


Fig. 3. Heat shrinkage of PVC-g-poly (aluminum acrylate) fibers prepared by direct method.

direct methods are compared, the former shows lower heat shrinkage.

The measurements of the properties other than the heat shrinkage were made on the PVC fiber directly grafted with aluminum acrylate (up to ca. 50%). The tensile strength, elongation and initial Young's modulus are not affected by the grafting. The hygroscopicity increases with the extent of grafting, and at 45% graft it is almost equal to that of cotton. The aluminum acrylate grafted PVC fiber of higher degree of grafting than 15% can be dyed with cationic dyes, although the untreated PVC fiber cannot be dyed. Fire retardance test reveals that self-extinguishing property is the same as that of the original fiber. (I. Sakurada, T. Okada, K. Kaji)

- 1) K. Kaji, T. Okada, and I. Sakurada, Sen-i Gakkai-shi (J. of the Society of Fiber Science and Technology, Japan), 33, T-12 (1977).
- 2) K. Kaji, T. Okada, and I. Sakurada, *ibid.*, 33, T-494, (1977).

3. Radiation-Induced Graft Polymerization of Acrylic Acid onto Poly (Vinyl Chloride)

The purposes of the present work are to prepare polymer having hydrophobic and hydrophilic groups in one molecule by radiation-induced grafting technique and to study the relationship between properties and structure of the polymer. The study is initiated with the grafting of acrylic acid to polyvinyl chloride. Graft polymerization was carried out on polyvinyl chloride powder suspended in aqueous solution of acrylic acid containing ethylenedichloride as swelling agent with the irradiation of Co-60 γ -rays. Products are extracted with hot water to remove homopolymer for 24 hrs, and dried under reduced pressure. Percent grafting is calculated from weight increase of the polymer.

Fig. 1 shows the rate of graft polymerization obtained under various ethylenedichloride concentrations at constant

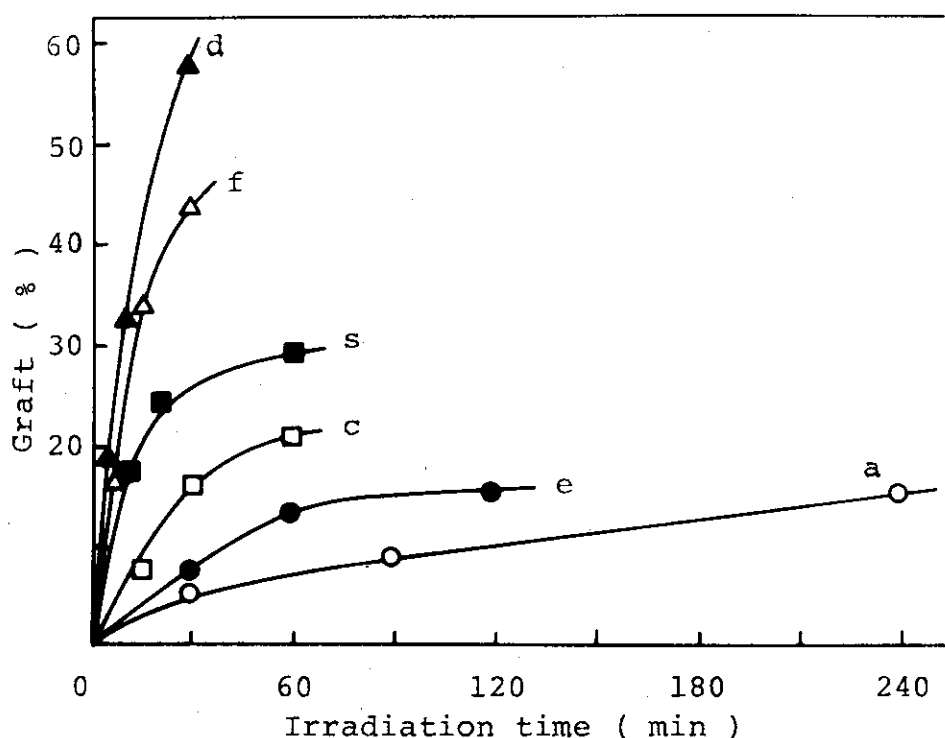


Fig. 1. Rate of graft polymerization under various ethylenedichloride concentrations.

(a) AA/H₂O/EDC: 40/54/6, (e) 50/40/10

(c) 50/34/15, (s) 50/25/25, (f) 50/20/30,

(d) 50/15/35.

Dose rate: 6.2×10^4 R/h, at room temp.

monomer concentration. Grafting rate increases with the increasing amount of ethylenedichloride in the system indicating that the swelling of the polyvinyl chloride with ethylenedichloride promotes monomer diffusion in the polymer.

Adsorption of cupric ion to the graft copolymer was tested by the following method. The graft copolymer was added to 20 ml aqueous solution of cupric sulphate containing 100 ppm cupric ion; the polymer was added to the solution so that the quantity of carboxylic group in the polymer was sixteen times that of cupric ion present in the solution in mole. Then the pH of the solution was adjusted to 11.5 with aqueous ammonia solution, and the solution was stirred for 3 minutes. The graft copolymer in the solution was separated and absorbance

of the supernatant at 610 nm was measured to determine the concentration of residual cupric ion.

Fig. 2 shows adsorption of cupric ion by the polymer obtained from systems a, e, s, and d in Fig. 1. The graft percents of the polymers are given in the caption of the figure. The polymers obtained from system a and e, in which the ethylene dichloride content is comparatively low show good adsorbability that 97% of the cupric ion is adsorbed by the polymers after 10 minutes standing. The adsorbability, however, decreases with increasing ethylene dichloride content in the systems s and d. This result may be explained by the uniformity of the distribution of carboxyl groups in the polymer particles; carboxyl groups which have affinity to metal ions are mainly distributed on the surface of the polymer particles in the cases a and e where the degree of swelling is low, resulting high rate of adsorption; on the other hand, in the polymer particles obtained from highly swelled system s and d, the carboxyl groups are uniformly distributed so that the cupric

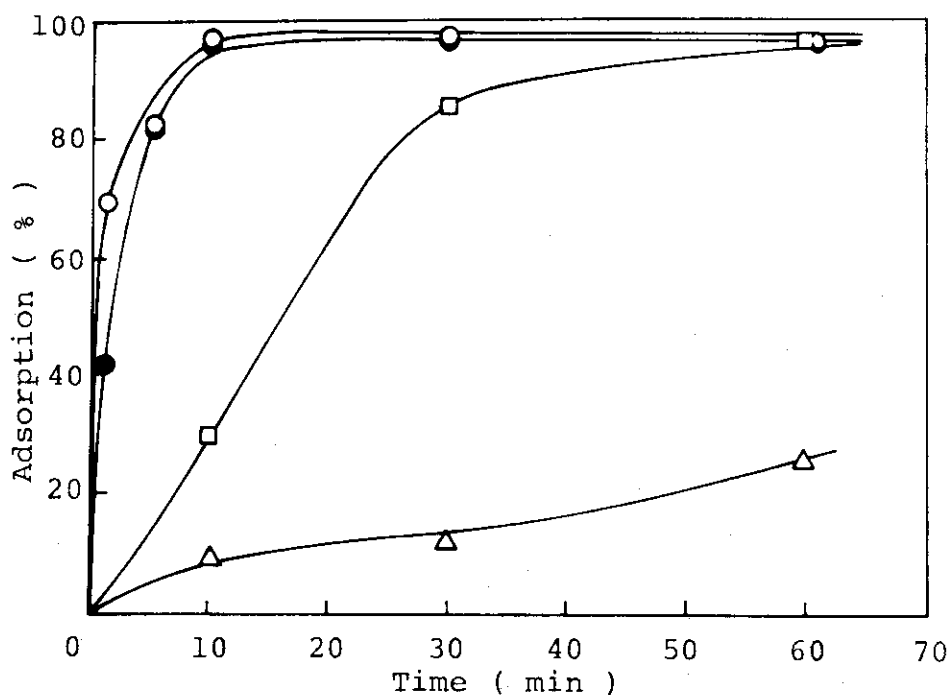


Fig. 2. Adsorption of the cupric ion by the graft polymer.

- o - a: Grafting % = 15.3, - ● - e: 15.4%,
 - □ - s: 17.8%, - △ - d: 18.4%.

ions have to diffuse into the polymer particles to be adsorbed.

In order to obtain further information about the distribution of the carboxylic groups in the polymer, electric conductivity was measured on the grafted film which was obtained

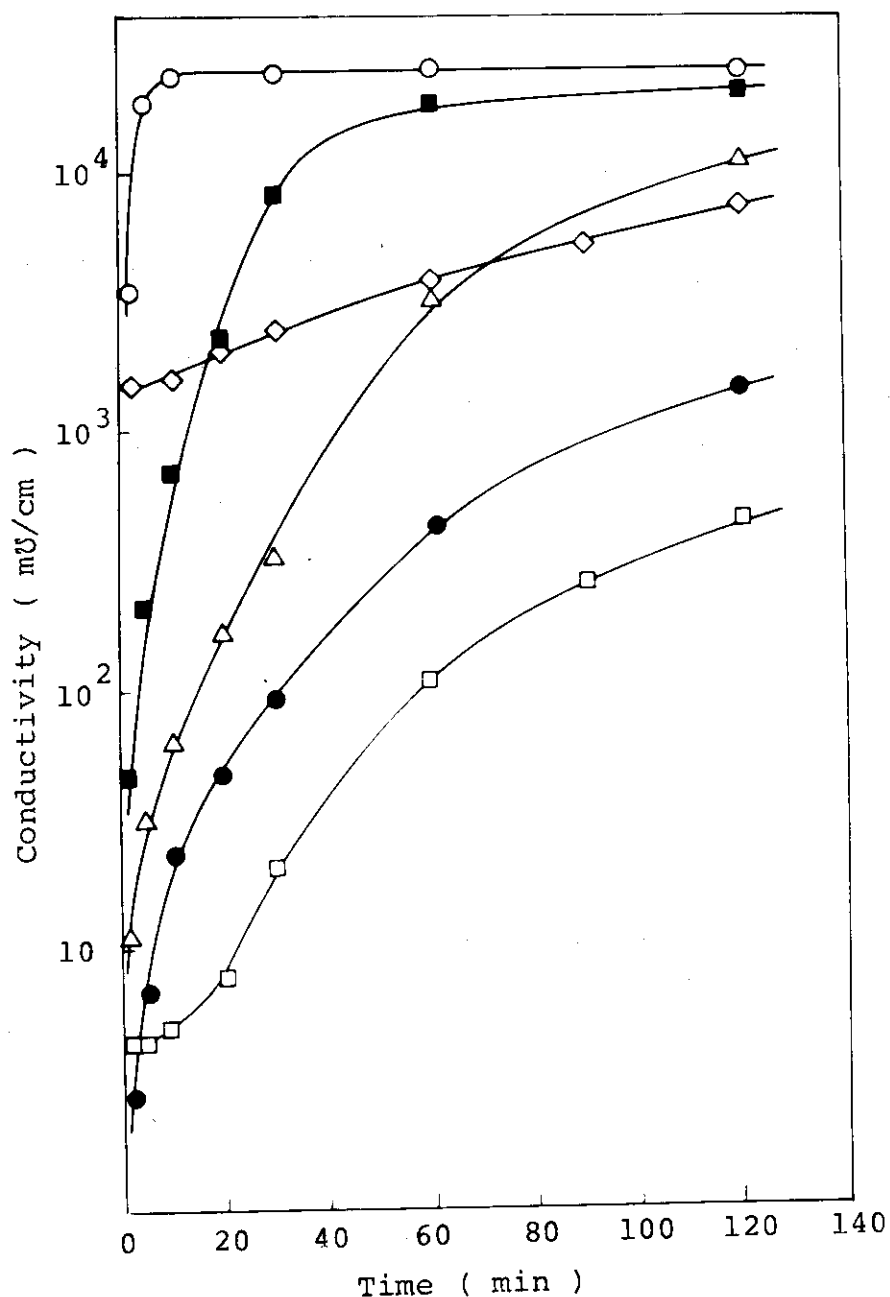


Fig. 3. Electric conductivity of the grafted films.

- o - a: 26.0%, - Δ - e: 30.0%,
 - ● - c: 30.3%, - □ - s: 29.0%,
 - ■ - f: 31.2%, - ◇ - d: 29.0%.

by grafting of polyvinyl chloride film in a similar way as that applied for the powder grafting. Two cells divided with grafted film, each mounted with silver electrode, were filled with 40% KOH solution. Conductivity was measured by connecting this cell to an a - c bridge. Original PVC films have low electric conductivity, but as shown in Fig. 3, the polymers obtained from systems a and f show comparatively high electric conductivity while the polymers by other systems, especially the polymer obtained from the system s of the highest degree of swelling, show low electric conductivity.

Since the carboxyl group plays an important role in carrying ion or charge, the highest electric conductivity would be expected for the polymers containing uniformly distributed carboxyl groups, which are obtained from the system of the highest degree of swelling, e.g., system s. The fact that the polymer obtained in system s gave rather low conductivity

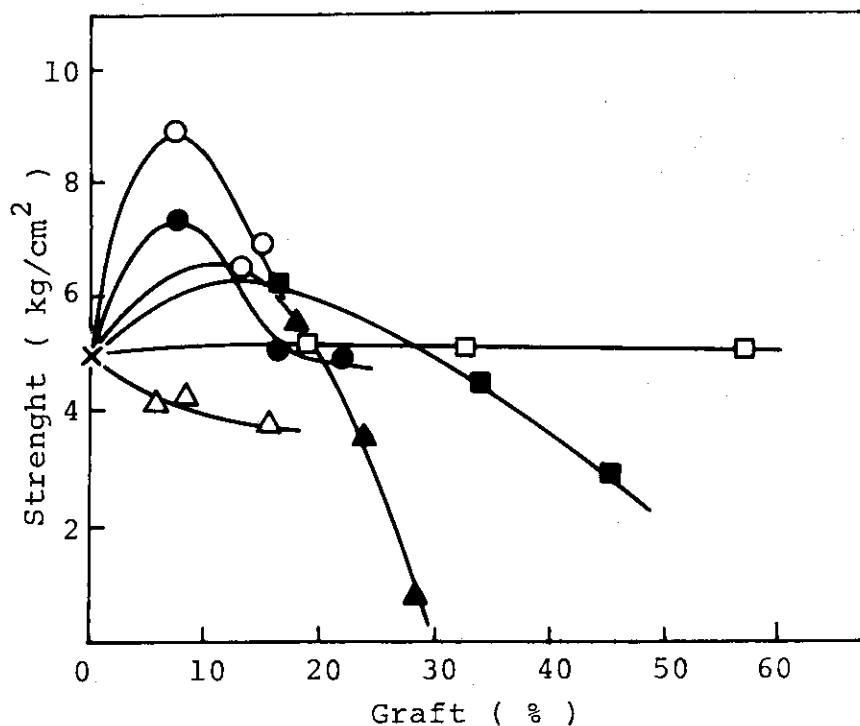


Fig. 4. Peeling strength of copper test pieces joined with the graft polymers.

- Δ - a, - ○ - e, - ● - c,
 - ▲ - s, - ■ - f, - □ - d.

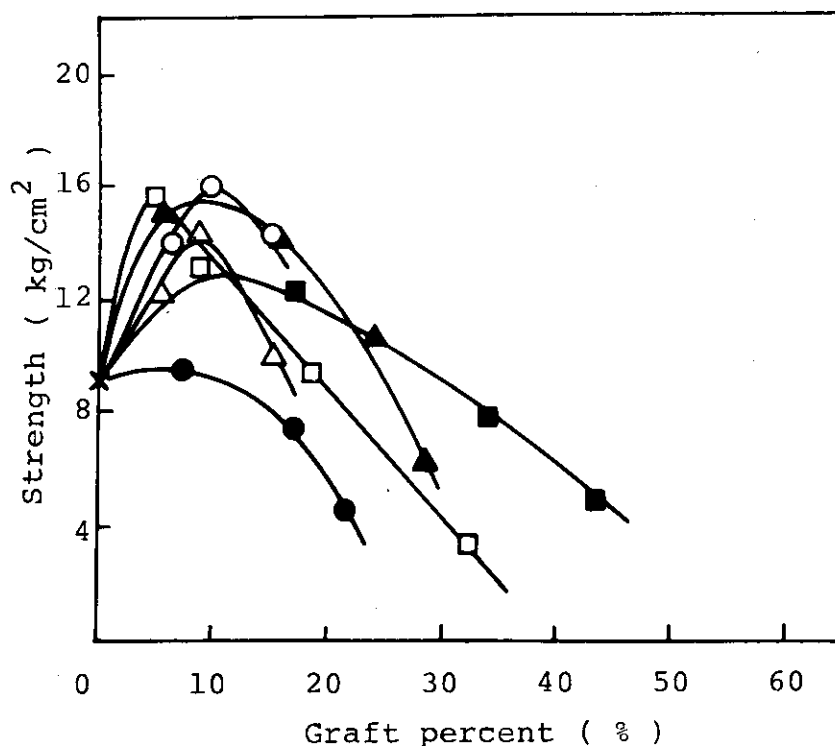


Fig. 5. Peeling strength of iron test pieces joined with the graft polymers.

Symbols are the same as in Fig. 4.

against the above expectation suggests that the mechanism of the conductivity is not simple and remains as the problem for the further studies.

Adhesion ability to copper or iron was measured in order to consider the structure of the graft copolymer through the affinity of carboxylic group to metal surface. Graft polymer (powder) was molded into 80 - 100 μ thickness with hot press at 190°C, 50 kg/cm², the hot plates being covered with Mylar film to avoid adhesion of polymer to the hot plates. The polymer sheet is sandwiched with a pair of metal test pieces, and hot-pressed under the same conditions as the molding. Peeling strength was measured by an Instron tester at the drawing rate of 20 mm/min.

The results are given in Fig. 4 and 5 for copper plates and iron plates, respectively. The system from which the graft copolymers were obtained and graft percents of the graft

polymer are given in the caption of Fig. 4. It is noted that the polymer effective to iron does not always show good adhesivity to copper, e.g., the polymer obtained by system a shows poor adhesion to copper but shows good adhesion to iron. The inhomogeneous distribution of carboxyl group may not contribute to adhesivity, because grafted chain can easily change its conformation to give uniform distribution of carboxyl groups in molten state during hot melt process of the adhesion test. Therefore, the marked difference observed between the adhesion to copper and iron might not be attributable to the distribution of carboxyl groups, but may result from higher order structure of the polymer such as steric configuration.

(Y. Kusama, T. Yagi, T. Okada)

4. Wettability of Hydrated Cellulose and Poly (Vinyl Alcohol)

Films

As described in the previous report¹⁾, a variety of hydrogels, mostly prepared by radiation-crosslinking of water-soluble polymers, do not exhibit complete wettability against water in spite of their high water content, in other words, a water droplet does not spread out completely on the hydrogels. Polysaccharides such as cellulose and dextran have the lowest contact angle to water among the hydrogels studied. It seems that the hydroxyl groups of these polymers may be responsible for the high water wettability. More detailed studies are, however, needed to reach a decisive conclusion on the wettability of hydrogels. The aim of the present work is to determine the water contact angles of hydrated cellulose and poly (vinyl alcohol) (PVA) more precisely than in the case of the previous study and to present a model on the surface structure of hydrogels. Previously we measured the contact angle with the usual sessile droplet method allowing the water droplet neither to advance nor to recede. For the contact angle determination of hydrophilic polymers swollen with water, this sessile drop method has some disadvantages such as drying of specimens and a long time to reach an equilibrium.

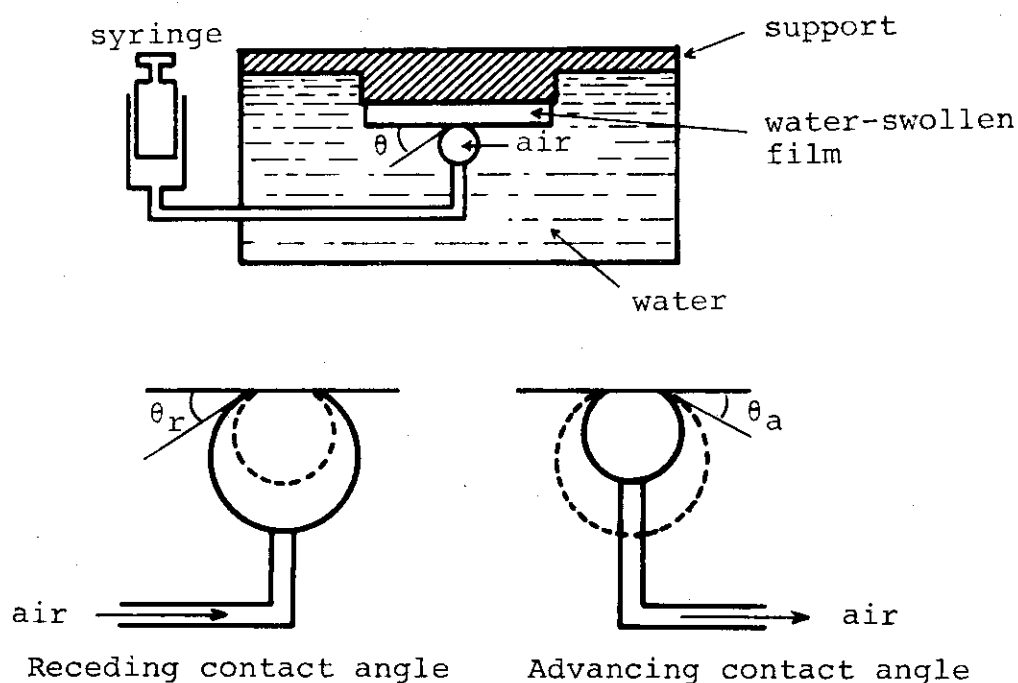


Fig. 1. Apparatus for measuring the contact angle by the inverted bubble method.

Therefore, we adopted the inverted bubble method to study the contact angle of cellulose and PVA films. Figure 1 illustrates schematically the outline of the method. The drawbacks mentioned above with respect to the sessile drop method disappear in this inverted bubble method. As is given in Table 1, the measurement with this method also confirms that cellulose has a much lower contact angle than PVA. It is interesting to note that the contact angles are almost independent of the equilibrated water content of polymers. The difference in wetting between cellulose and PVA may be explained in terms of the molecular structure. PVA has a hydrophilic group $>\text{CH}-\text{OH}$ and a hydrophobic group $>\text{CH}_2$ in the repeating unit, whereas the repeating unit of cellulose should be rather regarded as hydrophilic group as a whole. Accordingly, as demonstrated in Fig. 2, it will be difficult for the cellulose molecule to make its own surface more hydrophobic even when the surface comes in contact with a hydrophobic environment. This is in contrast with PVA, in which both hydrophilic and hydrophobic

groups are able to change their direction to some extent according to the outer phase in contact.

Table 1 Contact angles of several cellulose and PVA films swollen with water

Film	Water fraction	Contact angle/deg.		
		advancing	receding	average
Cellulose				
Cuprophane	0.51	12.5	11.9	12.2
Visking	0.51	11.8	11.3	11.6
Cast	0.27	12.0	11.8	11.9
PVA				
Commercial	0.37	50.0	20.6	37.9
Cast	0.73	50.3	20.6	38.1

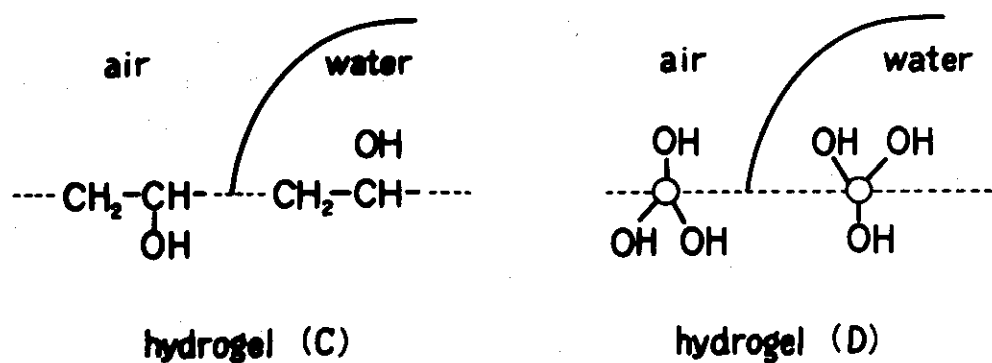


Fig. 2. Schematic representation of orientation of hydrophilic and hydrophobic groups at intersurfaces air/gel and water/gel.

Hydrogel C has a lower surface energy than hydrogel D.

The low contact angle on cellulose may be attributed to the high concentration of OH groups at the surface, compared with other water-soluble polymers. To confirm this expectation determination of the OH concentration at the surface is currently in progress with a fluorescence assay technique. (Y. Ikada, T. Matsunaga)

1) JAERI-M 7355, 60 (1977).

5. Formation of Electret in Polymers by High Energy Electron Irradiation

In the last annual report¹⁾, it is described that electrets are formed in polymers by electron beam irradiation, and the amounts of charge accumulated in the polymers are independent of the accelerating voltage and dose rate, but depend on dose. Studies are carried out on the relationship between the amount of charge formed in the polypropylene film and electrostatic field which is formed on poly (methyl methacrylate) substrate by irradiation.

Surface charge density, σ , on the polymer film is found to increase with time after irradiation, t , according to equation (1):

$$\sigma = k \cdot \ln t \quad (1)$$

where k is a constant which depends on dose received by polymer film (Fig. 1). Voltage generated on the substrate after irradiation is measured as a function of time and logarithm of the rate of the voltage increase is plotted in Fig. 2 as a function of time for substrate irradiated with different dose rates and doses. The plots lie on parallel straight lines, the intercepts of which depend only on dose received by the substrate; in other words, the plots lie on a straight line if the readings of these points on the ordinate are multiplied by factors depending on the dose. In Fig. 3, the multiplication factor, defined as shift factor, is plotted

against dose ratio D_2/D_1 where D_1 and D_2 are the doses at which the two rate curves were obtained. The plots lie on a straight line passing through the original point and having the slope of unity. This fact indicates that the rate of voltage increase can be related with t by the following equation:

$$\frac{dV}{dt} = \frac{D}{D_0} \frac{1}{t} \quad (2)$$

where D is the dose at which the rate curve was taken and D_0 is the dose which gives curve: $dV/dt = 1/t$. Equation (1) can be rewritten as $d\sigma/dt = k/t$; combining with equation (2), one can demonstrate that the surface charge density is proportional to voltage induced in the PMMA substrate. The fact that the voltage induced in the PMMA substrate is independent of electron accelerating voltage and dose rate as evident from Eq. (2)

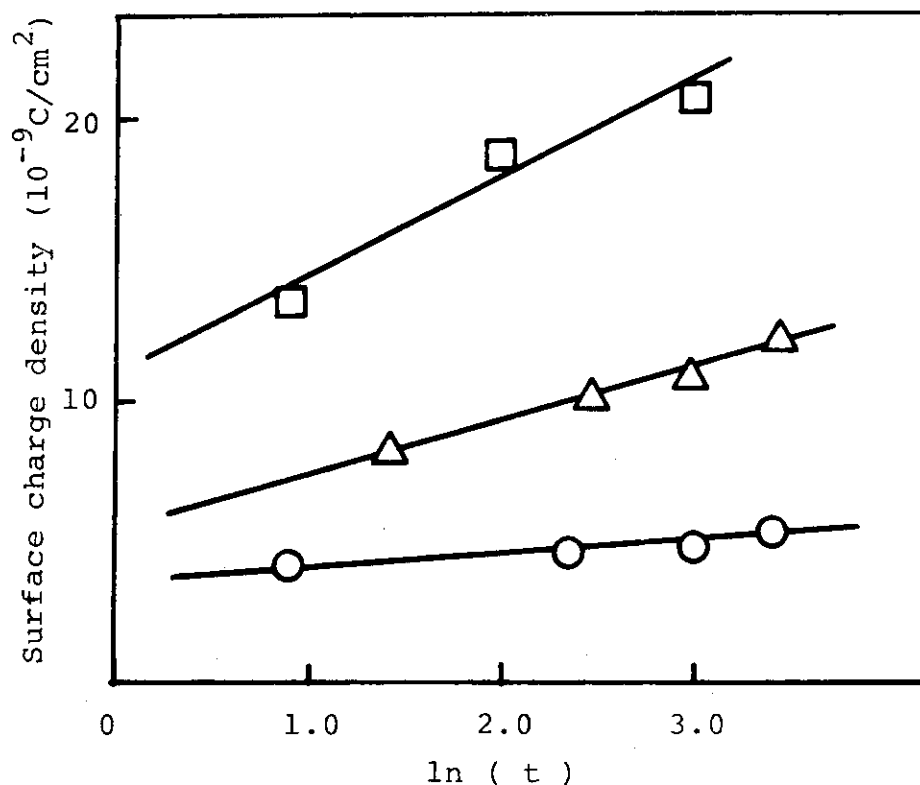


Fig. 1. Surface charge density vs. time after irradiation.

○ , 0.05 Mrad; Δ , 0.12 Mrad; □ , 0.18 Mrad;

Dose rate, 1.8×10^4 rad/sec.

agrees with the previous finding that the surface charge density is independent of the electron accelerating voltage and dose rate, and depends on dose alone.

The surface charge density decreases linearly with the reciprocal of the distance between the film and the substrates

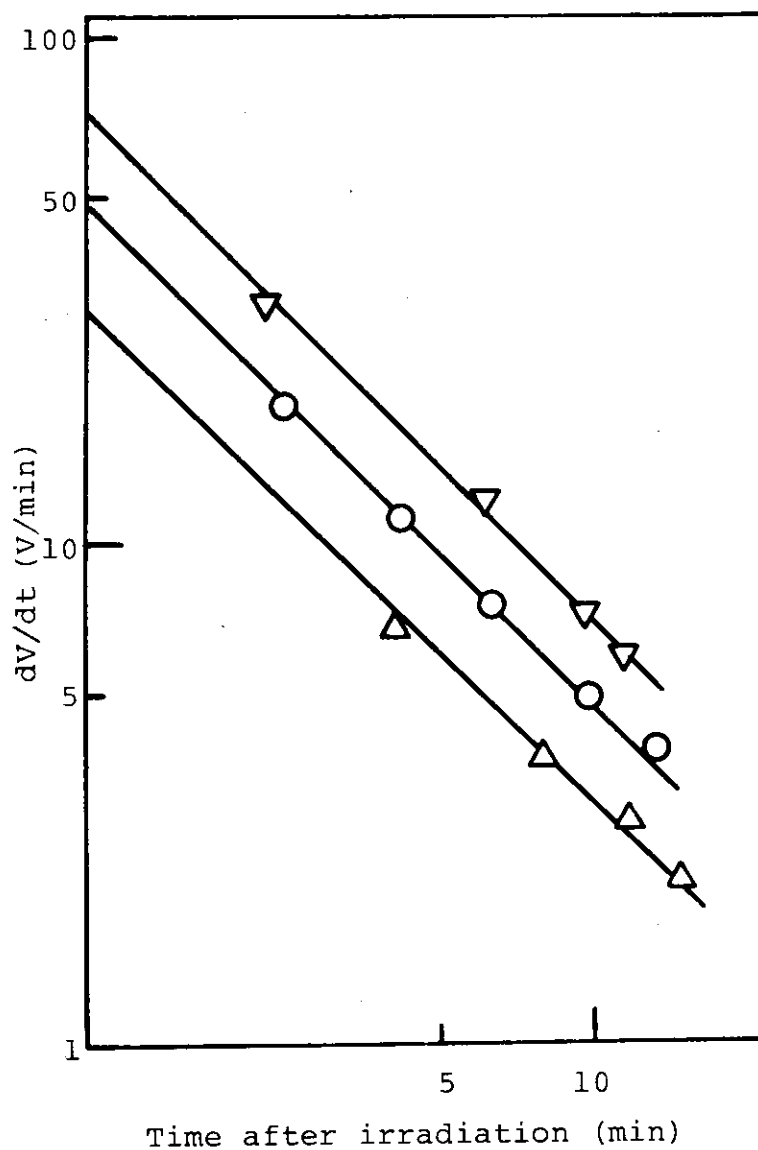


Fig. 2. Plots of dV/dt as a function of time after irradiation; electron accelerating voltage: 1.5 MeV.

- ▽ : 0.2×10^4 rad/sec, 0.26 Mrad
- : 0.29×10^4 rad/sec, 0.17 Mrad
- Δ : 1.44×10^4 rad/sec, 0.11 Mrad

during irradiation. The voltage of the PMMA substrate at the end of the irradiation is constant for the experiments and the voltage of the film surface against the irradiation window is considered to be zero because of ionization of air on the surface. Therefore, the strength of the electric field across the film is inversely proportional to the distance between the film and PMMA substrate. This again indicates that the surface charge density is proportional to the electric field strength.

The irradiations are carried out on the polymer film sandwiched between PMMA plates, the depth against radiation, dose, and dose rate being varied.

The dependence of the surface charge density on depth (Fig. 4) is similar to the electric field strength as a function of depth obtained by Araki²⁾ for polyethylene film taking into consideration the correction for PMMA.

The above results lead to the conclusion that the surface charge of the polymer electret is formed in proportion to

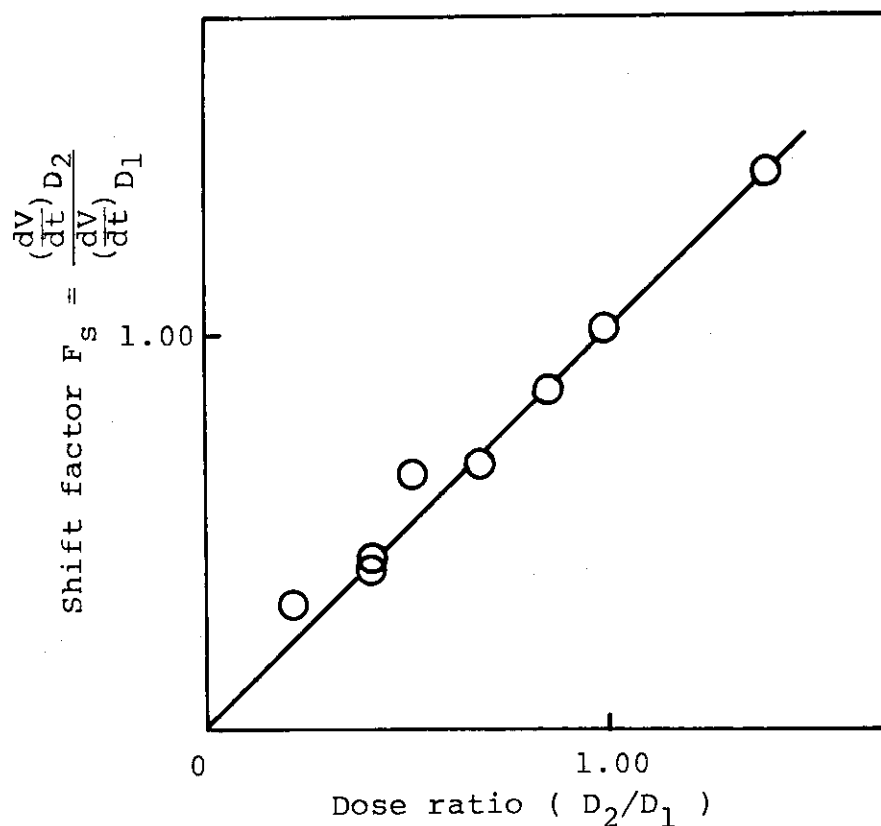


Fig. 3 Shift factor vs. dose ratio.

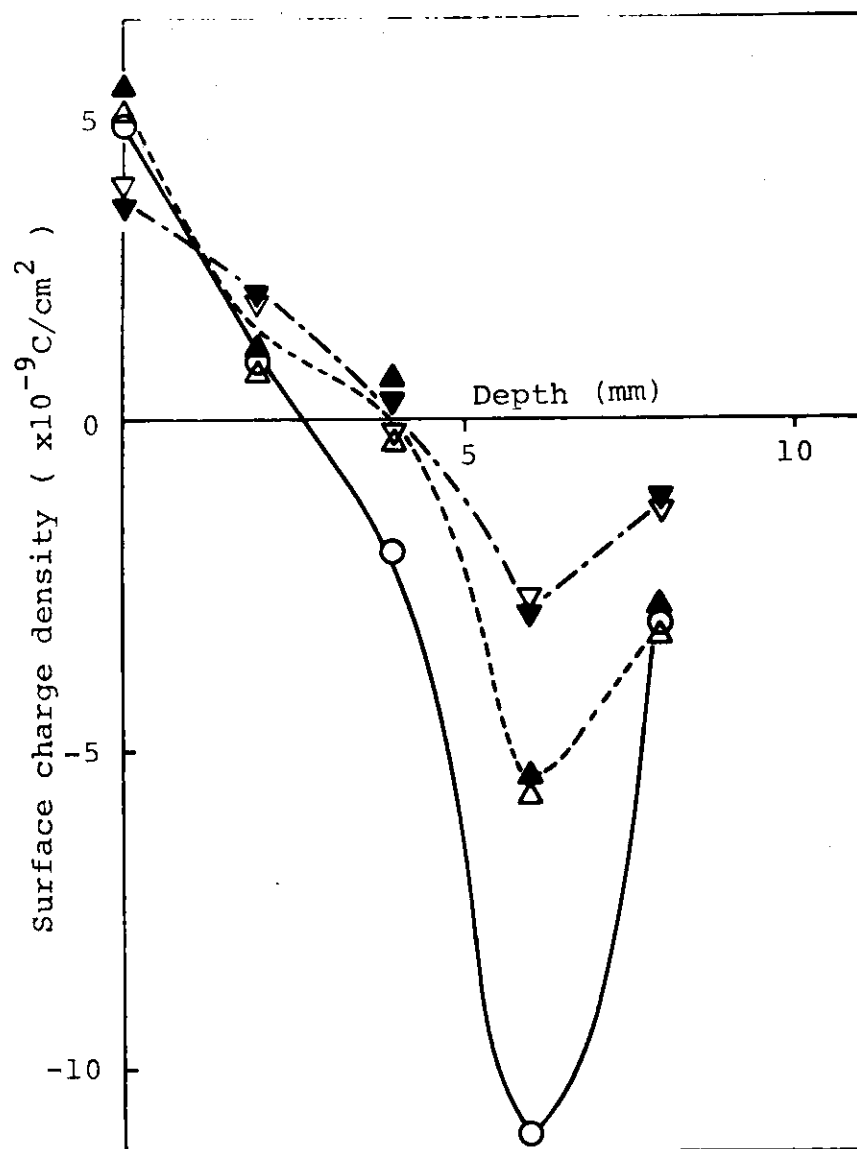


Fig. 4. Effect of depth in PMMA on surface charge density of PP-film; Accelerating voltage: 1.5 MeV.

	Current density ($\mu\text{A}/\text{cm}^2$)	Injected charge density
o	0.043	$0.203 \times 10^{-6} \text{ C}/\text{cm}^2$
Δ	0.043	0.104
▽	0.043	0.052
▲	0.017	0.033
▼	0.017	0.042

electric field strength across the polymer film induced by electric potential of PMMA substrate which is in contact with or close to the polymer film. However, we do not obtain a

model which explains the surface charge formation for different types of polymer films. (M. Kajimaki, T. Okada)

- 1) M. Kajimaki and T. Okada, JAERI-M 7355, 52 (1977).
- 2) K. Araki, et al., IEEE Trans. Nucl. Sci., NS-23 (No. 5), 1447 (1976).

[5] Studies of Chain Rupture in Polyamides by Radiation and Mechanical Stretching

1. Chain Rupture in Nylon 6 Fibers

Previous studies of radiation effects on aliphatic and aromatic polyamides^{1),2)} indicate that degradation predominates over crosslinking when polyamides are irradiated in air. Degradation or chain rupture has also been observed to take place in mechanically deformed polymers including aliphatic polyamides. Therefore, studies of radicals resulted from chain rupture by mechanical deformation of polyamides would provide valuable information concerning the mechanism in the radiation-induced degradation.

For studying radicals produced during mechanical loading, we have constructed an apparatus for stretching fibers, as shown schematically in Fig. 1. Fibers supported by brass rods are stretched in the ESR cavity downward by a servo-motor. Stretching can be made to a desired strain or load at a constant strain rate of five different speeds from 5 to 100% elongation/min.

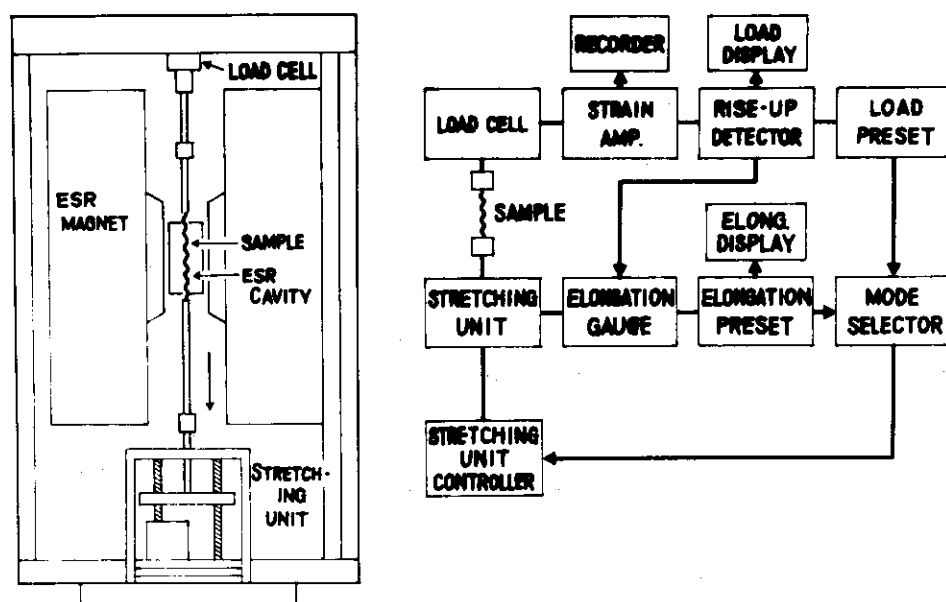


Fig. 1. Stretching apparatus.

We have used the apparatus to study radical formation of regular and high tenacity (HT) nylon 6 fibers both supplied by Unitika Co. Radicals are found to be produced by stretching nylon 6 fibers in a N_2 stream. The ESR spectrum observed agrees well to the one reported previously and ascribed to the secondary radicals produced subsequently to the chain rupture³⁾.

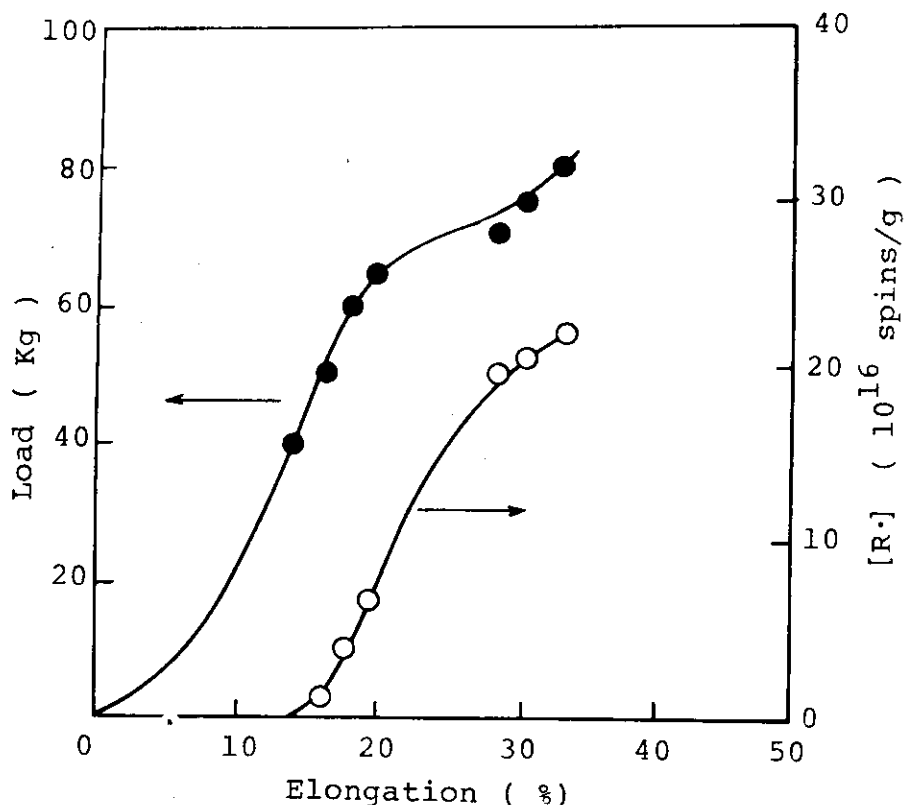


Fig. 2. Load and number of radicals vs. elongation for regular nylon 6 by the tensile force.
(2d x 8270 f)

Fig. 2 shows the concentration of radicals produced against percent elongation when the load is stepwise applied to regular nylon 6 fibers. Radicals become observable at ca. 15% of elongation and increase in concentration with the elongation. The concentration at break is 2×10^{17} spins/g which is well within the range of the various values reported previously.

Stretching of the HT-nylon 6 in N_2 gives rise to the ESR

spectrum identical with that for regular nylon 6 described above. The spectrum for the HT-nylon 6 fibers, however, becomes observable at elongation lower than that for regular nylon 6 fibers.

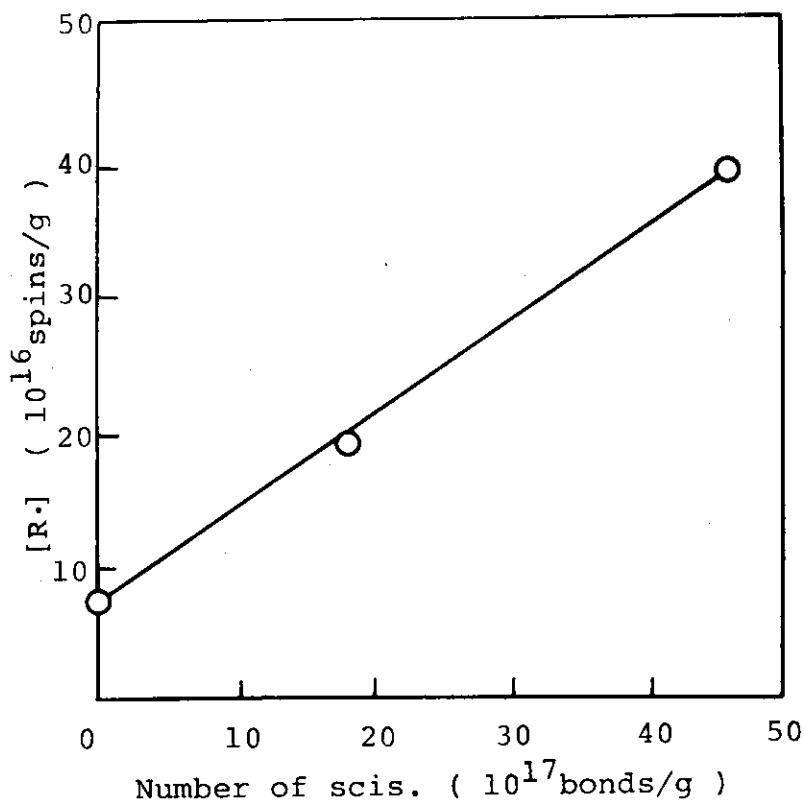


Fig. 3. Scission and radical formation of regular nylon 6 by the tensile force.

Dilute-solution viscosities of the unstretched and stretched nylon 6 fibers were measured with Ubbelohde capillary viscometers and changes in the viscosity-average molecular weight (\bar{M}_v) were estimated. Fig. 3 shows the number of chain rupture calculated from the changes in \bar{M}_v against the concentration of radicals determined by ESR. The linearity strongly indicates that the radicals observed by ESR are produced by chain rupture of regular nylon 6. (K. Kaji, S. Nagai, T. Takagaki, T. Okada, I. Sakurada)

- 1) K. Kaji, T. Okada, and I. Sakurada, JAERI 5027, 26 (1971).

- 2) K. Kaji, T. Okada, and I. Sakurada, JAERI-M 7355, 48 (1977).
- 3) H.H. Kausch-Blecken von Schmeling, J. Macromol. Sci.-Revs., Macromol. Chem., C4, 243 (1970).

2. Radical Formation in Wholly Aromatic Polyamides

Preliminary results were reported last year¹⁾ on ESR studies of radicals produced by γ -irradiation of two types of wholly aromatic polyamides, m-phenylene isophthalamide (m-PIA) and p-phenylene terephthalamide (p-PTA). As described in the preceding report, we have constructed a loading apparatus which permits ESR studies of radicals formed during stretching of fibers. With the apparatus studies were carried out on m-PIA and p-PTA fibers.

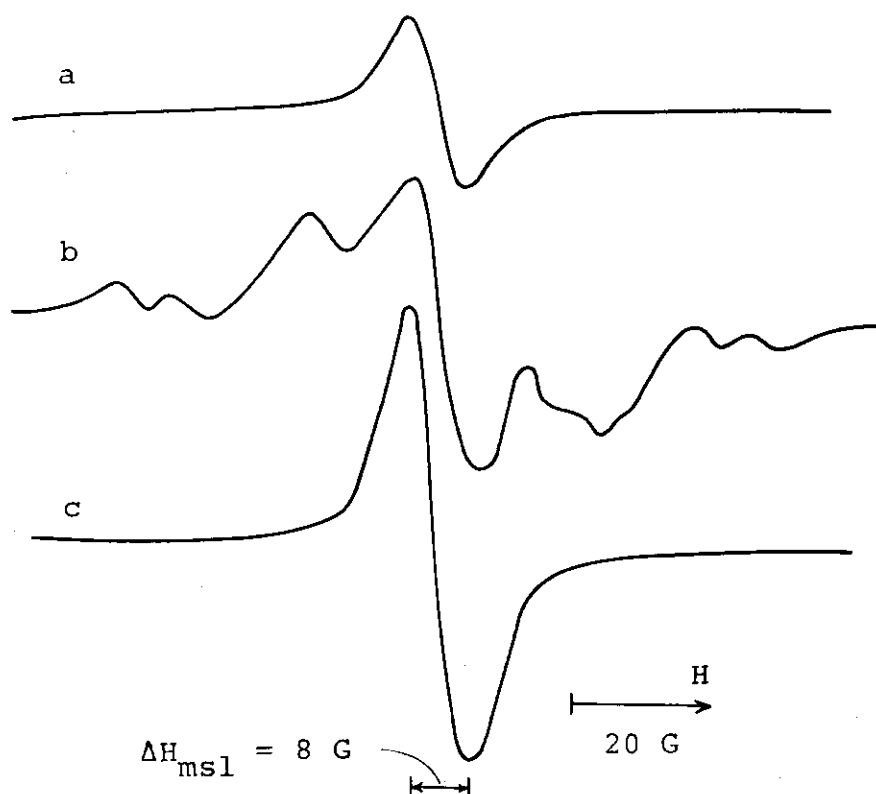


Fig. 1. ESR spectra observed during stretching of m-PIA fibers. (a) in N_2 , elongation 15.2%; (b) in N_2 , elongation 40.5%; (c) in air, elongation 40.5%.

The wholly aromatic polyamides used in this study are drawn and undrawn conex of Teijin Co. as m-PIA and Kevlar of Du Pont Co. as p-PTA. The fibers of 7900 filaments were stretched in an ESR cavity using the loading apparatus.

Radical formation was successfully observed for m-PIA by stretching both in air and in a N₂ stream while no radicals were detected in the case of p-PTA. The results for m-PIA are described below.

Stretching of m-PIA in air produces a singlet ESR spectrum with $\Delta H_{msl} = 8G$ as shown in Fig. 1 a, which is identical with that observed previously in the fibers after γ -irradiation. The spectrum grows in intensity with elongation of the fibers. Fig. 2 shows the load applied to the fibers and radical concentration produced against percent elongation of the fibers.

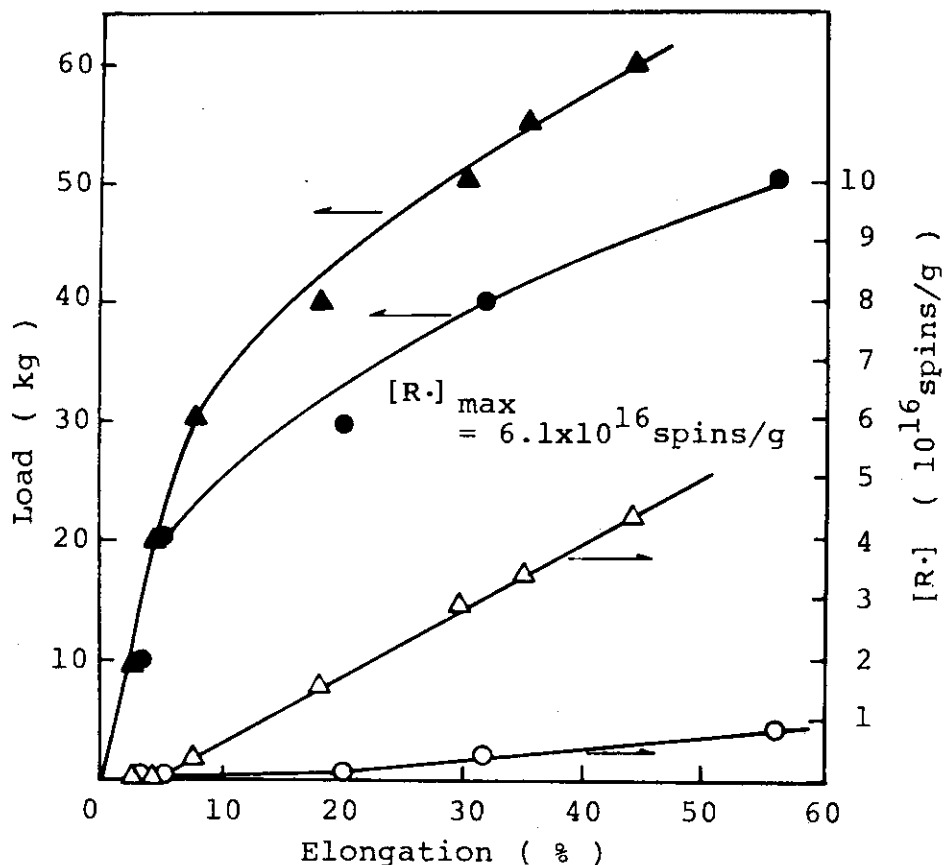


Fig. 2. Load & radical concentration vs. elongation of drawn (Δ) and undrawn (\circ) m-PIA fibers (7900 filaments). Stretching was carried out in air.

The concentration of radicals increases linearly with the elongation, which strongly indicates that the radicals are formed by molecular chain rupture of the fibers. It may also be seen from Fig. 2 that the radical concentration in the undrawn fibers is lower than that in the drawn fibers by an order of magnitude.

Stretching of m-PIA in a N_2 stream, on the other hand, gives a complex spectrum shown in Fig. 1 b. The spectrum is fairly stable in N_2 while it changes irreversibly to the singlet, same as observed from m-PIA stretched in air, when the N_2 flow is stopped. The concentration of radicals produced by stretching in N_2 is shown in Fig. 3 against elongation of the fibers. This behavior is quite similar to that by stretching in air except that more radicals are produced in N_2 . The concentration of radicals in the undrawn fibers is again lower than that in the drawn fibers. A similar phenomenon was already found in the case of regular nylon 6 fibers²⁾.

In an attempt to examine if the spectrum observed in N_2 flow are due to primary or secondary radicals produced after the chain scission, ESR studies were made for the fibers stretched at low temperatures. It is found that stretching at -100°C produces a triplet spectrum with 23G splitting which is quite different from the spectrum in Fig. 1 b. The spectrum is ascribed to the acyl radical $\cdot\text{C}(=\text{O})\text{NH}\phi$ formed by scission of $\text{C}(=\text{O})-\phi$ bond. On warming the fibers, the spectrum gradually decreases in intensity and changes at room temperature to a complex one consisting of a singlet with 8 G of width and an asymmetric spectrum possibly due to peroxy radicals. The spectral change observed may result from the reaction of the acyl radical with oxygen contained in liquid N_2 , and our attempt was unsuccessful to correlate the acyl radical with the radical responsible for the complex spectrum observed in N_2 at room temperature. The structure of the latter radical is not understood at present.

It is of interest to compare the present results with those for nylon 6. Radicals are detectable in m-PIA by stretching in air or in N_2 as described above. In contrast, stretching

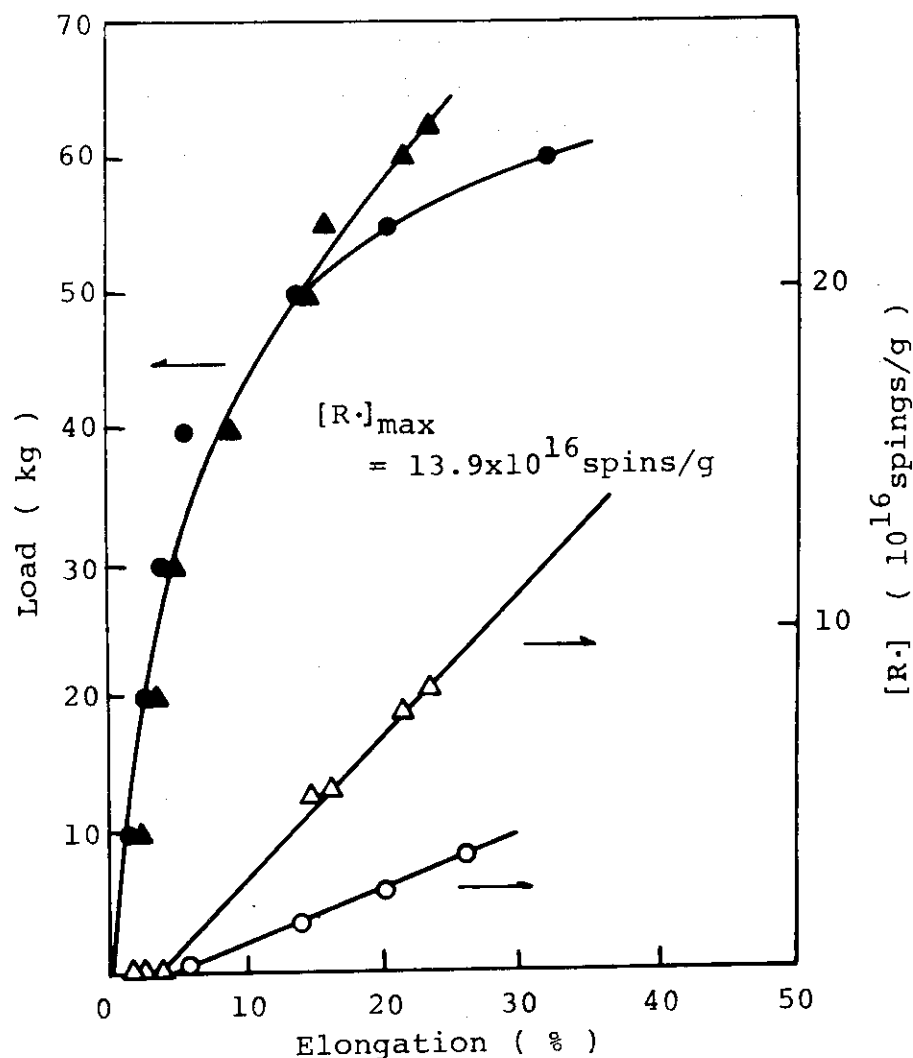


Fig. 3 Load & radical concentration vs. elongation of drawn (Δ) and undrawn (o) m-PIA fibers (7900 filaments). Stretching was carried out in a N_2 flow.

of nylon 6 in air permits no detection of radicals, which is due to the instability of produced radicals in air at room temperature. The concentration of radicals formed in m-PIA is lower than that in nylon 6. In addition, radical formation becomes observable in m-PIA at elongations greater than 5% in contrast to 15% in regular nylon 6, which may reflect the difference in orientation of molecular chains in both fibers. (S. Nagai, K. Kaji, I. Sakurada)

- 1) S. Nagai, K. Kaji, T. Takagaki, T. Okada and I. Sakurada, JAERI-M 7355, (1977).
- 2) T.C. Chiang and J.P. Sibilila, J. Polym. Sci. Polymer Phys., Ed., 10, 2249 (1972).

[6] Studies on Radiation Dosimetry1. Survey of Wavelength Suitable for Optical DensityMeasurement Used for CTA Film Dosimeter

Cellulose triacetate (CTA) film dosimeter which contains triphenyl phosphate (TPP) in 15 % by weight is reported to have excellent sensitivity and linearity between dose and optical density change when the optical density measurements are made at 280 nm¹⁾.

This wavelength is recommended by Numelec Co. in France because background optical density of unirradiated film is low so that dosimetry is possible over a wide range of dose.

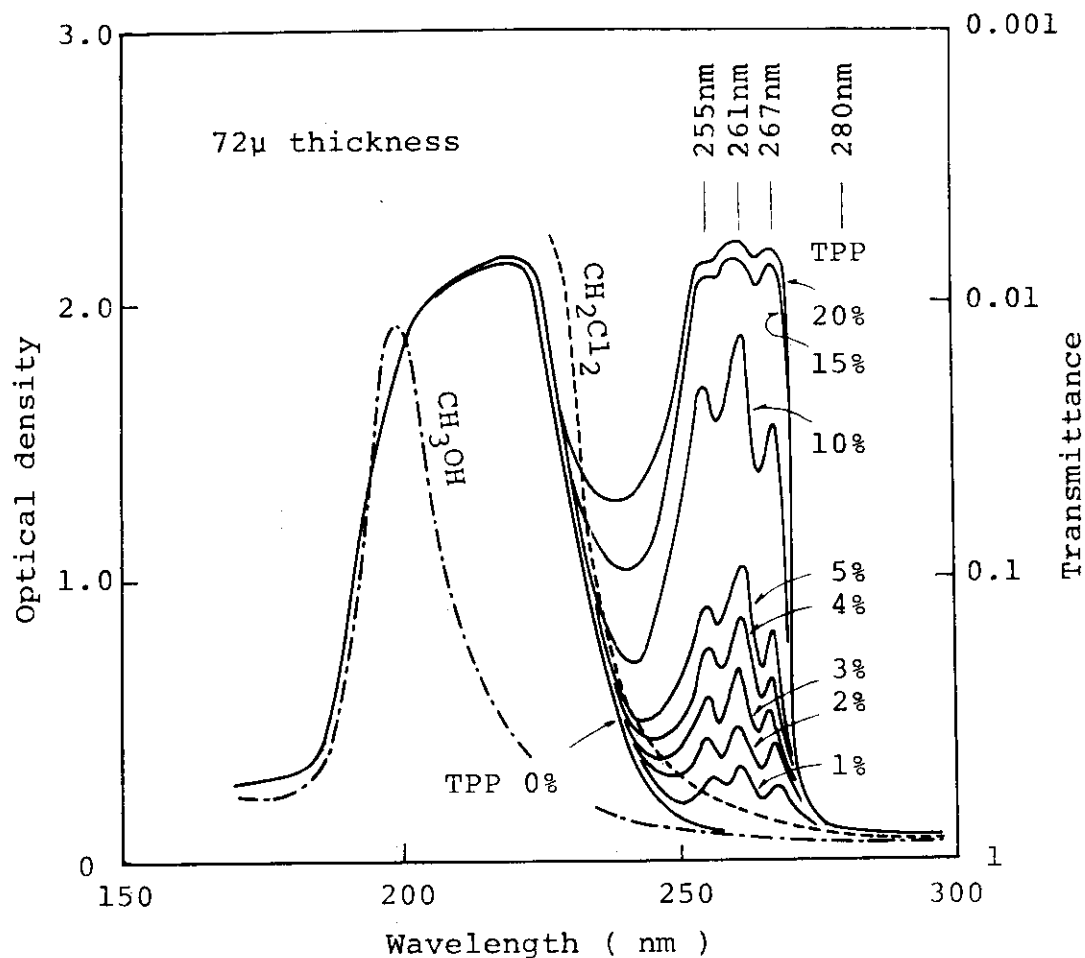


Fig. 1. Spectra of CTA films containing different amounts of TPP.

However, no definite basis for selection of this wavelength seems to be given and small deviation of the wavelength setting may cause a substantial error because of steep change in optical density (O.D.) around 280 nm in the UV spectrum of the dosimeter after irradiation. Therefore, a survey has been made to find the possibility whether better dosimetry can be made at other wavelength for the CTA film containing different amounts of TPP.

The CTA films containing no additives were supplied by Fuji Photo Film Co. Triphenyl phosphate (TPP) by Nakarai Chemicals Co. was recrystallized using zone melting method. The CTA films containing 1 - 20% by weight TPP were prepared by casting solutions of CTA and TPP in methylene dichloride and methanol (85 : 15 by vol). The thickness of the films thus prepared was 40 - 120 μm . Irradiations were carried out with electron beams of 1.5 MeV and 50 μA from a VdG accelerator. The samples to be irradiated are placed on a PMMA plate cooled by running water to avoid temperature rise due to the irradiations. The dose rate was estimated to be 7.5×10^4 rad/sec by the CTA dosimeter of Numelec Co. The UV spectra before and

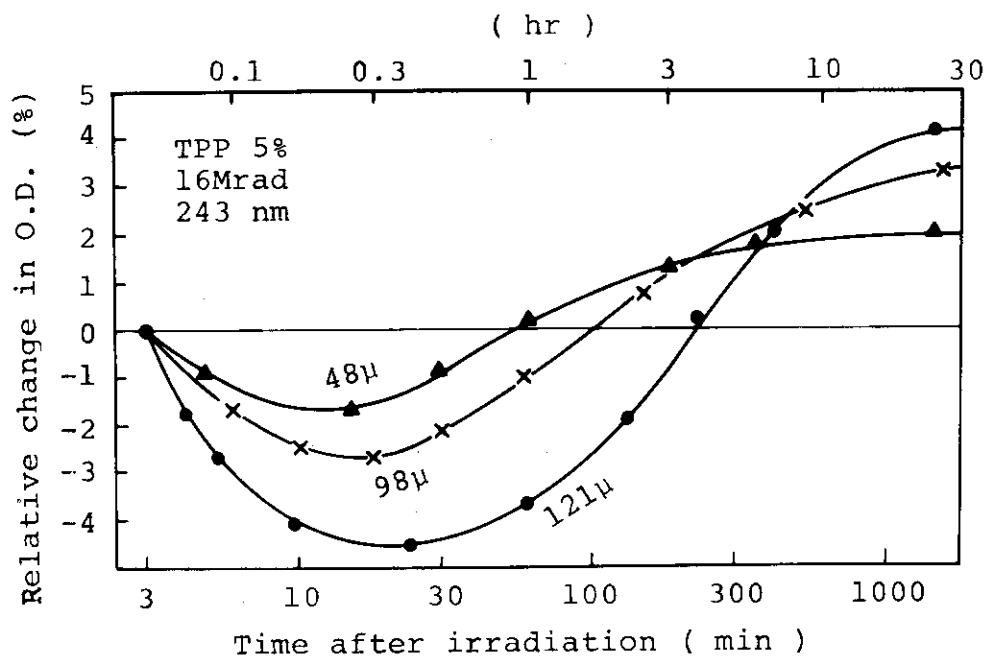


Fig. 2. Relative change in OD with time after irradiation.

after irradiation were recorded on a Shimadzu UV-210A spectrophotometer.

The UV spectra of unirradiated CTA films containing different amounts of TPP are shown in Fig. 1. The absorption band centered around 260 nm arises from transition of π electrons of benzene rings in TPP. It is seen that the O.D. at 280 nm recommended for use in dosimetry is fairly low and little dependent on TPP content while the wavelength of 280 nm corresponds to no definite peaks. The wavelengths of 255, 261 and 267 nm at peaks cannot be adopted because of the high O.D.'s. On the other hand, the wavelengths at bottoms lying

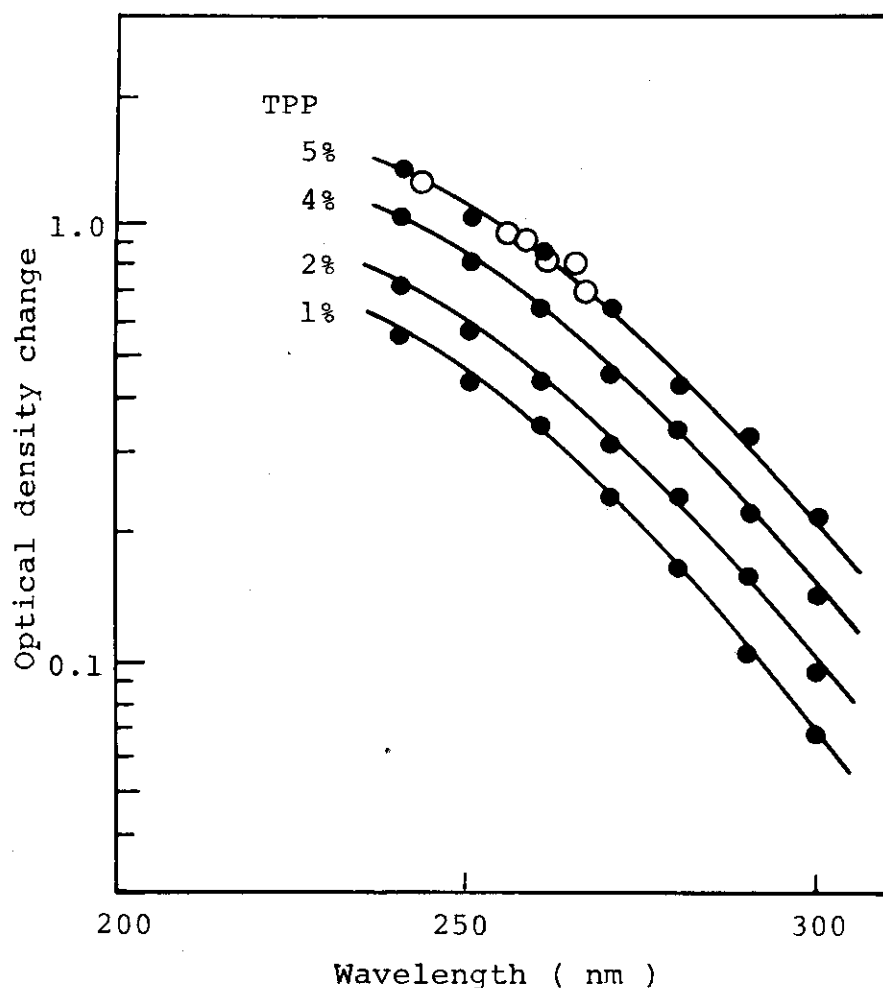


Fig. 3. Optical density change of CTA films containing different amounts of TPP as a function of wavelength by 16 Mrad irradiation. The optical density is normalized to that of 125 μ thickness.

in 240 - 250 nm, and at 257, and 265 nm seem worth examining further if their choice is appropriate for dosimetry, since the O.D.'s are rather low so long as TPP content in the film does not exceed 10%.

Fig. 2 shows the change in optical density (ΔOD_R) at 243 nm, the wavelength at one of the bottoms, relative to the value immediately after irradiation, with time after irradiation of CTA films containing 5% TPP to a dose of 16 Mrad.

The ΔOD decreases with time until 30 min after irradiation, and thereafter increases gradually, in agreement with the behavior found for the CTA dosimeter of Numelec Co. Since the increase in the ΔOD_R at time longer than 24 hr is quite slow, the value of ΔOD 24 hr after irradiation will be discussed below. When the irradiation dose increased from zero to 20

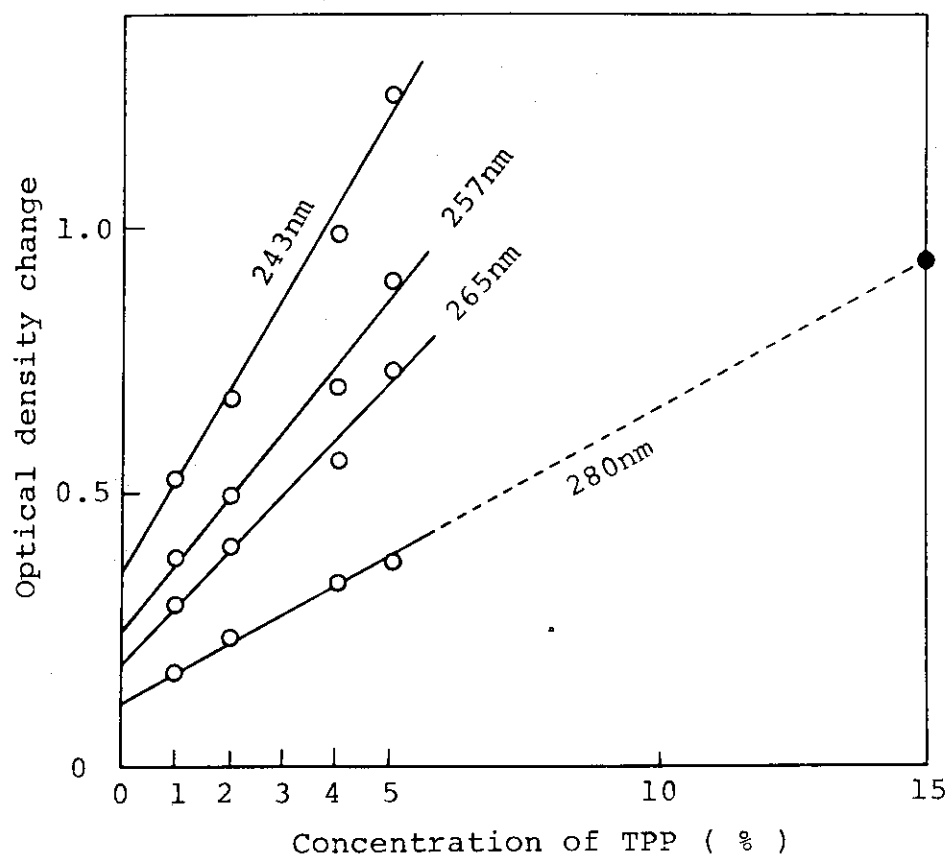


Fig. 4. Optical density change at different wavelengths by 16 Mrad irradiation as a function of TPP concentration. The optical density is normalized to that of 125 μ thickness.

Mrad, no shift from 243 nm was observed for the wavelength at the bottom.

In Fig. 3, the change in optical density (ΔOD) are plotted against wavelength for the CTA films containing different amounts of TPP. The irradiation dose was kept constant at 16 Mrad and film thicknesses are normalized to 125 μ m thickness since the film thickness deviates a little from batch to batch. It is evident from the figure that ΔOD becomes larger as the OD readings are taken at shorter wavelength and the content of TPP increases.

In Fig. 4 the data are replotted from Fig. 3 to give the ΔOD change as a function of TPP content at 243 nm, 257, 265 and 280 nm. The sensitivity of CTA film containing 5% TPP at 243 nm is three times higher than that at 280 nm, and even high by 1.3 when compared with that for CTA film containing 15% TPP at 280 nm.

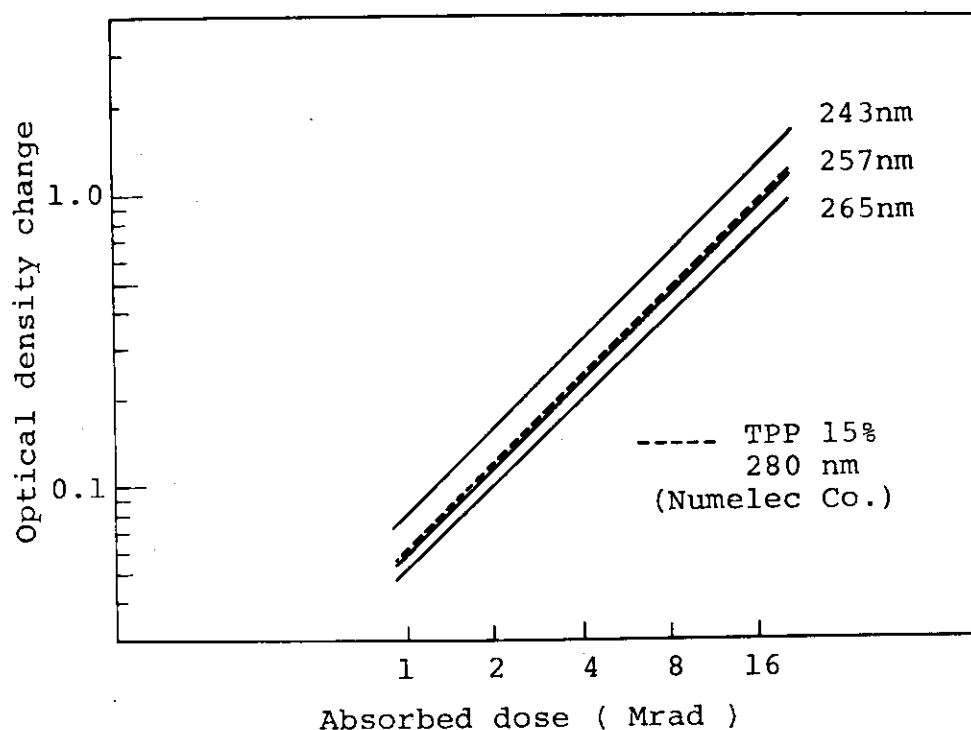


Fig. 5. Optical density change vs. absorbed dose for CTA film containing 5% TPP at 243, 257 and 265 nm; the ΔOD is normalized to that of 125 μ m thickness. Data for CTA obtained from Numelec Co. is also shown for comparison.

The linearity test for dose- ΔOD relationship also gives satisfactory results at 243 nm without sacrifice of the sensitivity as shown in Fig. 5.

In conclusion, dosimetry can be performed more accurately by the measurement of optical density change at 243 nm for the CTA films containing TPP. (K. Matsuda, T. Takagaki, T. Kasamatsu)

- 1) Y. Nakai, K. Matsuda, and T. Takagaki, JAERI 5029, 153 (1973).

2. Coloration Mechanism of the CTA Dosimeter

The dosimetry using the CTA film consists of measurement of optical density change in the UV region before and after irradiation¹⁾. The origin of such coloration, however, seems not to be known. The present study was carried out in an attempt to get insights into the mechanism for the coloration.

The CTA film dosimeter containing 15 weight % triphenyl phosphate (TPP) employed in this study was obtained from Numelec Co., France. Radiation effects on the dosimeter were studied spectroscopically using UV, IR, and ESR spectrometers. For comparison, similar studies were made on CTA films containing no additives supplied from Fuji Photo Film Co., and TPP powder from Nakarai Chemicals Co. Irradiations were performed with electron beams from a VdG accelerator.

Fig. 1 shows the relative change of the optical density (ΔOD_R) at 280 nm with time after irradiation of the film dosimeter irradiated in air and in vacuo. The ΔOD for the dosimeter irradiated in air decreases gradually with time until 30 min after irradiation and thereafter increases with storage time. Thus, the coloration of the dosimeter consists of two different phenomena, one occurring during irradiation and the other proceeding after irradiation. These are, for convenience, referred to hereafter as in situ-coloration, and post-coloration, respectively. In situ-coloration was also found to occur in the dosimeter irradiated in vacuo and the CTA film containing no additives. On the other hand, no or

little post-coloration occurs in the dosimeter irradiated in vacuo with or without subsequent exposition to air as may be seen from Fig. 1. This is also the case for the pure CTA film irradiated in air. Accordingly, the post-coloration would be attributed to some radiation effect on TPP in the presence of air.

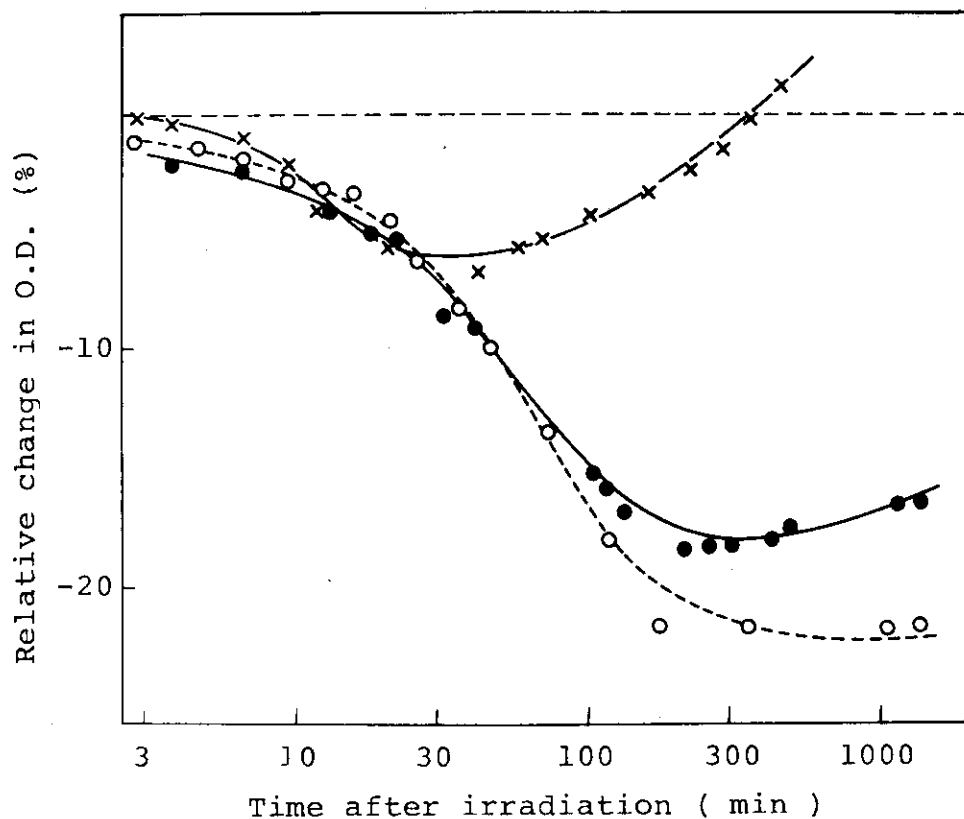


Fig. 1. Relative change of optical density at 280 nm with time after irradiation of the CTA film dosimeter in air (x), in vacuo (o). The data (•) are for the dosimeter irradiated in vacuo, followed by exposition to air.

The in situ-coloration may arise from non-radical species produced in CTA films by irradiation in view of the following findings obtained from ESR studies. The ESR spectrum of the dosimeter after irradiation in vacuo or in air consists of a triplet with the approximate separation of 12 G. A nearly identical spectrum was observed from the irradiated CTA film

containing no additives, so that the triplet spectrum is ascribed to CTA radicals. Irradiation of TPP powder produces an ESR spectrum showing the presence of two distinct radicals. The predominant component is ascribed to the phenoxy radicals and the minor one to cyclohexadienyl-type radicals produced by H atom addition to the benzene ring in TPP. Fig. 2 shows the decay curves of the radicals produced in the CTA films and powder, and in TPP powder. It can be seen from the figure that the CTA radicals in the dosimeter disappear nearly completely in air within 100 min while they are fairly stable in vacuo. The behavior is quite different from that for the ΔOD_R described above so that the CTA radicals may not be responsible for the in situ-coloration.

It is known in liquid phase²⁾ that some types of substituted phenoxy radicals react with O_2 to produce peroxides and quinones which give rise to strong absorptions in UV and visible region. By analogy, it is likely that the phenoxy radicals trapped in the dosimeter react with O_2 to produce

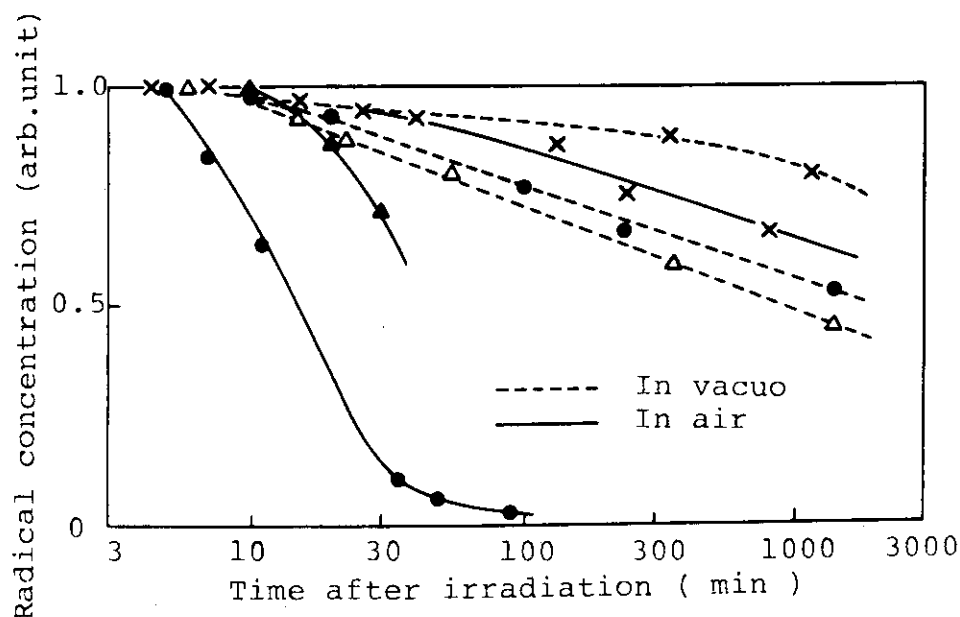


Fig. 2. Decay curves of radicals produced by irradiation of CTA film containing 15% TPP (●), pure CTA film (Δ), pure CTA powder (▲), and TPP powder (x) at room temperature. Dose, 20 Mrad.

some color centers for the post-coloration. This hypothesis was, however, ruled out by the finding that the dosimeter irradiated in O_2 exhibits no post-coloration. In addition, it was found in a preliminary experiment that the dosimeter exposed to 7 torr NO_2 shows an increase in OD at 280 nm with time. This fact suggests that the post-coloration proceeds through reactions of NO_2 , produced by irradiation and confined in the dosimeter, with TPP. Further study is in progress to support this hypothesis. (K. Matsuda, S. Nagai)

- 1) Y. Nakai, K. Matsuda, and T. Takagaki, JAERI 5029, 153 (1973).
- 2) A.R. Forrester, J.M. Hay, and R.H. Thomson, "Organic Chemistry of Stable Free Radicals", Chap. 7, Acad. Press, London and New York (1968).

III. LIST OF PUBLICATIONS

[1] Published Papers

1. M. Hatada and K. Matsuda, "Radiation Effects on Fischer-Tropsch Synthesis", *Radiat. Phys. Chem.*, 10, 195 (1977).
2. S. Nagai, K. Matsuda, and M. Hatada, "Application of the Spin Trapping Technique to the Study of Radiation Effects on Gaseous Mixtures of Carbon Monoxide and Hydrogen", *J. Phys. Chem.*, 82, 322 (1978).
3. K. Matsuda, S. Nagai, H. Arai, and M. Hatada, "Fluidized Bed Catalytic Reactor for Radiation Chemical Gaseous Reaction Induced by Electron Beams", (1977)
4. S. Nagai and T. Gillbro, "Anion Radicals of 2-Chlorothiophene. A σ^* Radical", *J. Phys. Chem.*, 81, 1793 (1977).
5. J. Takezaki, T. Okada, and I. Sakurada, "Radiation-Induced Polymerization of Styrene at High Dose Rate", *J. Appl. Polym. Sci.*, 21, 2683 (1977).
6. I. Sakurada, "Radiation-Induced Polymerization of Vinyl Monomers", *Nippon Kagakusen-i Kenkyusho Koenshu* (Annual Report of the Research Institute for Chemical Fibers, Japan), 34, 41 (1977).
7. I. Sakurada, T. Okada, and J. Takezaki, "Polymerization of Water Saturated Styrene with Electron Beams", Report of the 70th Poval Committee, 70, 67 (1977).
8. M. Hatada and M. Nishii, "Polymerization Induced by Electron-Beam Irradiation of Octadecyl Methacrylate in the Form of a Multilayer or Monolayer", *J. Polym. Sci., Polym. Chem. Ed.*, 15, 927 (1977).
9. K. Kaji, T. Okada, and I. Sakurada, "Radiation-Induced Graft Polymerization onto Poly (Vinyl Chloride) Fiber", *Sen-i Gakkai-shi* (J. of the Society of Fiber Science and Technology, Japan), 34, 1 (1977).
10. K. Kaji, T. Okada, and I. Sakurada, "Radiation-Induced Grafting of Calcium Acrylate onto Poly (Vinyl Chloride) Fiber", *Sen-i Gakkai-shi* (J. of the Society of Fiber Science and Technology, Japan), 33, T-494 (1977).
11. Y. Ikada, "Platelet Adhesion and Non-Thrombogenic Materials", *Nippon Setchaku Kyokai-shi* (J. of the Adhesion Society of Japan), 13, 264 (1977).

12. Y. Ikada and F. Horii, "Properties of Hydrogels", Nippon Kagakusen-i Kenkyusho Koenshu (Annual Report of the Research Institute for Chemical Fibers, Japan), 34, 1 (1977).
13. Y. Ikada, "Surface Effect on Blood Coagulation", Hyomen (Surface), 15, 718 (1977)
14. Y. Ikada, H. Iwata, and S. Nagaoka, "Chain Transfer in Radical Polymerization and End Group Content of Resultant Polymers", Macromolecules, 10, 1364 (1977).

* * * *

15. M. Hatada, "Radiation Chemical Reactions of Mixtures of Carbon Monoxide and Hydrogen", Nuclear Engineering, 24, (No. 4), 24 (1977).
16. T. Okada, "Electron Beam - and U.V.-Radiation Induced Cross-Linking and Adhesion", Nippon Setchaku Kyokai-shi (J. of the Adhesion Society of Japan), 13, 465 (1977).
17. M. Hatada, "Polymerization of Monomers in a Form of Monolayer or Multilayers", Nippon Setchaku Kyokai-shi (J. of the Adhesion Society of Japan), 13, 344 (1977).
18. M. Gotoda, T. Okada, K. Murata, and A. Takahashi, "Separator for Electrolytic Cells", Japan Kokai (Patent Application), Jun. 23 (1977).

[2] Oral Presentations

1. S. Sugimoto, M. Nishii, and T. Sugiura, "Radiation Effects on the Reaction of Mixtures of Carbon Monoxide and Hydrogen (V). Irradiation Using a Gas Circulation System", The 20th Discussion Meeting on Radiation Chemistry, Oct. 6, 1977.
2. K. Matsuda, S. Nagai, H. Arai, and M. Hatada, "Radiation Effects on the Reaction of Mixtures of Carbon Monoxide and Hydrogen (VI). Irradiation in the Flow System", The 20th Discussion Meeting on Radiation Chemistry, Oct. 6, 1977.
3. S. Nagai, K. Matsuda, and M. Hatada, "Application of the Spin Trapping Technique to the Radiation Chemistry of Mixture of CO and H₂", The 20th Discussion Meeting on Radiation Chemistry, Oct. 6, 1977.
4. H. Arai and H. Hotta, "Decline of the Self-Focusing of a Pulsed High-Intensity Electron Beam Due to Gas Breakdown", The 20th Discussion Meeting on Radiation Chemistry, Oct. 6, 1977.
5. J. Takezaki, T. Okada, and I. Sakurada, "Polymerization of Water-Saturated Styrene with Electron Beams", The 26th Annual Meeting of the Society of Polymer Science, Japan, Jun. 27, 1977.
6. I. Sakurada, T. Okada, and J. Takezaki, "Formation of Radical and Ionic Polymers in the Radiation-Induced Polymerization of Styrene", The 26th IUPAC Congress, Sep. 8, 1977.
7. K. Hayashi, "Molecular Weight Distribution of Polymers Obtained in Polymerization by Electron Beams and Its Change with Dose Rate", The 20th Discussion Meeting on Radiation Chemistry, Oct. 7, 1977.
8. N. Kotani and K. Hayashi, "Polymerization of α -Methylstyrene by Radiation", The 26th Discussion Meeting of the Society of Polymer Science, Japan, Oct. 29, 1977.
9. M. Gotoda, T. Yagi, and K. Ishikawa, "Electron Beam Curing of Chlorinated Polymer/Vinyl Monomer Mixtures", Discussion Meeting of the Society of the Synthetic Plastic Industries, Oct. 1977.
10. S. Nagai, K. Kaji, T. Takagaki, and T. Okada, "ESR Studies of Radicals Produced in Wholly Aromatic Polyamides", Discussion Meeting on ESR, Oct. 12, 1977.

11. T. Okada, K. Kaji, K. Ohkura, and I. Sakurada, "Flame-Retardant Polyester Fiber Prepared by Surface-Polymerization of Vinyl Phosphonate with Irradiation of Electron Beams", Annual Meeting of the Society of Fiber Science and Technology, Jun. 15, 1977.
 12. K. Kaji, T. Okada, and I. Sakurada, "Radiation Effects of Wholly Aromatic Polyamide Fibers", Annual Meeting of the Society of Fiber Science and Technology, Jun. 13, 1977.
 13. M. Gotoda, T. Yagi, and K. Ishikawa, "Curing of Diepoxy Compounds by Electron Beam-Induced Ionic Polymerization", The 26th Annual Meeting of the Polymer Society, Japan, May 27, 1977.
 14. T. Okada, J. Takezaki, and I. Sakurada, "Preparation of Low Molecular Weight Products such as Oligomer with Electron-Beam Irradiation", The 15th Discussion Meeting on Adhesion Research, Jun. 1977.
 15. T. Okada, K. Kaji, and I. Sakurada, "Modification of Polyester Fiber by Radiation-Induced Chlorination", The 23rd Regional Meeting of the Society of Polymer Science (Kobe), Jul. 12, 1977.
 16. Y. Ikada, T. Mita, H. Iwata, and S. Nagaoka, "Surface Grafting onto PVA Films", The 26th Annual Meeting of the Society of Polymer Science, Japan, May 26, 1977.
 17. T. Mita, H. Iwata, and Y. Ikada, "Immobilization of Amylase onto Film of Ethylene-Vinyl Alcohol Copolymer", The 23rd Regional Meeting of the Society of Polymer Science (Kobe), Jul. 13, 1977.
 18. Y. Ikada, H. Iwata, and S. Nagaoka, "Grafting of Plasma Proteins onto Film Surfaces", The 26th International Congress of Pure and Applied Chemistry (Tokyo), Sep. 7, 1977.
 19. Y. Ikada, H. Iwata, T. Mita, and S. Nagaoka, "Grafting onto Film Surfaces of PVA and its Derivatives", The 35th Annual Meeting of the Research Institute for Chemical Fibers, Japan, Oct. 1977.
 20. H. Iwata, Y. Ikada, and R. Kitamaru, "Kinetics of Acetalization Coupling of PVA", The 26th Discussion Meeting of the Society of Polymer Science, Japan, Oct. 31, 1977.
- * * * *
21. T. Kasamatsu, "Present Status and Future of Irradiation Processing", The Chubu Regional Meeting of Japan Atomic Industrial Forum, Feb. 23, 1978.

22. T. Kasamatu, "Present Status and Prospect of RI Utilization (3). Large Radiation Source", The 16th Joint Symposium on Atomic Energy Research, Feb. 16, 1978.
23. T. Okada, "Application of Electron Beam and UV Induced Cross-Linking to Adhesion", The 26th Seminar on Adhesion, Jun. 22, 1977.

IV. LIST OF SCIENTISTS

(Aug. 31, 1978)

[1] Staff Members

Tomomichi KASAMATSU	Radiation physicist, Head
Ichiro SAKURADA	Professor emeritus, Kyoto University, Former head
Seizo OKAMURA	Professor emeritus, Kyoto University
Toshio OKADA*	Dr., polymer chemist
Motoyoshi HATADA	Dr., physical chemist
Kanae HAYASHI	Dr., polymer chemist
Shun'ichi SUGIMOTO	Physical chemist
Koji MATSUDA	Radiation physicist
Jun'ichi TAKEZAKI	Physical chemist
Yasuo KUSAMA	Polymer chemist
Masanobu NISHII	Dr., polymer chemist
Siro NAGAI	Dr., physical chemist
Hidehiko ARAI	Physical chemist
Torao TAKAGAKI	Radiation physicist
Kanako KAJI	Polymer chemist
Toshiaki YAGI	Engineering chemist

[2] Advisors and Visting Researchers

Isamu NITTA	Professor emeritus, Osaka University, Advisor
Kozo HIROTA	Professor emeritus, Osaka University, Advisor
Kochiro HAYASHI	Professor, Osaka University, Advisor
Shun'ichi OHNISHI	Professor, Kyoto University, Advisor
Yoshito IKADA	Assoc. Professor, Kyoto University, Advisor
Masao KAJIMAKI	Physicist, Duskin Co., Ltd. (May 1975 - Jun. 1978)

*) Appointed chief, The second research and development division, Takasaki Research Establishment since Jun. 1st, 1978.